NASA/USRA UNIVERSITY ADVANCED DESIGN PROGRAM 1992-1993

PROJECT CENTER MENTOR:
NASA-AMES DRYDEN FLIGHT RESEARCH FACILITY

FINAL DESIGN PROPOSAL

The RTL-46

A Simulated Commercial Air Transportation Study

April 1993

Department of Aerospace and Mechanical Engineering
University of Notre Dame
Notre Dame, IN 46556

AEROSPACE DESIGN

SENIOR DESIGN PROPOSAL

RTL - 46

PROPOSED BY RTL AERONAUTICS

TEAM LEADER, CHRISTIAN DUNBAR

CHIEF ENGINEER, JOHN PRETTE

DIRECTOR OF MANUFACTURING, GERALD ANDERSEN

SECRETARY, MARTIN SPRUNCK

AERODYNAMICS CONSULTANT, CHRISTINE VOGEL

STABILITY AND CONTROL SPECIALIST, FRANCISCO RIVERA

PROPOSAL DATE, 8 APRIL 1993

TABLE OF CONTENTS

EXECUTIVE SUMMARY

i. SUMMARY

The RTL-46 (**R**eason **t**o **L**ive **f**or the **S**ix group members) provides an aircraft which utilizes advanced technology within the Aeroworld market to better service the air travel customers and airlines of Aeroworld. The RTL-46 is designed to serve the portion of the travel market which flies less than 10,000 feet per flight. The design cruise velocity for the aircraft is 35 ft/sec, which rapidly expedites travel through Aeroworld.

The major focus of the endeavor was to design an aircraft which would serve the Aeroworld market better than the existing aircraft, the HB-40. This could have been done through targeting another portion of the Aeroworld market or through serving the current HB-40 market more effectively. Due to the fact that approximately 70% of the potential Aeroworld passengers desired flights of 10,000 ft or less, this range became the target market for the RTL-46.

The driving forces behind the design for the RTL-46 were economic in nature, consisting of reducing the direct operating costs, and thus the cost per seat per thousand feet of the aircraft, and gaining a higher share of the potential market than the HB-40. The first method of decreasing the costs and increasing the market arose through the design of an aircraft which holds 2.5 times as many passengers as the existing aircraft. The 100 passenger capacity RTL-46 decreases the cost per seat by increasing the number of seats, and achieves the increased market share goal by servicing a higher percentage of the passengers desiring flights. The second major aspect of the design, which increases the available, market consists of the use of high lift devices (full span flaps) which shorten the takeoff distance to 15.4 ft, well below the 20 ft maximum distance for service to all airports. Through strong structural engineering and weight analysis, these

increases in the aircraft performance are achieved while only minimally increasing the aircraft weight from the HB-40 (less than 15% more).

The Aerodynamics of the RTL-46 consist of a SD7062 airfoil section modified with 25% chord full span flaps which have a maximum deflection angle of 20° for takeoff and landing maneuvers. The SD7062 was chosen for its lifting abilities and fairly flat bottom surface design which allows for ease of construction and lower costs of construction (labor and material) than more cambered airfoils. The flaps increase the aircraft C_{Lmax} from 1.1 to 1.8 when deflected to the maximum angle. The tail section is mounted on the top of the fuselage with the horizontal section mounted at the base of the vertical stabilizer. This clears the tail of most vortices trailing off the low mounted wing. The wing aspect ratio was set at 8.46 to allow for minimal losses in the lift due to 3-D effects, while at the same time maintaining structural integrity.

The propulsion system consists of the Astro 15 motor and 12 Panasonic NiCd batteries which will provide the necessary voltage and current draw to achieve the required takeoff and cruise conditions over the range of the flights targeted by the RTL-46. The aircraft uses a modified Zinger 13-6 propeller cut to yield the effects of a 12.5-6 propeller.

The landing gear of the RTL-46 provides much ground control through the use of tricycle landing gear with the steerable nose gear. This formation provides better maneuverability and eliminates the potential for tip over nose first when landing and ground loop during maneuvers while on the ground. The drawbacks to this type of gear are the increased technology integration costs and the critical placement of the gear for takeoff rotation.

The use of flaps led to the elimination of ailerons in the design for roll control, therefore, the dihedral of 10° combined with the rudder size and deflection provide the lateral stability necessary to control the aircraft. This

system also provides the necessary means to bank the aircraft into the turns at a slightly faster rate than the HB-40 while the total bank remains the same. This improvement aids the pilot in the limited confines of Aeroworld. The horizontal stabilizer provides the necessary pitch stability and when combined with the elevators, pitch control is achieved. The overall handling qualities of the aircraft are expected to be better for the pilot than those of the HB-40. The static margin of 28% provides more than adequate response time for the pilot of the aircraft

The interior of the RTL-46 is designed to maximize the comfort of every one of its 100 passengers, first class and coach. The seating arrangement provides every passenger with both a window view and aisle access from his or her seat. Passengers will be served their food from the aircraft's galley located towards the nose of the aircraft and lavatories are located in the rear. The multiple deck configuration (see diagrams) provides each individual with enough room to move while not causing long walks to the front or rear of the aircraft to get to these lavatories or the exits.

While the RTL-46 increases the size and performance over the existing aircraft, the aircraft weight is only 4.9 lb. This low weight, through sound structural design provides a dramatic cost decrease through the fuel savings or direct operating costs per flight. The relatively square fuselage is simple yet the drag is reduced by tapering the shape towards the nose and tail. The light weight, compared to similar aircrafts in the market, allows for better performance. Economically the aircraft has a CPSPK of .46 cents for the designed mission flight range and a total manufacturing cost estimated at $2185.00 +/- 10%.

The major areas of design for the aircraft lie within the cost effectiveness through improved aerodynamics of the wing and fuselage. Although the benefits of these areas are readily apparent, their drawbacks are slightly more

subtle. The increased drag of the wing with flaps down could negate the lift gain, and the increased complexity could lead to higher costs of construction than the revenue gain from the service to the shorter runway airports.

ii - SUMMARY OF SPECIFICATIONS:

AERODYNAMICS:		PROPULSION:	
Wing Area	9.93 ft^2	Engine	Astro 15
Aspect Ratio	8.46	Propeller	Zinger 12.5-6
Chord	13 in	Number of Batteries	12
Span	9.17 ft	Battery Pack Voltage	19.4 V
Taper Ratio	1.0	Cruise gear RPM	4314
Sweep	0 degrees		
Dihedral	10 degrees		
C_{Do}	0.0247		
Airfoil section	SD7062		
Wing Incidence angle	1.5 degrees		
Flap cf/c	0. 25		
Flap max deflection	20 degrees		

STABILITY AND CONTROL EMPENNEGE:		PERFORMANCE:	
Hor. and Ver. Tail Airfoil sections	flat plate	Takeoff distance	15.4 ft
		Takeoff velocity	23ft/s
Hor. Tail area	1.92 ft^2	Cruise velocity	35 ft/s
Elevator area	0.23 ft^2	Range(cruise)	19451ft
Elevator max deflection	45 degrees	Endurance(cruise)	9.26 min
Vertical Tail area	0.73 ft^2	Max Range	19788 ft
Rudder area	0.39 ft^2	Max Endurance	13.52 min
Rudder max deflection	30 degrees	Max Rate of Climb	13.06
		Turn Radius	60 ft

STRUCTURES:		ECONOMICS:	
Weight	5.1 lbs	CPSPK	$0.42
Fuselage length	5.5 ft	DOC	$4.09
Fuselage width	6 inches	Total aircraft cost	$2185.00
Fuselage height	6 inches		

THREE VIEW EXTERNAL SCHEMATICS

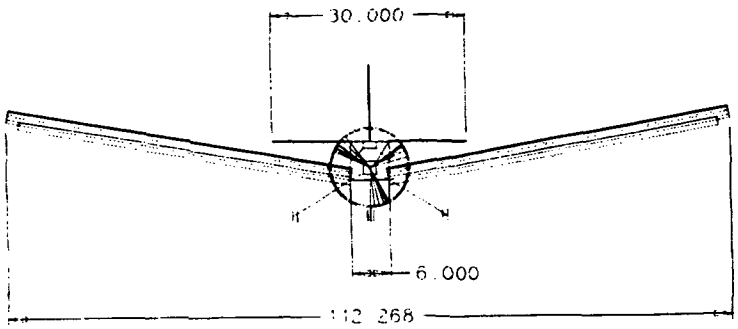

FRONT VIEW

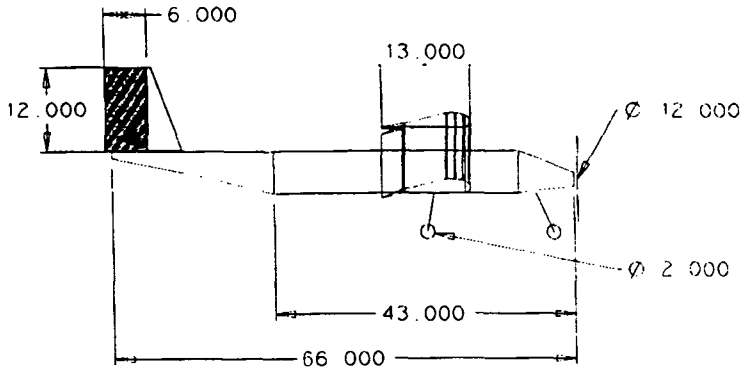

SIDE VIEW

TOP VIEW

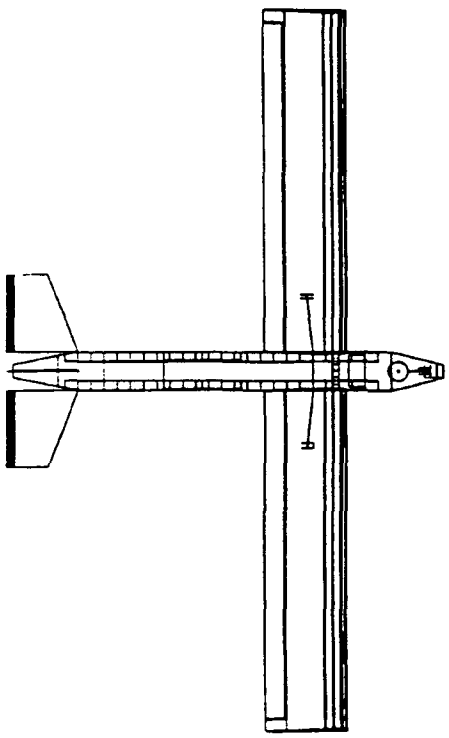

TWO VIEW INTERNAL CONCEPT SCHEMATIC

TOP VIEW

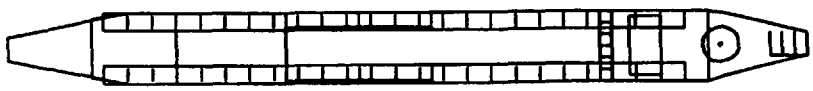

SIDE VIEW

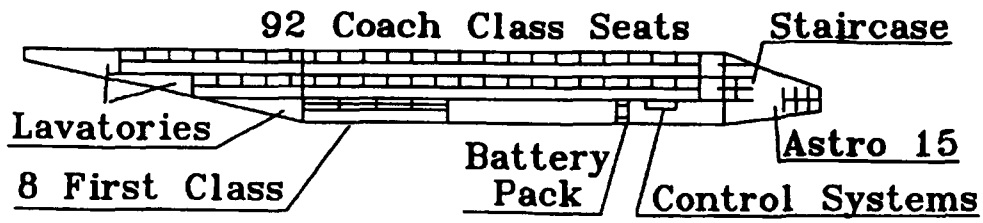

POST FLIGHT MANAGEMENT REVIEW: **RTL -46**

April 30, 1993

The following observations were made during the flight test validation for this aircraft design. This assessment is obviously quite qualitative and is based primarily upon the pilot's comments and instructor's observations.

1. Initial takeoff was conducted without flaps.

2. The aircraft was somewhat sluggish in the turns but this is indicative of a low-wing aircraft which turns with rudder/dihedral.

3. Second flight with half flaps and was o.k. but there was not a readily obvious improvement in take-off length. This may be due to increased drag with flap deflection and its effect on acceleration.

4. Second flight landing with full flaps but had real problems keeping the nose up to flare. Doesn't seem to have a large enough elevator to compensate for the nose down moment when flaps are deployed. There appeared to be enough elevator deflection, just not enough area.

5. In-field fix was attempted to increase the elevator size (approximately double). It took off full flaps (although it was somewhat difficult to get it to rotate at takeoff) and then it flew fine with full flaps.

6. Successful validation of basic flight concept. Flew under control through entire closed course at approximately the required loiter speed. Landing and take-off performance was acceptable based upon the requirements.

	A	B	C
1	Parameter	Initials	Value
2	DESIGN GOALS:		
3	V cruise	all	35 ft/s
4	Max # of passengers	all	100
5	#passengers-coach	Dunbar	8
6	# passemgers-1st class	Dunbar	92
7	# crew	Dunbar	5
8	Max Range at Wmax	all	13000 ft
9	Altitude cruise	all	15 ft
10	Minimum turn radius	all	60 ft
11	Max range at Wmin	all	20000 ft
12	Maximum TO Weight-WMTO	Dunbar/Anderson	5.5 lbs
13	Minimum TO Weight - Wmin	Dunbar/Anderson	5.0 lbs
14	Total Cost per Aircraft	all	$2,350.00
15	DOC	all	$10.00
16	CPSPK(max design conditions	all	$0.90
17			
18	BASIC CONFIG.		
19	Wing Area	Vogel	9.93 ft^2
20	Maximum TO Weight-WMTO	Dunbar	5.1 lbs
21	Empty Flight Weight	Dunbar	4.6 lbs
22	Wing Loading(WMTO)	Vogel/Dunbar	7.9 oz/ft^2
23	max length	Dunbar	5.5 ft
24	max span	Dunbar	6 inches
25	max height	Dunbar	6 inches
26	Total Wetted Area	Dunbar	33.46 ft^2
27			
28	WING		
29	Aspect Ratio	Vogel	8.46
30	Span	Vogel	9.17 ft
31	Area	Vogel	9.93 ft^2
32	Root Chord	Vogel	13 inches
33	Tip Chord	Vogel	13 inches
34	Taper Ratio	Vogel	1
35	C mac-MAC	Rivera	-0.083
36	leading edge Sweep	Vogel	none
37	1/4 chord Sweep	Vogel	none
38	Dihedral	Vogel	10 degrees
39	Twist(washout)	Vogel	none
40	Airfoil section	Vogel	SD7062
41	Design Reynolds number	Vogel	200000
42	t/c	Vogel	13.98%
43	Incidence angle(root)	Vogel	1.5 degrees
44	Hor. pos of 1/4 MAC	Rivera	18.25 inches
45	Ver. pos of 1/4 MAC	Rivera	2.5 inches
46	e-Oswald efficiency	Vogel	0.79
47	CDo-wing	Vogel	0.011
48	CLo-wing	Vogel	0.32
49	Clalpha-wing	Vogel	4.58/rad
50			
51	FUSELAGE		
52	Length	Dunbar	5.5 ft
53	Cross section shape	Dunbar	square
54	Nominal Cross Section Area	Dunbar	0.25 ft^2
55	Finess Ratio	Dunbar	11
56	Payload volume	Dunbar	0.75 ft^3
57	Planform area	Dunbar	2.75 ft^2
58	Frontal area	Dunbar	0.25 ft^2
59	CDo -fuselage	Vogel	0.00583
60	CLalpha-fuselage	Vogel	0.41/rad
61			
62	EMPENNAGE		
63	Horizontal tail		
64	Area	Rivera/Prette	1.92 ft^2
65	Span	Rivera/Prette	30 inches

	A	B	C
66	Aspect Ratio	Rivera/Prette	3.26
67	Root chord	Rivera/Prette	11 inches
68	Tip chord	Rivera/Prette	6.5 inches
69	Average chord	Rivera/Prette	9.33 inches
70	Taper ratio	Rivera/Prette	0.6
71	l.e. sweep	Rivera	15.7 degrees
72	1/4 chord sweep	Rivera	11.9 degrees
73	incidence angle	Rivera	- 2 degrees
74	hor. pos. of 1/4 MAC	Rivera	59 inches
75	ver. pos. of 1/4 MAC	Rivera	3.0 inches
76	Airfoil section	Rivera	flat plate
77	e - Oswald efficiency	Rivera	0.73
78	CDo horizontal	Vogel	0.0012
79	CLo-horizontal	Vogel	0
80	CLalpha - horizontal	Vogel	3.89/rad
81	CLde - horizontal	Rivera	0.237
82	CM mac-horizontal	Rivera	0
83			
84	**Vertical tail**		
85	Area	Rivera/Prette	0.73 ft^2
86	Aspect ratio	Rivera/Prette	2.2
87	root chord	Rivera/Prette	11 inches
88	tip chord	Rivera/Prette	7.66 inches
89	average chord	Rivera/Prette	9.33 inches
90	taper ratio	Rivera/Prette	0.7
91	l.e. sweep	Rivera/Prette	20.6 degrees
92	1/4 chord sweep	Rivera/Prette	15.7 degrees
93	hor. pos. of 1/4 MAC	Rivera	59 inches
94	vert. pos. of 1/4 MAC	Rivera	3.0 inches
95	Airfoil section	Rivera	flat plate
96			
97	**SUMMARY AERODYNAMICS**		
98	Cl max (airfoil)	Vogel	1.5
99	CL max(aircraft) w/o flaps	Vogel	1.1
100	CL max(aircraft) w/ flaps	Vogel	1.8
101	lift curve slope(aircraft)	Vogel	4.87/rad
102	CDo (aircraft)	Vogel	0.0247
103	efficiency-e(aircraft)	Vogel	0.73
104	Alpha stall(aircraft) w/o flaps	Vogel	9.8 degrees
105	Alpha stall(aircraft) w/ flaps	Vogel	8.1 degrees
106	Alpha zero lift (aircraft)	Vogel	3.5 degrees
107	L/D max(aircraft)	Vogel	14
108	Alpha L/D max(aircraft)	Vogel	5 degrees
109			
110	**WEIGHTS**		
111	Weight total (empty)	Dunbar	4.4 lbs
112	C. G. most forward-x&y	Dunbar	x=17.7 inches
113	C. G. most aft-x&y	Dunbar	x=19 inches
114	Avionics	Dunbar	9.44 oz
115	Payload-Crew and Pass-max	Dunbar	8.82 oz
116	Engine & Engine controls	Dunbar	11.5 oz
117	Propeller	Dunbar	0.87 oz
118	Fuel(battery)	Dunbar	14.75 oz
119	Structure	Dunbar	35.3 oz
120	Wing	Dunbar	21 oz
121	Fuselage/emp	Dunbar	8.9 oz
122	Landing gear	Dunbar	3.6 oz
123	lcg - max weight	Dunbar	x=19.0 inches
124	lcg - empty	Dunbar	x=16.5 inches
125			
126	**PROPULSION**		
127	Type of engines	Sprunck	Astro-15
128	number	Sprunck	1
129	placement	Sprunck	forward
130	Pavil max at cruise	Sprunck	85 watts

	A	B	C
131	Preq cruise	Sprunck	23.6 watts
132	max current draw at TO	Sprunck	12.1 amps
133	cruise current draw	Sprunck	5.6 amps
134	Propeller type	Sprunck	Zinger 12.5-6
135	Propeller pitch	Sprunck	6 inches
136	Number of blades	Sprunck	2
137	max. prop, rpm	Sprunck	6510
138	cruise prop. rpm	Sprunck	4314
139	max thrust	Sprunck	2.7 lbs
140	cruise thrust	Sprunck	0.5 lbs
141	battery type	Sprunck	P-90SC
142	number	Sprunck	12
143	individual capacity	Sprunck	900 mah
144	individual voltage	Sprunck	1.2 V
145	pack capacity	Sprunck	900 mah
146	pack voltage	Sprunck	14.4 V
147			
148	STAB AND CONTROL		
149	Neutral point	Rivera	0.58c
150	Static margin %MAC	Rivera	0.273
151	Hor. tail volume ratio	Rivera	0.61
152	Vert. tail volume ratio	Rivera	0.027
153	Elevator area	Rivera	0.23 ft^2
154	Elevator max deflection	Rivera	15 degrees
155	Rudder area	Rivera	0.39 ft^2
156	Rudder max deflection	Rivera	30 degrees
157	Aileron area	Rivera	none
158	Aileron max deflection	Rivera	none
159	Cm alpha	Rivera	1.233/deg
160	Cn beta	Rivera	0.092
161	Cl alpha tail	Rivera	6.28/rad
162	Cl delta e tail	Rivera	-0.743
163			
164	PERFORMANCE		
165	Vmin at WMTO	Sprunck	19.4
166	Vmax at WMTO	Sprunck	54 ft/s
167	Vstall at WMTO	Prette	19.4
168	Range max at WMTO	Sprunck/Prette	19,430
169	Endurance @Rmax	Sprunck/Prette	11 min
170	Endurance Max at WMTO	Sprunck/Prette	13.52 min
171	Range at Emax	Sprunck/Prette	16224 ft
172	Range max at Wmin	Sprunck/Prette	19,760
173	ROC max at WMTO	Sprunck	13.06
174	Min Glide angle	Sprunck	4.1 degrees
175	T/O distance at WMTO	Sprunck	15.4 ft
176			
177	SYSTEMS		
178	Landing gear type	Dunbar	tricycle
179	Main gear position	Dunbar	x=20 inches
180	Main gear length	Dunbar	4.5 inches
181	Main gear tire size	Dunbar	d=2 inches
182	nose/tail gear position	Anderson	x=4.5 inches
183	n/t gear length	Dunbar	5.5 inches
184	n/t gear tire size	Dunbar	d=2 inches
185	engine speed control	Dunbar	1
186	Control surfaces	Dunbar	3
187			
188	TECH DEMO		
189	Max Take-off Weight		
190	Empty Operating Weight		
191	Wing Area		
192	Hor. Tail Area		
193	Vert. Tail Area		
194	C. G. position at WMTO		
195	1/4 MAC position		

	A	B	C
196	static margin %MAC		
197	V takeoff		
198	Range max		
199	Airframe struc. weight		
200	Propulsion sys. weight		
201	Avionics weight		
202	Landing gear weight		
203			
204	ECONOMICS		
205	raw materials cost	Anderson	$120.00
206	propulsion system cost	Sprunck	$530.90
207	avionics system cost	Anderson	$430.00
208	production manhours	Anderson	$1,000.00
209	personnel costs	Dunbar	$1,000.00
210	tooling costs	Anderson	$150.00
211	total cost per aircraft	Dunbar	$2,185.00
212	Flight crew costs	Dunbar	$0.40
213	mantenance costs	Dunbar	$0.04
214	operation costs per flight	Dunbar	$0.44
215	current draw at cruise WMTO	Dunbar	$5.81
216	flight time-design Range max	Dunbar	0.079 hrs
217	DOC	Dunbar	$4.09
218	CPSPK	Dunbar	$0.42

Nomenclature

a	3-D lift curve slope
a_0	2-D lift curve slope
A_π	Component reference area
AR	Aspect ratio
C_{Di}	Induced drag coefficient for entire aircraft
C_{Do}	Aircraft parasite drag coefficient
C_{Dp}	Component parasite drag coefficient
cf/c	Flap chord to wing chord ratio
c.g.	Center of gravity location in percent of chord (measured from the leading edge)
C_L	Lift coefficient
$C_{L\alpha v}$	Vertical tail lift curve slope
$C_{L_{\alpha f}}$	Fuselage lift curve slope
$C_{L_{\alpha t}}$	Horizontal tail lift curve slope
$C_{L_{\alpha w}}$	Wing lift curve slope
$C_{l\beta}$	Lateral stability derivative
$C_{l\delta r}$	Roll control power due to the rudder
C_m	Pitching moment coefficient
C_{mac}	Pitching moment coefficient about the aerodynamic center
C_{m_α}	Pitching moment coefficient slope
$C_{m_{\alpha f}}$	Fuselage contribution to pitching moment coefficient slope
$C_{m\delta e}$	Change in pitching moment coefficient with elevator deflection
$C_{n\beta}$	Directional stability derivative
$C_{n\beta wf}$	Wing-fuselage contribution to directional stability derivative
$C_{n\delta r}$	Yaw moment coefficient due to rudder deflection
CPPPK	Cost per passenger per thousand feet
CPSPK	Cost per seat per thousand feet
$\frac{d\varepsilon}{d\alpha}$	Change in downwash with angle of attack
DOC	Direct operating cost
E	Aircraft Endurance
e	Aircraft Oswald efficiency
$e_{fuselage}$	Fuselage efficiency factor
e_{wing}	Wing efficiency factor
G	Acceleration of gravity
h	Altitude
L	Aircraft lift force
L/D	Aircraft lift to drag ratio
i_t	Tail incidence (measured from fuselage reference line)
l_t	Tail moment arm
R	Aicraft Range
SM	Static margin in percent of mean chord
S_e	Elevator area
S_H	Horizontal tail area
S_r	Rudder area
S_{ref}	Wing planform area
S_v	Vertical tail area

S_w	Wing area
S_{wet}	Aircraft component wetted area
t/c	Maximum thickness to chord ratio
V_{crs}	Cruise velocity of the aircraft
V_H	Horizontal tail volume ratio
V_{stall}	Stall Velocity
V_{TO}	Takeoff velocity
V_v	Vertical tail volume ratio
W	Total aircraft weight
W/S	Wing Loading
$\frac{X_{ac}}{\bar{c}}$	Aerodynamic center location in percent of mean chord (measured from leading edge)
$\frac{X_{np}}{\bar{c}}$	Neutral point location in percent of mean chord (measured from leading edge)
$\alpha_{L=0}$	Angle of attack at zero lift
α_{stall}	Angle of attack at stall with respect to the fuselage
β	Sideslip angle
δ_e	Elevator deflection
η	Propeller efficiency
η	Horizontal tail efficiency
η_v	Vertical tail efficiency
Γ	Dihedral angle
γ	Glide Angle
λ	Wing taper ratio
ρ	Freestream density at sea level
τ	Flap effectiveness parameter

A. DESIGN MISSION EVALUATION WITH REQUIREMENTS AND OBJECTIVES

A.1 - MISSION STATEMENT

RTL AERONAUTICS will set forth to design and manufacture an aircraft which will:

- use advanced design technology to enable service to a larger share of the current Aeroworld service market than the existing aircraft,
- achieve the aforementioned at a lesser cost to the airlines per seat per 1000 feet of flight,
- thus providing an optimal situation for the customers of Aeroworld through lower costs, better service, and increased comfort.

While providing this aircraft, designated the RTL-46 (Reason To Live-46), RTL Aeronautics will maintain the ethical standards from which the corporation was built.

A.2 - MARKET ANALYSIS

Based upon the market data and the distances between the airports of Aeroworld, the following market analysis was performed. Aeroworld is displayed in figure A-1, which shows the airport locations and their corresponding coordinates. With a distance of 500 feet between longitudinal and latitudinal increments, the actual distances were calculated between each airport. Then, along with the route distances and the flight demand of passengers per day, it was decided that although only 54 of the 105 routes in Aeroworld were under 10,000 feet in distance (slightly over 50%), over 70% of the total daily passenger demand was for these designated routes. Elimination of service to airports C and O (because of their short runway length) would result in a sizable 10% decrease in total passenger demand served. Therefore, with the extra 10% of

the passengers in mind, it was decided that the plane would attempt to take off in under twenty feet.

Figure A-1 - Aeroworld Airport Layout and Relative Distances

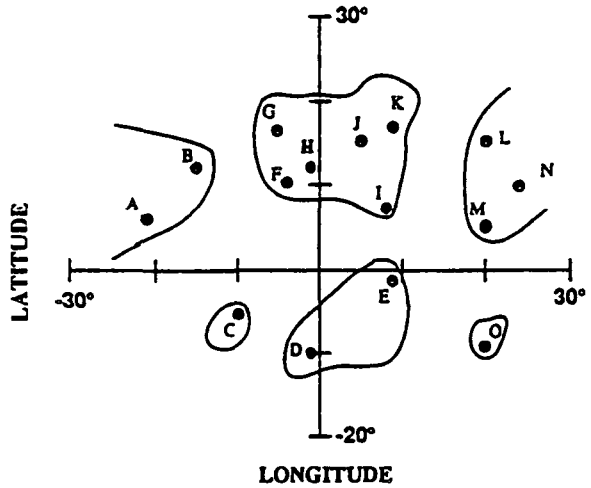

City	Longitude	Latitude	Runway Length Factor
A	-21	6	1
B	-15	12	0.8
C	-10	-5	0.6
D	-1	-10	1
E	9	-1	1
F	-4	10	1
G	-5	17	1
H	-1	12	1
I	8	7	1
J	5	15	1
K	9	17	1
L	20	15	1
M	20	5	1
N	24	10	1
O	20	-9	0.5

The market decision set the basis for sizing an aircraft which would best satisfy the proposed market focus. In order to do this, the number of flights per day had to be calculated so that the aircraft could maximize efficiency of service to the desired market. The number of flights per day was calculated using a relationship between the length of the flight and the necessary flights per day to

make the option of flying more beneficial than other modes of transportation. This relationship was provided in the Request for Proposals as:

$$\textbf{Flights per day} = \frac{30{,}000}{\textbf{Travel distance (ft)}}$$

This relationship shows that, the shorter the flight is, the more flights per day one must fly to gain that part of the market. This also means that there will be empty seats on some of the flights and in some markets, the number of flights per day will not satisfy the entire demand. Therefore the aircraft size analysis shown in Table A-1 shows the specific numbers for the unused seats per day of Aeroworld market. These numbers are calculated by taking the passenger data per route provided and then filling up the RTL-46 as many times as allowed (or needed) by the flights per day designated above. This process left some flights under booked, and these are shown as the per cent of excess seats.

Table A-1 - Passenger data for different RTL -46 sizing (10,000 ft range)

Passenger Capacity	65	75	85	95	105
Total Aeroworld Passengers	28,400	28,400	28,400	28,400	28,400
Target Market Passengers	20,145	20,145	20,145	20,145	20,145
Total Passengers Flown	13,985	15,390	16,920	17,525	18,465
% of All Passengers Flown	49.24	54.19	59.58	61.70	65.02
% of Market Passengers Flown	69.42	76.40	83.99	86.99	91.66
% Excess Seats	-13.11	1.97	13.50	22.61	29.98

As the aircraft size increased, the percent of the passengers being serviced on the flights that they desired increased, but that also meant that there would be more empty seats on the flights where the demand is not as high. Another consideration was that the cost per seat per thousand feet (CPSPK) of the aircraft

decreased as the number of seats was increased (as will be discussed in Chapter I). Therefore, it was decided that, although an increase in passenger capacity caused an increase in weight, this weight penalty was negligible when compared with gains achieved by a higher capacity. Thus, a capacity of 100 passengers was chosen in order to best serve the desired market.

A.3 - PERFORMANCE

The requirements set forth by the initial mission proposal consist of those values listed in table A-2. These values were restrictions based upon the physical characteristics of Aeroworld. For example, if the aircraft were unable to take off in under the 40 ft requirement, it will not be able to service any of the market of Aeroworld, thus rendering it useless.

From the requirements designated, the objectives became the selling points of the design, making the RTL-46 the design of choice over other new entrants into the market as well as existing aircraft. Initially, the takeoff distance of 32 feet was chosen for the RTL-46 to allow for service into airport B. With the introduction of flaps into the design to increase the maximum lift coefficient for

Table A-2 - Performance Requirements and Objectives

Performance Characteristic	Requirement	Initial Objective	Final Objective
Turn Radius	60 feet	N/A	N/A
Turn Velocity	25 feet/second	N/A	N/A
Loiter Time	2 minutes	2 minutes	2 minutes
Takeoff Distance	40 feet	32 feet	20 feet
Max Altitude	25 feet	N/A	N/A
Max Lifetime	50 hours (flight)	N/A	N/A
Max Range (Des)	N/A	10,000 feet	10,000 feet
Max Range (Total)	N/A	13,000 feet	13,000 feet
Takeoff Velocity	< 30 feet/second	22.5 feet/second	20 feet/second
Stall Velocity	< 25 feet/second	19 feet/second	16.7 feet/second
Endurance	N/A	6.2 minutes	6.2 minutes

takeoff (as will be discussed in Section C - Aerodynamics), the objective was modified to include airports C and O which have runway lengths of 24 and 20 feet, respectively.

The addition of flaps also allowed the designated takeoff velocity to be decreased from the initial objective of 22.5 feet per second to 20 feet per second. The initial objective was set to achieve a takeoff speed 10% slower than the required turn velocity. The modified objective was based on the use of flaps in the take off configuration. The required values for the takeoff speed and maximum stall speed were dictated by the turn velocity. That is, the stall velocity had to be lower than the turn velocity of 25 ft/s, and the takeoff velocity was calculated as 1.2 times the stall velocity - a conventional estimate.

Based upon the market analysis of section A.2, it was decided that the most competitive section of the market, the flights of 10,000 feet or less served such a large portion that they should be the ones emphasized in the design of the RTL-46. By allowing for a two minute loiter at 25 ft/s, an additional 3000 feet of range became necessary. Therefore the design range of the RTL -46 became 10,000 feet with a maximum range of 13,000 feet, including loiter.

A.4 - PASSENGER SERVICE

As a commercial transport aircraft, the RTL-46 must maintain a standard of service and comfort for the passengers on board. Each passenger in coach seating is required to have no less than 8 in^3 of space and each first class passenger is to have 12 in^3 of space. With these requirements in mind the objective of carrying 100 passengers as discussed in section A.2 was further quantified into a breakdown of 92 coach class seats and 8 first class seats on the aircraft in its basic seating configuration. The passengers would have access to

multiple lavatories, and a galley would be provided for the service of beverages and meals. Seating would be provided for the required maximum of 3 flight attendants required (one per forty passengers) on board the aircraft.

A.5 - PROPULSION

The required propulsion system will consist of an electric motor driven propeller system. The battery and motor system must be attached such that they can be removed and installed in twenty minutes or less. The objectives are set such that the aircraft will have a total flight endurance time of 6.2 minutes based upon the maximum range while cruising at the desired velocity of 35 ft/s.

A.6 - FLIGHT CONTROL SYSTEMS

It was required that the aircraft have no more than four servo motors, although an option was available for a fifth servo, which would be required when using both ailerons and flaps. The initial objective of the aircraft was to use the combination of rudder, ailerons, elevators, and the flaps along with the throttle control for a total of five controls for the aircraft. But, as the design progressed past the preliminary stage, this objective was modified to eliminate the ailerons and the rudder - wing dihedral combination was chosen to provide the roll control necessary for the aircraft. The elimination of ailerons will be discussed more fully in Chapter B.

A.7 - MANUFACTURING AND WEIGHTS

The aircraft must be able to be constructed in the allotted two week time frame. The construction of the aircraft will minimize disposal of parts due to the large expense incurred for the disposal. The design will also utilize the commonalty of parts thus allowing for similar materials to be used in various

parts of the aircraft. This system of part production not only reduces labor costs but increases accuracy. The final weight of the aircraft was initially set at under seven pounds, based upon the size of the RTL-46 with respect to its competitor, the current HB-40. After a preliminary, level zero weight build up, the maximum weight at takeoff was set at 5.5 lb - a much more realistic and beneficial value.

A.8 - SUMMARY OF REQUIREMENTS AND OBJECTIVES

A summary of the design requirements and objectives which will be achieved through the concept discussed in the following chapter are as follows:

- REQUIREMENTS
    - Takeoff distance of under 40 feet
    - 60 ft turn radius at 25 ft/sec velocity
    - 50 hour flight lifetime
    - 2 minute loiter capability beyond maximum range
    - 8 in3 per coach seat and 12 in3 per first class seat
    - Motor and battery removal in under 20 minutes
    - One flight attendant per 40 passengers
    - No more than four servo motors for control
- OBJECTIVES
    - Takeoff distance of 20 ft at 20 ft/sec
    - Cruise velocity of 35 ft/sec
    - 10,000 ft cruise range (13,000 with loiter)
    - 100 passengers (92 coach and 8 first class)
    - Maximum takeoff weight of 5.5 lb
    - Endurance of 6.2 minutes

A.9 - SUMMARY OF SELLING POINTS

A summary of the major selling points of the RTL-46 based upon these requirements and objectives is thus:

- Range serving approximately 70% of Aeroworld passenger demand
- Flap configuration allowing for take off and landing at all airports
- Faster cruise velocity than existing aircraft allowing for shorter flights
- Relatively simple and symmetric design for ease of construction
    - Lower cost of aircraft
    - Lower costs to consumers (than existing competition)
- First Class Seating
- Better ground handling qualities (more comfort to passengers)

B. CONCEPT FORMATION AND SELECTION

B.1 - INITIAL INDIVIDUAL CONCEPTS

The initial concepts submitted by the design group consisted of many similar design configurations for the proposed aircraft. All concepts were based upon a monoplane aircraft which included the use of throttle control, rudder and elevator servos to control the aircraft. Other aspects of the designs are listed in Table B-1. The vanilla designs lacked major advantages over the existing HB-40 outside of the size increase from the existing aircraft in the market. The proposed aircrafts would all satisfy the mission at hand, but they would not be marketable as achievers of the mission set forth in Chapter A. The only true selling points from the initial concepts were shown in Concept G which integrated the tricycle landing gear and ailerons for roll control. Sketches of the three main

Table B-1 Initial Concept Descriptions

Concept	J	G	C
Wing placement	High	Mid	High
Control Surfaces	Rudder Elevator	Rudder Elevator Aileron	Rudder Elevator
Number of Passengers	96	80	100
Deck Configuration	2 decks of 2 rows apiece	2 decks of 2 rows apiece	2 decks of 2 rows apiece
Landing Gear	Tail dragger	Tricycle	Tail dragger
Fuselage Shape	Square	Square	Rounded

group concepts are shown in figures B-1 through B-3. As can be shown by these concept descriptions, there lacked a major selling point (either performance or cost) to wrestle control of the market away from the Hot Box. This point led to the formation of the REASON TO LIVE concept (RTL-46) for the six design team members.

Figure B-1 - Concept J

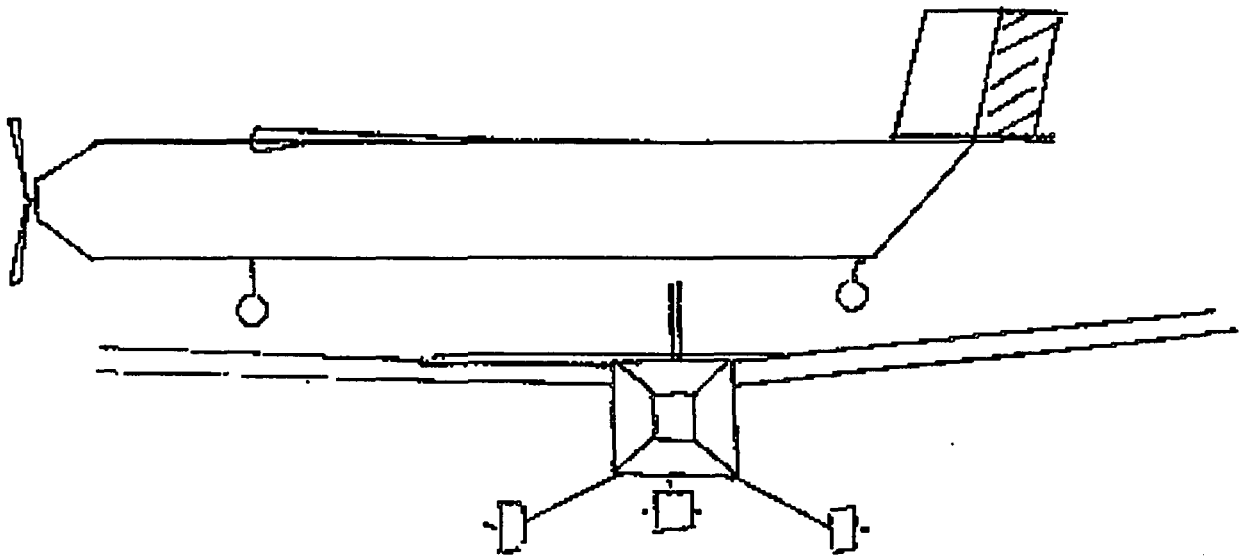

Figure B-2 - Concept G

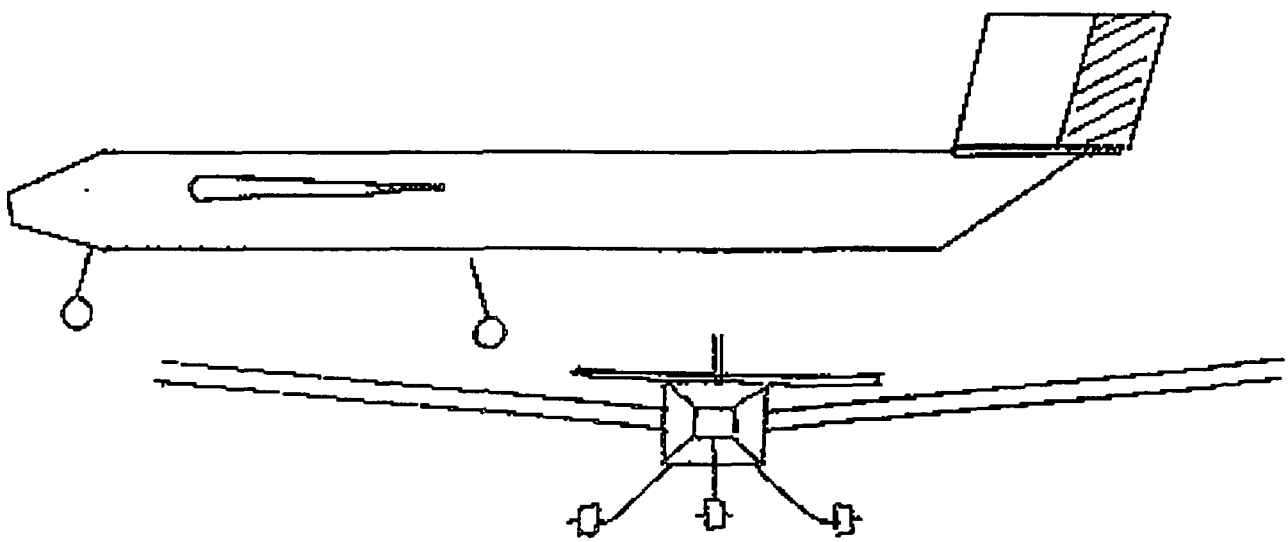

Figure B-3 - Concept C

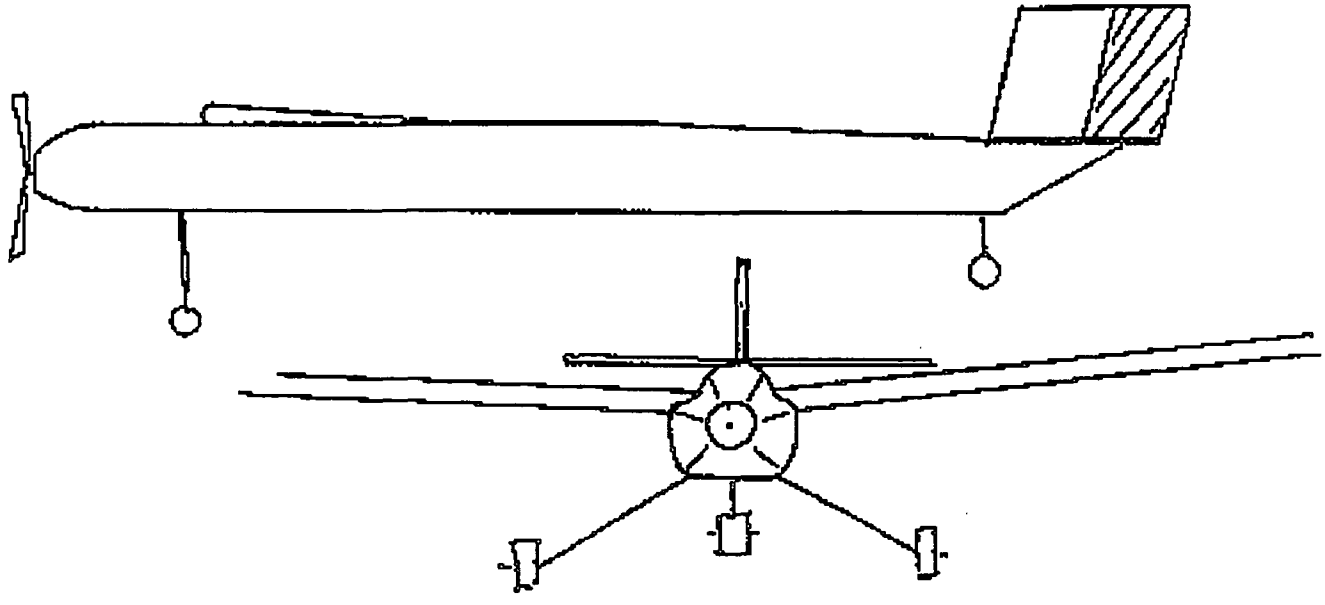

B.2 - THE RTL-46

The new concept formed around the idea of being able to reach the Aeroworld markets of airports C and O with the short runway lengths as discussed in Chapter A. Being able to reach this market involved integrating the idea of high lift devices to the aircraft wing. The original RTL-46 configuration included the use of flaps and ailerons along the wing as well as the rudder, elevators, and throttle control considered in the initial concepts. Although this configuration consisted of five servos, which exceeded the design limit of four, it was concluded that the particular design was feasible, if that what was decided. Also, a tricycle landing gear was chosen to bring about better handling qualities while on the ground, as Concept G had suggested. The RTL-46 first concept description can be seen in Table B-2.

The integration of flaps into the design provided the increased lifting potential required to achieve the necessary takeoff distance. The flaps, relatively simple in nature, do not cause a major addition to the work load in design and construction. The one main problem with the initial RTL-46 design arose when the idea of flaps and ailerons were integrated. The use of ailerons caused a reduction in flap sizing along the span thus bringing about either an increase in the percent of the chord, or an increased deflection angle (Chapter C). After discussing the concept with Reference [8] and analyzing the ability of the rudder-wing dihedral combination to compensate for the absence of ailerons for roll control, it was concluded that the flaps would

Table B-2 RTL-46 Concepts

Concept	Preliminary	Final
Wing Location	Low with dihedral	Low with dihedral
Tail Location	High fuselage mount with low mount horizontal tail	High fuselage mount with low mount horizontal tail
Control surfaces	Rudder, elevator, aileron, flaps (not full span)	Rudder, elevator, full span flaps
Number of Passengers	90 +/- 5	100(92 coach, 8 first class)
Deck Configuration	2 Decks of two columns	2 Decks of two columns of coach and third, lower deck, of first class
Landing Gear	Steerable tricycle	Steerable tricycle
Fuselage Shape	Slightly rounded	Square and tapered towards the nose and tail

be full span and that ailerons would be removed from the concept. This removal provided the more simplified design for the wing which lessens construction time and thus lower the cost of the aircraft. Along with the cost reduction, the removal of the ailerons leaves the aircraft within the required limit of four servo motors and eases the work load on the pilot flying the plane.

The tricycle landing gear, although more risky in the balancing of the aircraft weights for gear placement and the possible inability of rotation for takeoff if the gear is not placed correctly, the benefits outweighed the risks. The tricycle gear prevents the aircraft from going into ground loop during ground maneuvers, and it also provides better landing performance by not allowing the aircraft to tip, tumble forward nose down, into the propeller. Since the aircraft will spend the majority of its life on the ground between flights, the steerable landing gear provides the aircraft and its crew and passengers better quality ground handling and maneuverability in to and out of the gates. The landing gear configuration can be seen in figures B-4 and B-5.

Figure B-4 Front View of Final RTL-46 Configuration

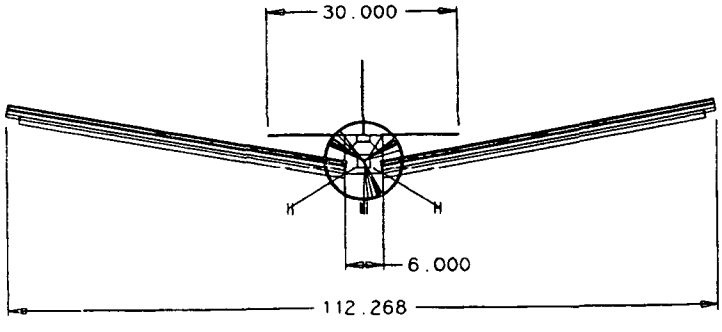

B.3 - FUSELAGE CONFIGURATION

The final fuselage configuration needed to be large enough to fly 100 passengers. This translated to a volume in excess of 1200 cubic inches. The reduction in pressure drag was also a great influence. Concepts were debated

Figure B-5 Side View of Final RTL-46 Configuration

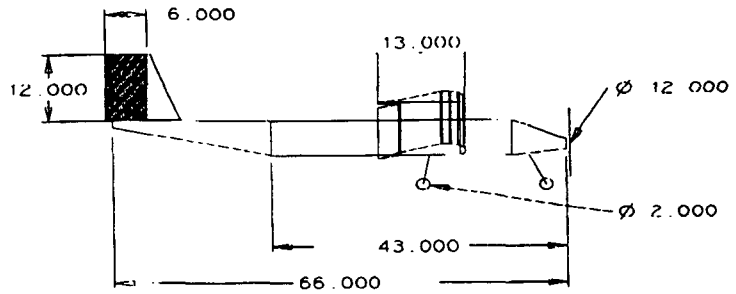

and evaluated and referenced. The current geometry (see figures B-6 and B-7) provides a gentle upsweep of the forward, nose section of the fuselage to present a more streamline body to the airflow and decrease frontal surface area which decrease the drag of the fuselage and actually cause a slight lifting surface because of the airfoil like shape. The taper and upsweep in the rear of the aircraft were designed to reduce the pressure drag associated with sharp edges at the aft end of bluff bodies. The upsweep also allows trailing vortices of the fuselage to not interfere with the tail lifting surface. The low-wing concept decreased interference as well as, in conjunction with the high tail, decreased trailing vortices interference of the wing onto the tail. These concepts will be discussed in detail in the Chapter C.

Figure B-6 Side View of RTL-46

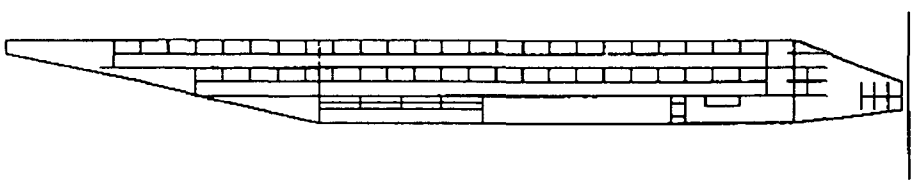

Figure B-7 Top View of RTL-46

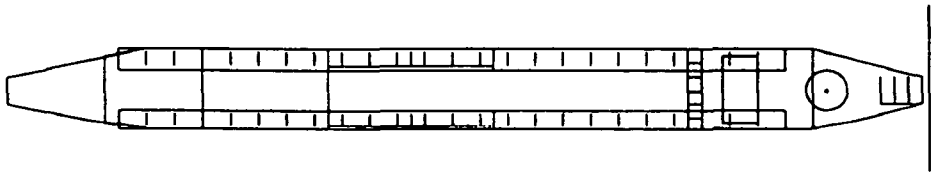

B.4 - INTERNAL LAYOUT AND CONFIGURATION

Internally, the RTL-46 consists of seating for 100 passengers in the arrangement listed in Table B-2. This three deck seating arrangement allows for separate areas for the first class passengers and the coach passengers. The first class seats are on the bottom deck and near the entrance to the aircraft. To get to the coach seating, a spiral staircase is used to climb to the upper levels. The galley is located in the front of the plane along with the seating for the flight attendants during takeoff and landing procedures. The lavatories are located in the rear. This configuration allows for symmetric weight balance about the centerline of the fuselage and the symmetry allows for ease in construction.

B.5 - SUMMARY OF CONCEPTS STRENGTHS AND WEAKNESSES

The following table lists some of the most important strengths and weaknesses of the major design aspects of the RTL-46. The four areas addressed are the major design drivers of the RTL-46 and the aircraft is designed to yield the strengths of all of these engineering concepts while minimizing or eliminating the effects of the associated weakness.

Table B-3 Major Concept Strengths and Weaknesses

CONCEPT	STRENGTHS	WEAKNESSES
Full Span Flaps	• Increased maximum lift • Lower stall velocity • Shorter takeoff and landing distances • More marketable aircraft	• Increased drag • Loss of aileron control • Increased construction complexity
Steerable Tricycle Landing Gear	• Better ground handling • Less chance for tumbling forward • Eliminates ground loop	• Incorrect placement effecting rotation for takeoff • increased servo connection complexity
Multiple Deck Aircraft	• Increased passenger potential • Better balance about centerline than if more columns of passengers • Smaller internal volume than single deck	• Multiple floors needed increases weight • Passenger access difficulty
Simple fuselage shape	• Shorter construction time • Less unused space than circular • Lower cost • Tapered fuselage decreases drag	• Circular has much lower C_{Do}

C. AERODYNAMICS

C.1 - OVERALL OBJECTIVES:

The overall objectives for the aerodynamic design of the RTL-46 aircraft include the need to provide sufficient lift during takeoff, cruise, and maneuver and the desire to minimize aircraft drag. High lift devices are included in the wing design to improve the aerodynamic performance of the aircraft to meet the design requirements and objectives of the proposal which emphasize the aircraft's competitiveness in the target market.

C.2 - AIRFOIL SELECTION:

The RTL-46 aircraft will operate in a low Reynold's number regime($1x10^5$ - $3x10^5$). The selection of the airfoil section was a significant part of the wing design. The parameters that drove this process were C_{lmax}, lift curve slope, C_d, airfoil thickness, and camber. Airfoil sketches and lift and drag curve data from Reference [15] were examined. Based on the criteria above, a set of four airfoils were chosen from the set in the Reference [15] for further analysis.

Table C-1 - Airfoil Characteristics:

Airfoil Type	C_{lmax}	C_{do}	t/c(%)	camber(%)	α_{stall}(deg)
Clark-Y	1.2	0.010	11.72	3.55	10
S3010	1.2	0.010	10.32	2.82	11
SD7062	1.5	0.011	13.98	3.97	14
Spica	1.4	0.012	13.53	3.75	14

The takeoff requirements imposed in the design requirements and objectives dictated that the chosen airfoil should have the highest C_{lmax} possible. This criteria, however, became less important with the addition of high lift devices in the design. A high stall angle was also desirable for more freedom in performance. Figure C-1 shows the 2-D lift curves for the airfoils listed above.

All the airfoil sections have only a small degree of camber for simplicity of construction. The thickness of the airfoil section became an important parameter because high lift devices were implemented in the wing design. Drag was a consideration because one of the aerodynamic design objectives was to minimize the drag of the aircraft. As shown in Reference [15], the SD7062 and S3010 airfoils had the lowest drag characteristics, of the four examined, over the entire range of Reynold's numbers that covered all regimes of flight.

Figure C-1 - Comparison of 2-D Lift Curve Slopes for 4 Airfoils

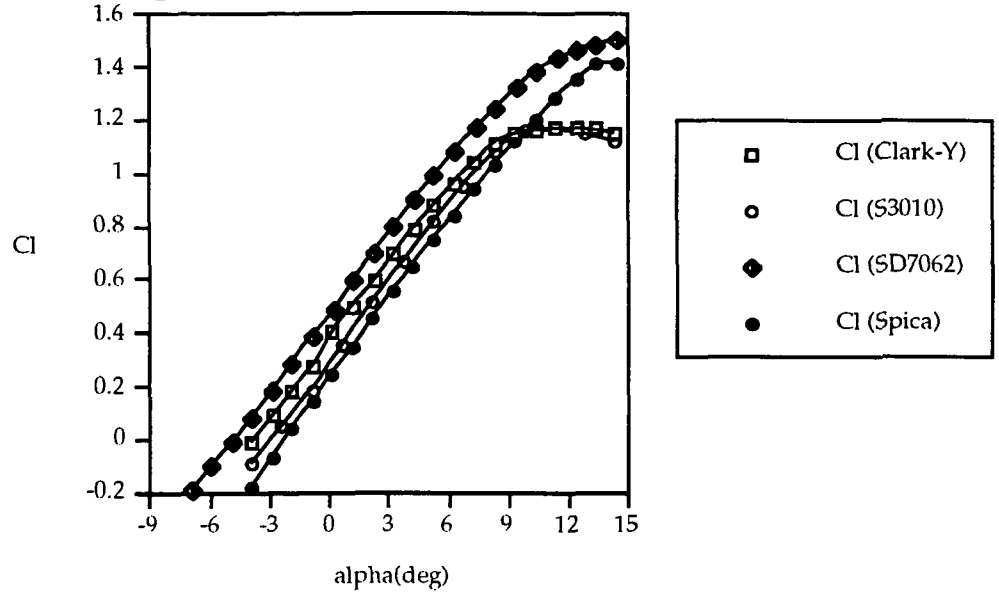

The SD7062 airfoil was selected because it had the best combination of characteristics. The SD7062 airfoil had the highest C_{lmax} of the set, which was deemed an important precaution in the event of failure of the flaps, a high stall angle, and desirable drag characteristics. Manufacture of the airfoil also played a role in the selection. The SD7062 airfoil, as shown in Figure C-2, had a small amount of camber which will not significantly hinder the effectiveness of the monokote covering at keeping the airfoil shape along the wing span. It had the largest maximum thickness of the set which will aid in flap construction. In particular, it will affect the size of cut for flap attachment. The SD7062 airfoil characteristics are given below.

Figure C-2 - SD7062 Airfoil

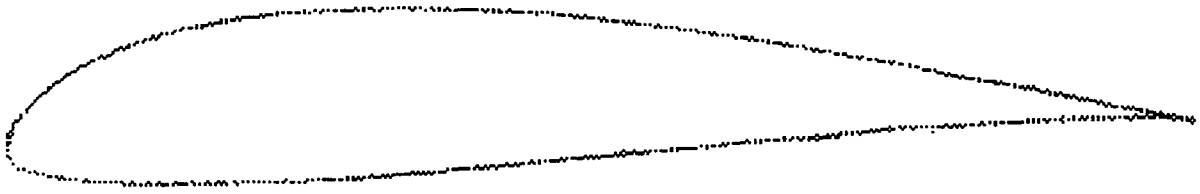

thickness = 13.98%
camber = 3.97%
Cl_{max} = 1.5
α_{stall} = 14 degrees
$\alpha_{L=0}$ = -2.5 degrees

The SD7062 airfoil is shaped to produce lift. By using a flap, the camber of the airfoil is changed which results in a change in its lifting characteristics. Design of the flaps will be discussed in the next section. The addition of a flap with a 0.25 flap chord to wing chord ratio deflected at twenty degrees shifted the 2-D airfoil lift curve upward by 1.16 and the maximum lift coefficient of the airfoil was increased by 0.63, as shown in Figure C-4. These values were calculated using the methods concerning airfoil lift with and without flaps in Appendix 2. Thus, the addition of flaps caused a 72% increase in the lift of the airfoil which is a significant improvement. The stall angle at which maximum lift occurred was estimated because the relation used to correct the lift curve slope for wing aspect ratio, which is given below, was only valid for the linear portion of the curve.

$$a = \frac{a_0}{1 + \frac{a_0}{\pi AR e}}$$

However, with knowledge of the change in maximum lift coefficient gained from the relations in Reference [14], it was observed that deflection of flaps decreased the airfoil stall angle. This is a drawback associated with the use of flaps.

However, with the large increase in lift that flap deflection produces at lower angles of attack, this is a small penalty to incur.

C.3 - WING DESIGN:

The decision to design a rectangular wing without aerodynamic twist, taper, or sweep was driven by simplicity of design and construction, as well as the desire to implement high lift devices in the wing design. The wing sizing was driven by the aircraft takeoff performance, in particular the minimum takeoff distance requirement of twenty feet. To meet this requirement, the takeoff speed was set initially at 22 ft/s. The takeoff speed is defined as $1.2V_{stall}$. Thus, the stall speed was estimated as $V_{takeoff}$ / 1.2 which gave it a value of 18.3 ft/s. The wing loading, which is defined below as the total aircraft weight per unit wing area, was used to size the wing. A maximum lift coefficient was estimated to be between 1.2 and 1.4, which would be obtained with flaps deflected. At an initial estimated maximum aircraft takeoff weight of 5.5 lbs, which was obtained by scaling the HB-40 aircraft weight up to account for the increase in fuselage size of the RTL-46, a wing planform area range from 9.87 ft^2 to 11.5 ft^2 was obtained.

$$\frac{W}{S} = \frac{1}{2}\rho V_{stall}^2 C_{Lmax} \qquad S = \frac{W}{\frac{1}{2}\rho V_{stall}^2 C_{Lmax}}$$

Thus, the range of wing loading values obtained were from 0.478 lbs/ft^2 to 0.577 lbs/ft^2. For the final wing design, the wing chord was set at 13 inches to give the wing the necessary thickness and chord length for flap construction, as well as to give it a large aspect ratio. With the chord set, the range of values for the span were between 9.11 ft and 10.6 ft. The values for the wing aspect ratio were ranged from 8.4 to 9.8. As shown in Figure C-3, for aspect ratios of seven and above, only a small decrease in lift curve slope occurs. Thus, the smallest wing span that fell within the design range was selected to minimize wing weight and

construction. A wing with a larger span would need a stronger carry through structure which would also increase the aircraft weight. The final wing design has a 9.93 ft^2 wing planform area with a 13 inch chord and a 9.17 ft span giving a wing aspect ratio of 8.46.

Figure C-3- The Effect of Aspect Ratio on Airfoil Lift Curve Slope

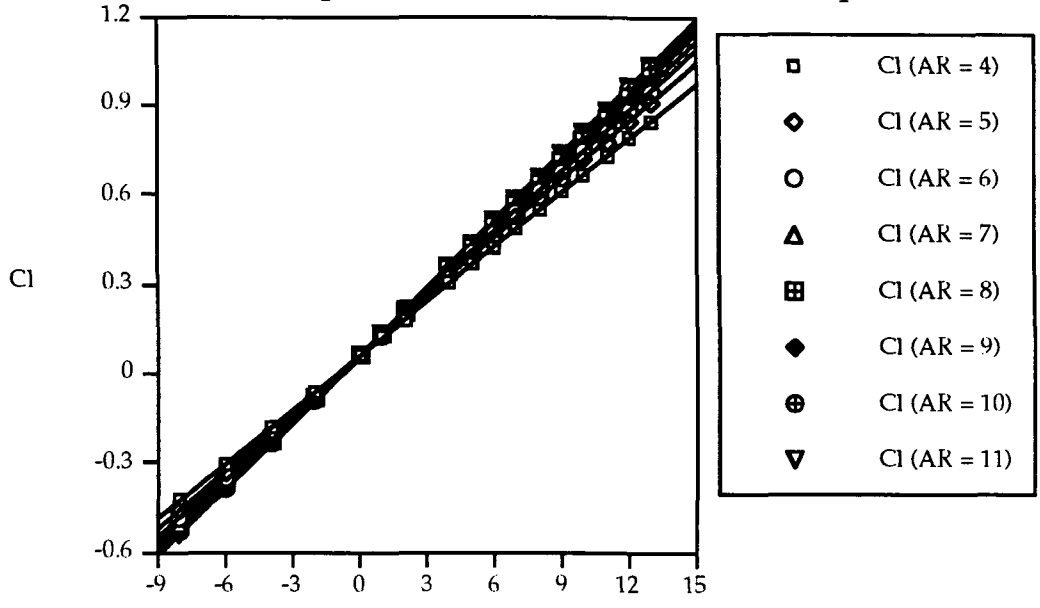

The decision for the use of high lift devices was driven by the desire to meet the needs of all the customers of the Aeroworld market that was targeted. This meant setting the takeoff distance requirement to twenty feet. In order to meet this requirement the aircraft needed considerable lift for takeoff. The first wing design concept included both ailerons and flaps. However, taking into consideration construction and weight penalties, as well as increased difficulty in aircraft control for the pilot associated with this design, the concept was changed to full span flaps excluding ailerons. These flaps run the full span of the wing because this is the easiest flap configuration to integrate in the wing design. An analysis was conducted, as outlined in Appendix 2, to determine the optimum flap size in percent chord. Figure C-4 shows that a range of flap chord to wing

chord ratio, cf/c, values of 0.15 to 0.25 will produce comparable lifting characteristics. The final flap design was set at 0.25 cf/c because this would produce the largest cut for flap construction. When deflected a maximum of twenty degrees, the flaps increase the camber of the wing and improve the aircraft lift by approximately 67%. The stall angle of the aircraft is decreased by approximately 20 % due to flap deflection. This penalty is outweighed by the significant increase in lift at lower angles of attack.

Figure C-4 - Wing Lift Curve as a Function of Flap Size for a Twenty degree Flap Deflection:

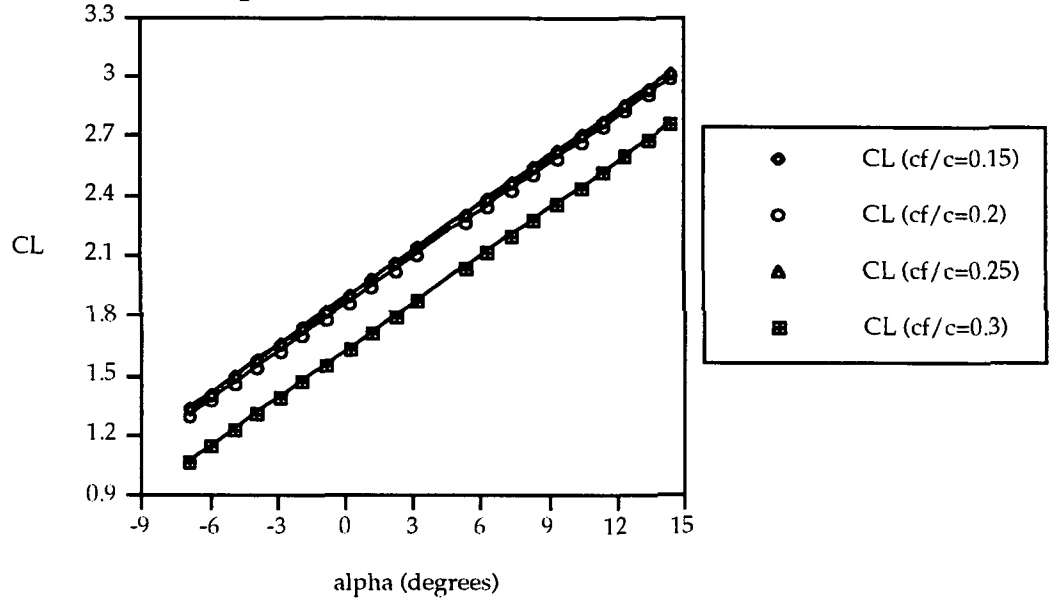

Dihedral was included in the wing design to provide roll control along with the rudder, in place of ailerons. A ten degree dihedral angle was set for stability and control purposes as explained in Chapter F. The wing with and without dihedral was modeled in an aerodynamics software program, Reference [6] to obtain its lifting characteristics. From these results it was found that this amount of dihedral decreases the lift coefficient of the wing by approximately 2% for both wing configurations, with and without flaps deflected. This is an insignificant consequence in comparison to the desirable affects obtained for aircraft control. The stall angle of the wing was increased by approximately 5%

for both wing configurations and the wing stalled near the root both with and without dihedral.

The lift curve for the SD7062 airfoil corrected for an aspect ratio of 8.46 is shown in Figure C-5. The stall region was estimated because the correction for the lift curve slope was based on the constant slope of the 2-D airfoil lift curve data. Table C-2 gives the final design parameters for the RTL-46 aircraft wing.

Table C-2 - Wing Parameters:

Planform area, S	9.93 ft^2
Aspect Ratio, AR	8.46
Wing Span, b	9.17 ft
Mean Chord, c	13.0 inches
Airfoil Section	SD7062
Taper Ratio	1
Twist	none
Sweep	none
Incidence Angle	1.5 degrees
Dihedral	10 degrees
Cruise CL	0.34
Flap Size, cf/c	0.25
Maximum Deflection	20 degrees

Figure C-4 - Lift Curve for the SD7062 Airfoil With and Without Flap Deflection of Twenty Degrees (AR = 8.46):

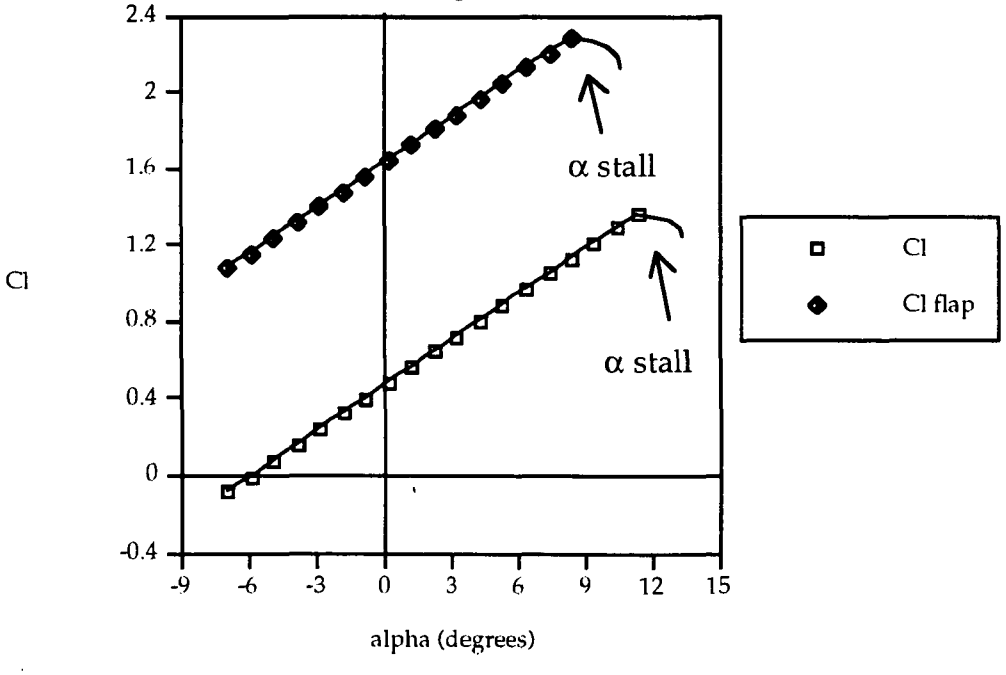

C-4 AIRCRAFT DRAG:

Drag is an important parameter which affects the design and performance of the aircraft. It gives a direct indication of the power required for flight, which drives the selection of the propulsion system and the propeller. This in turn is used to develop the range and endurance of the aircraft which are important considerations for the marketability of the aircraft.

Drag Prediction:

An initial aircraft drag prediction was made using Method 1 from Reference [5]. A two parameter drag polar was obtained in the form given below, where C_{Do} is the aircraft parasite drag and C_{Di} is the aircraft induced drag due to lift.

$$C_D = C_{Do} + C_{Di}$$

$$C_{Di} = \frac{C_L^2}{\pi A R e}$$

$$C_{Do} = 0.0055 \frac{S_{wet}}{S_{ref}}$$

The parasite drag calculation was dependent upon an estimated skin friction coefficient, C_f, of 0.0055 and the wetted area of the aircraft. Thus, by decreasing the surface area of the aircraft components, the parasite drag could be decreased. The aircraft Oswald efficiency factor of 0.73 was developed using the relation below. A wing efficiency of 0.79 and a fuselage efficiency of 19.9 were developed using the figures from Reference [12] for a rectangular configuration.

$$\frac{1}{e} = \frac{1}{e_{wing}} + \frac{1}{e_{fuselage}} + \frac{1}{e_{other}}$$

$$e_{fuselage} = \frac{E_{fuselage} S_{wing}}{S_{fuselage}}$$

This method did not take the drag due to the landing gear into consideration so 0.005 was added to the total parasite drag component. The value for the landing gear CDo was obtained from an estimation of the landing gear surface area and

the drag coefficient factors set in Reference [4]. The drag polar equation from this method was $0.0235 + 0.0514\,C_L^2$.

A second method used for aircraft drag estimation was taken from Reference [12]. The induced drag component calculations remained the same. The parasite drag component was obtained from the relation below.

$$C_{Do} = \frac{\Sigma C_{D\pi} A_\pi}{S_{ref}}$$

The values for A_π were defined and the values for $C_{D\pi}$ were given for each component in Reference [12], except the $C_{D\pi}$ for the landing gear which was taken from Reference [4] which gave a detailed description of all possible types. An additional 20% was included in the calculations to account for interference and roughness. Table C-3 shows the values for $C_{D\pi}$, the reference areas, and the percentage of the total drag for each aircraft component.

Table C-3 - Drag Breakdown:

Component	$C_{D\pi}$	A_π	% of total drag
Fuselage- frontal area component	0.11	0.25	
Fuselage- surface area component	0.0033	9.223	
Fuselage- total %			29
Front landing gear	0.25	0.0348	4
Back landing gear	0.5	0.0919	24
Wing	0.007	9.93	35
Horizontal tail	0.008	1.458	5
Vertical tail	0.008	0.729	3
Interference	20%		

The parasite drag for the fuselage was calculated as a sum of the skin friction drag due to the total surface area, as set down in Method III of Reference [5] and the drag produced by the fuselage cross-sectional area modeled as a flat plate, as set down in Reference [12]. The results from this method gave an aircraft parasite drag coefficient value of 0.0247. This value was used for the final design

drag polar because the second method was more accurate than the first. Thus, the final equation was $0.0247 + 0.0514C_L^2$ for the RTL-46 aircraft drag polar, which is shown in Figure C-6. The drag polar for flaps deflected twenty degrees was also obtained. A factor of 0.045 was added to the parasite drag component of the flaps up drag polar to account for the effects of flaps, as suggested in the drag analysis section of Reference [14]. The high lift gained from the flaps also increased the induced drag component of the drag polar. The deflection of flaps made the aircraft dirty and increased the aircraft drag by approximately 65%. This increase is acceptable because of the large increase in lift that is gained by flap deflection.

This drag prediction is only an estimate because many factors need to be included in the drag buildup which have not been sufficiently examined at low Reynold's numbers. The optimal verification of these calculations would be wind tunnel testing of the components. However, the facilities are not available. There is also the immediate effects of the propeller flow on the fuselage which may increase the drag significantly.

The cruise condition was examined to minimize aircraft drag. The cruise speed was set at 35 ft/s which dictated an aircraft lift coefficient of 0.34 for this regime. Thus, 80% of the drag produced by the aircraft in cruise will be parasite drag. Some changes were made in the structural design to reduce this component. A large percentage of the parasite drag initially was attributed to the fuselage because it was a bluff body with a large surface area. Thus, the nose was rounded and the body was tapered upward toward the tail to minimize drag. Another idea was to round the edges of the fuselage cross-section. However, no easy way has been found to implement this idea in construction. The cross sectional area was designed as compact as possible to limit bluff body drag, taking into account the limits on total aircraft length and still meeting the

passenger requirement. The horizontal and vertical tail surfaces were tapered to minimize drag.

Figure C-6 - Aircraft Drag Polar

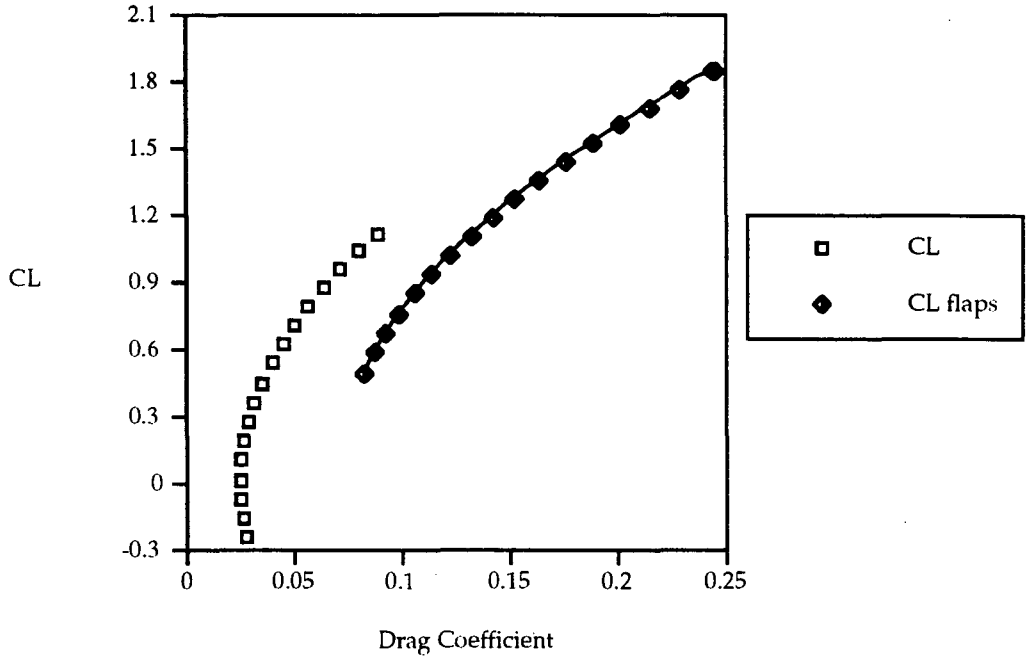

C.5 - Aerodynamic Summary:

The major aircraft lifting characteristics which include CL_{max}, lift curve slope, and α_{stall} were obtained by modeling the aircraft in an aerodynamics program, Reference [6]. This program used lifting line theory to develop the total forces on the aircraft. The wing was modeled after the mean camber line of the SD7062 airfoil section and the fuselage and horizontal tail were modeled as flat plates. Figure C-6 shows the LinAir model of the RTL-46.

Figure C-7 - LinAir Model of RTL-46 Aircraft

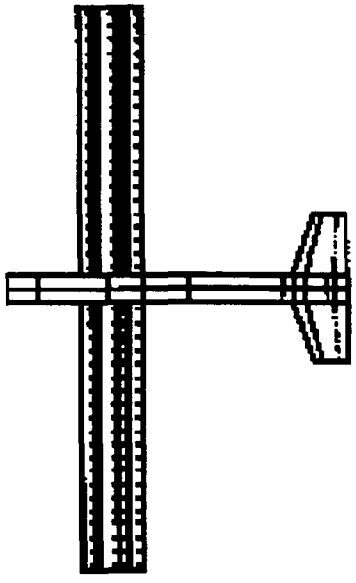

The stall angle of the RTL-46 was calculated for both the flaps up and the flaps down configurations by analyzing the lift distribution of the wing elements in LinAir. When the lift coefficient exceeded the SD7062 airfoil section C_{lmax} for flaps up and flaps down, the aircraft was considered stalled. The stall angle and lift characteristics of the RTL-46 were obtained from the program results. Thus, the stall angle for the flaps up configuration was 9.8 degrees and for flaps deflected twenty degrees it was 8.1 degrees. At these angles of attack, the aircraft attained its C_{Lmax} which was equal to 1.1 for flaps up and 1.8 for flaps down. The lift curve slope of the aircraft was obtained by plotting the lift coefficients calculated at various aircraft angles of attack as shown in Figure C-8. The RTL-46 lift curve slope was equal to 4.87/rad.

The value for L/D_{max} was obtained using the aircraft drag polar and knowing that the parasite drag is equal to induced drag at this point.

$$CD = 0.0247 + 0.0514CL^2$$

$$CL \text{ at } L/D_{max} = 0.693$$

$$CD \text{ at } L/D_{max} = 0.0494$$

Therefore, L/D_{max} was equal to 14 at an angle of attack of 5 degrees, as indicated in Figure C-9. The design cruise speed was set at 35 ft/s to decrease flight time and thus be competitive in the targeted market. An aircraft lift coefficient of 0.34 is necessary to achieve this speed at cruise conditions which produces a drag coefficient of 0.031 and gives an L/D of 11. It was acknowledged that the desired condition for cruise is to fly as close to L/D_{max} as possible for optimum performance. However, cost was also taken into consideration in the analysis of the aircraft and it was deemed more important to increase the cruise speed and significantly decrease the cost per seat per thousand feet which will decrease the direct operating cost of the aircraft. This will help in achieving the design objective of minimizing the overall cost of the aircraft, as will be discussed in Chapter I. The penalty incurred by this decision is that the aircraft will cruise at an L/D approximately 30% lower than L/D_{max}. This translates to an increase in drag at cruise and less than optimal conditions for the aircraft flight.

Figure C-8 - Aircraft Lift Curve With and Without High Lift Device Deflection of Twenty Degrees:

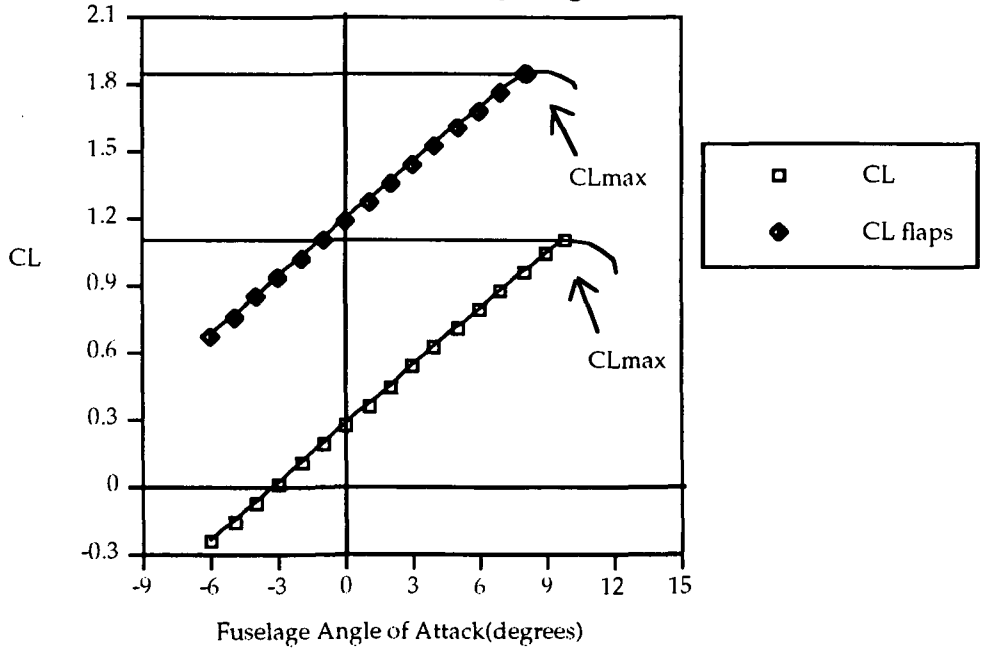

Figure C- 9 - Aircraft Lift to Drag Ratio Curve

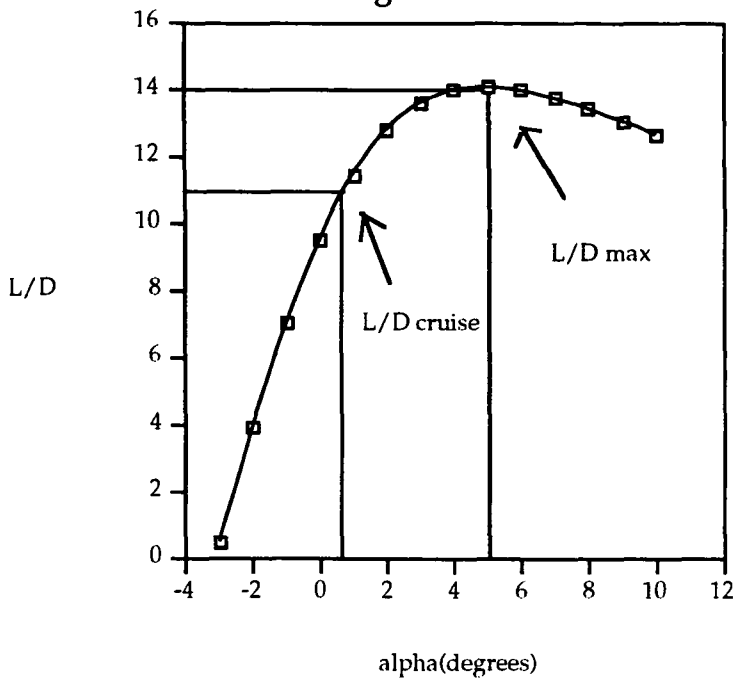

The aerodynamic design of the RTL-46 aircraft was driven by performance, weight, and construction. The SD7062 airfoil has sufficient aerodynamic characteristics and will aid in wing manufacture. The wing design is simple and should be conducive to flap construction. The most critical technology of the RTL-46 aircraft is the integration of flaps in the wing design. When deflected, they will allow the aircraft to achieve the minimum takeoff distance requirement. The lift to drag ratio is an indication of the aircraft performance. The maximum lift to drag ratio of the RTL-46 aircraft exceeds that of the HB-40 aircraft by approximately 17%. Thus, the RTL-46 aircraft will be competitive in the Aeroworld market.

D. PROPULSION SYSTEM DESIGN DETAIL

D.1 - GENERAL OVERVIEW

The propulsion system consists of three important and interconnected elements:

- The propeller
- The motor
- The fuel (i.e., the batteries - their number and capacity)

A wide selection in each of these areas was made available, so the selection of the ideal system for the RTL-46 was an intricate process involving many factors. These factors were limited by the issues discussed in the Design Requirements and Objectives. These limits are presented in Table D-1:

Table D-1 - Propulsion Requirements and Objectives

Takeoff Distance	≤ 20 ft with flaps; ≤32 feet without flaps
Takeoff Velocity	≤ 22.5 ft/s
Cruise Velocity	= 35 ft/s
Range	≤ 13,000
Installation/Removal Time	≤ 20 minutes

D.2 - SYSTEM SELECTION AND PERFORMANCE PREDICTIONS

The takeoff distance requirement depended on the weight of the aircraft, the power of the motor (governed by the motor type and battery pack voltage) and the propeller selection. Here, a higher battery pack voltage led to a shorter takeoff distance and an increased weight. A higher propeller diameter and pitch caused a decrease in takeoff distance and an increase in weight. Finally, as the motor size was increased, the power increased (leading to a shorter distance), but the motor, and thus, aircraft, weight also increased. The range requirement

depended on the battery capacity and total voltage. As the battery capacity increased, the range of the aircraft increased.

Based on the data base values of takeoff distance for previous aircraft, it was decided that the takeoff distance requirement of 20 feet was more restrictive than the cruise performance requirements, so the takeoff performance of the different motors was analyzed first. Initially, six Astro Cobalt motors, ranging from model 035 to 40, were considered. The Astro 035 motor was eliminated because its power ratings for a range of input current values were between 20 and 25% lower than the power values for the same current range of the Astro 05 - the next more powerful motor. By examining power values and motor selections of previous aircraft, it was decided that the power values of the Astro 035 were too low for the weight range of the RTL-46.

Motor/battery system weights for the motors with model numbers over 25 were found to be over 2.0 pounds. The database showed that motor/battery systems that weighed under 2.0 pounds would still be able to provide the power requirements needed for an aircraft weight in the area of 5 pounds. Therefore, the Astro 25 and 40 models were eliminated because their increased power did not justify the large weight penalty associated with those models.

The Astro 05, 05 FAI and 15 models were selected for more detailed analysis. Each of these motors was analyzed with its suggested battery voltage and, in order to isolate motor performance from dependence on propeller size, each of the three motors was analyzed using the same Zinger 12-6 propeller data. By using the Takeoff Performance Fortran program (References [1]), it was found that each of the three motors was capable of the 20 ft takeoff, depending on the battery voltage used. This program listing and a brief explanation of its input, output and iteration method may be found in Appendix 3. The Astro 15 had the highest required voltage for a 20 foot takeoff, but the lowest takeoff

battery drain. This motor also produced the longest takeoff ground roll distance of the three motors. The takeoff performances for the Astro 05 and the FAI 05 were nearly identical to each other. The weights of the Astro 05 and the FAI 05 motors were lower than that for the Astro 15 (by 1.0 ounce) and had the best takeoff performance. Thus, it appeared that the Astro 15 motor should have been eliminated.

However, the cruise performance of each of these motors (in combination with the Zinger 12-6 propeller) was also analyzed using Reference [3] (see also, Appendix 3 - Cruise Performance Spreadsheet). It was found that the Astro 05 and FAI 05 motors required such high current draw values that extremely heavy and costly batteries would be required to provide the battery capacity necessary to meet the range requirement 13,000 ft. The total weights and total costs of the three battery systems were compared to provide the combination that would minimize both cost and weight (see table D-2).

Table D-2 - Motor/Battery System Weights and Costs

	Astro 05	Astro 05 FAI	Astro 15
#Batteries & Weight	8X1400 mah = 13.6 oz	8X1400 mah = 13.6 oz	12X900 mah = 14.8 oz
Motor Weight	6.5 ounces	6.5 ounces	7.5 ounces
Total Weight	20.1 ounces	20.1 ounces	22.3 ounces
Battery Cost	$ 64.00	$ 64.00	$ 36.00
Motor Cost	$ 109.95	$ 99.95	$ 124.95
Total Cost	$ 173.95	$ 163.95	$ 160.95
Cost/Weight Ratio	$ 8.65/ounce	$ 8.1/ounce	$ 7.2/ounce

As this table shows, the Astro 15 motor/battery system, while having the highest weight, had the lowest purchase cost and the lowest cost-to-weight ratio. It was decided that the 2.2 ounce weight penalty associated with the Astro 15

system was acceptable for the savings in purchase cost of the system. Therefore, the Astro 15 motor and twelve 900 mah batteries were selected.

D.3 - PROPELLER DESIGN

Many propellers were analyzed for use with the Astro 15 motor, ranging from diameters between 10 and 14 inches and pitch values between 4 and 6 inches. As in the motor selection, the takeoff objective of 20 feet was the driving factor in selection of a propeller. A propeller performance program (Reference [17]) was used in order to find the propeller characteristics in flight for different flight velocities and propeller RPM values. This program used simple blade element theory and included the effects of induced velocity and tip losses in order to calculate thrust, power, and efficiency values for various advance ratios. Input data such as thickness, chord and blade angle values at different radial positions was required. This data was obtained by direct measurement in some cases and, in other cases, from the database of propeller sizes (reference [13]; see Appendix 3 for listing of that database).

By using the output from this program in conjunction with the takeoff performance program , it was found that the propellers with diameters under 12 inches could not takeoff in fewer than 20 feet, so those propellers were eliminated. It was also found, from a cruise analysis using Reference [3], that the propellers with higher pitch operated at higher efficiencies. Of the propellers with diameters greater than 12 inches and pitch values of 6 inches, this left the Zinger 12-6, 12.5-6, 13-6, 13.5-6 and the 14-6 propellers (see Figure D-1 for the propeller performance comparison). The propellers with non-integer diameters would be manufactured by cutting one half inch from the tips of the larger propeller. For example, the 12.5-6 propeller would be created by cutting 0.25 inches from the tip of each of the blades of a 13-6 propeller.

Because a range of total aircraft weight was being considered (4.9 lbs to 5.5 lbs), the takeoff and cruise performance of each of these propellers was calculated at each weight extreme. The Zinger 12-6 propeller was unable to meet the 20 foot requirement for the maximum of 5.5 pounds, so it was eliminated from consideration. The Zinger 13.5-6 propeller was eliminated because it produced the shortest range. This left the 12.5-6, 13-6 and 14-6 as possible selections. Because large diameter propellers require larger (and thus, heavier) landing gear to achieve the necessary ground clearance, the 14-6 propeller was eliminated. Finally, the 13-6 propeller was eliminated because its weight and battery drain at takeoff were higher than those of the 12.5-6 propeller. Thus, the 12.5-6 propeller was selected for use with the Astro 15 motor.

Figure D-1 - Propeller Comparison

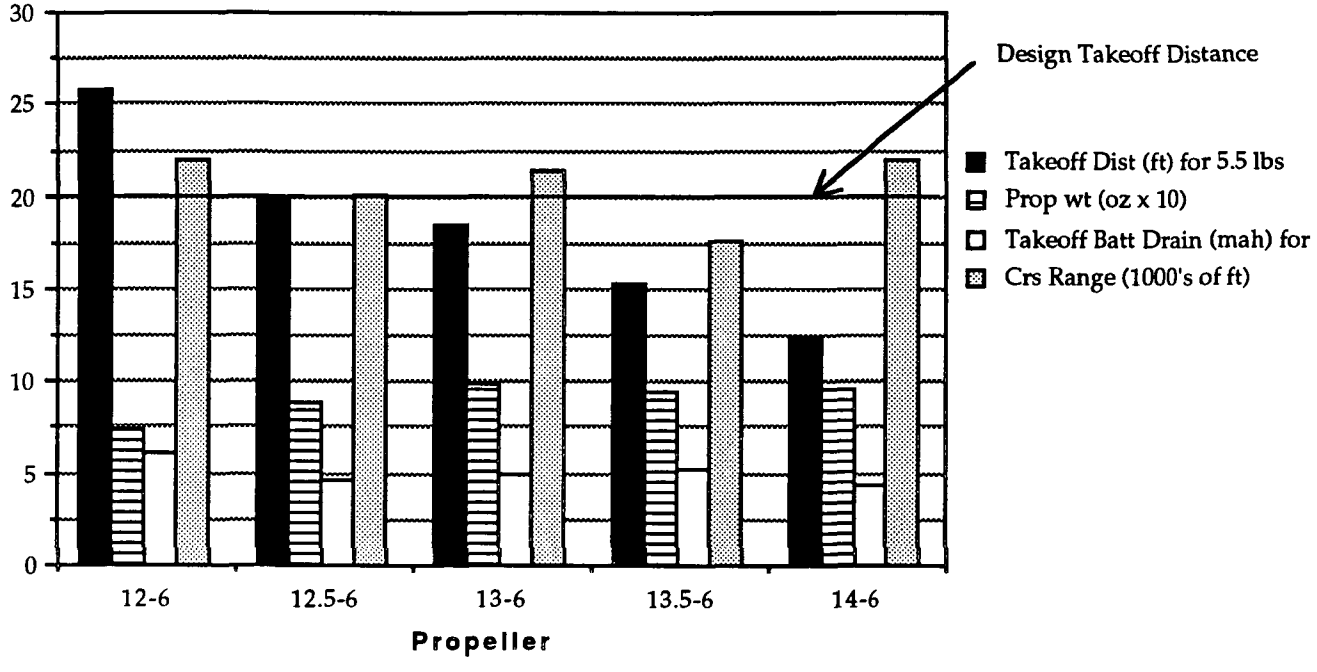

In order to validate the propeller choice, the performance values of propeller efficiency, thrust coefficient, and power coefficient were analyzed. This was done with the aid of Reference [17]. Performance graphs of the 12.5-6 propeller, as compared to the other propellers, are provided in Figures D-2

through D-5. Figure D-2 shows that, of the five propellers, the 12.5-6 propeller had the second highest values of efficiency. The 12-6 propeller operated at the highest efficiencies, but, as stated above, the 12-6 propeller was not able to meet all of the takeoff distance requirements, so the next best choice was the 12.5-6 propeller. As shown on the graph, the cruise propeller efficiency was 68%, which is within 1.4% of the value of maximum propeller efficiency, 69%.

Figure D-2 - Propeller Efficiencies vs Advance Ratio

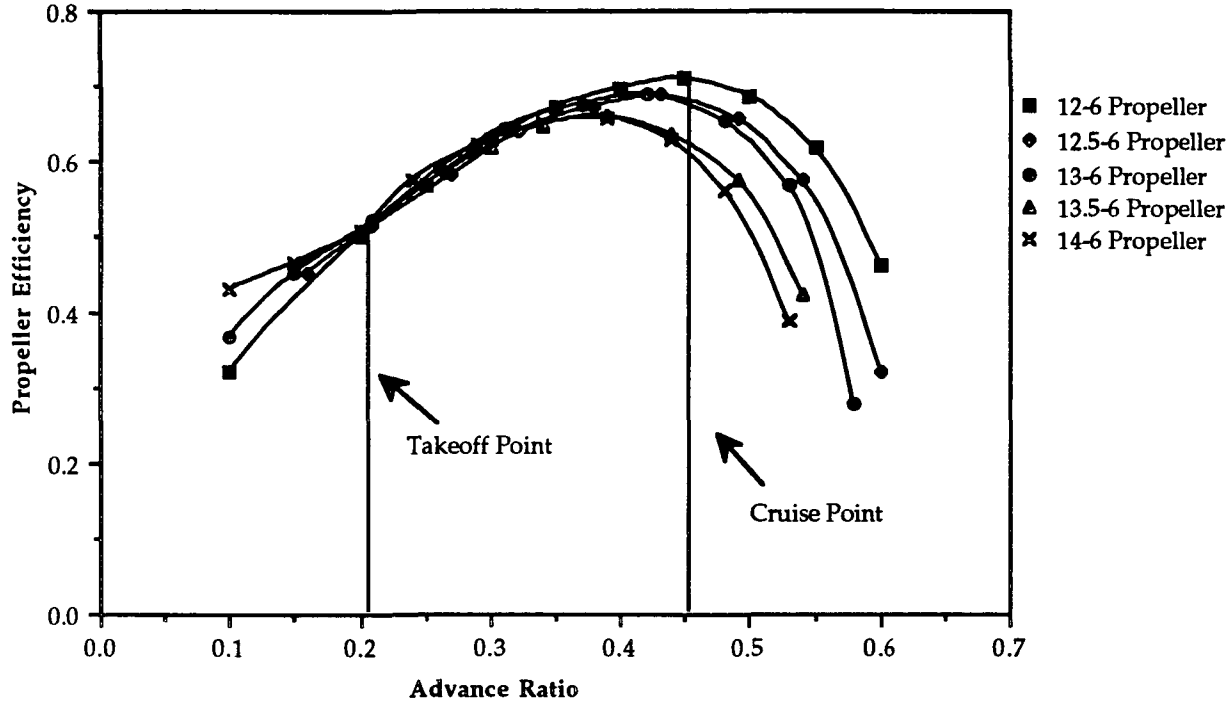

Figure D-3 shows the thrust coefficient curves for each of the propellers. The 12.5-6 propeller produced the most consistently high power for the range of advance ratios considered. At takeoff, the 13.5-6 propeller did have a higher thrust coefficient, but that value quickly dropped off until it had the second lowest thrust coefficient at the cruise condition. Therefore, the 12.5-6 propeller had the most advantageous thrust coefficient characteristics.

Figure D-3 - Propeller Thrust Coefficient vs. Advance Ratio

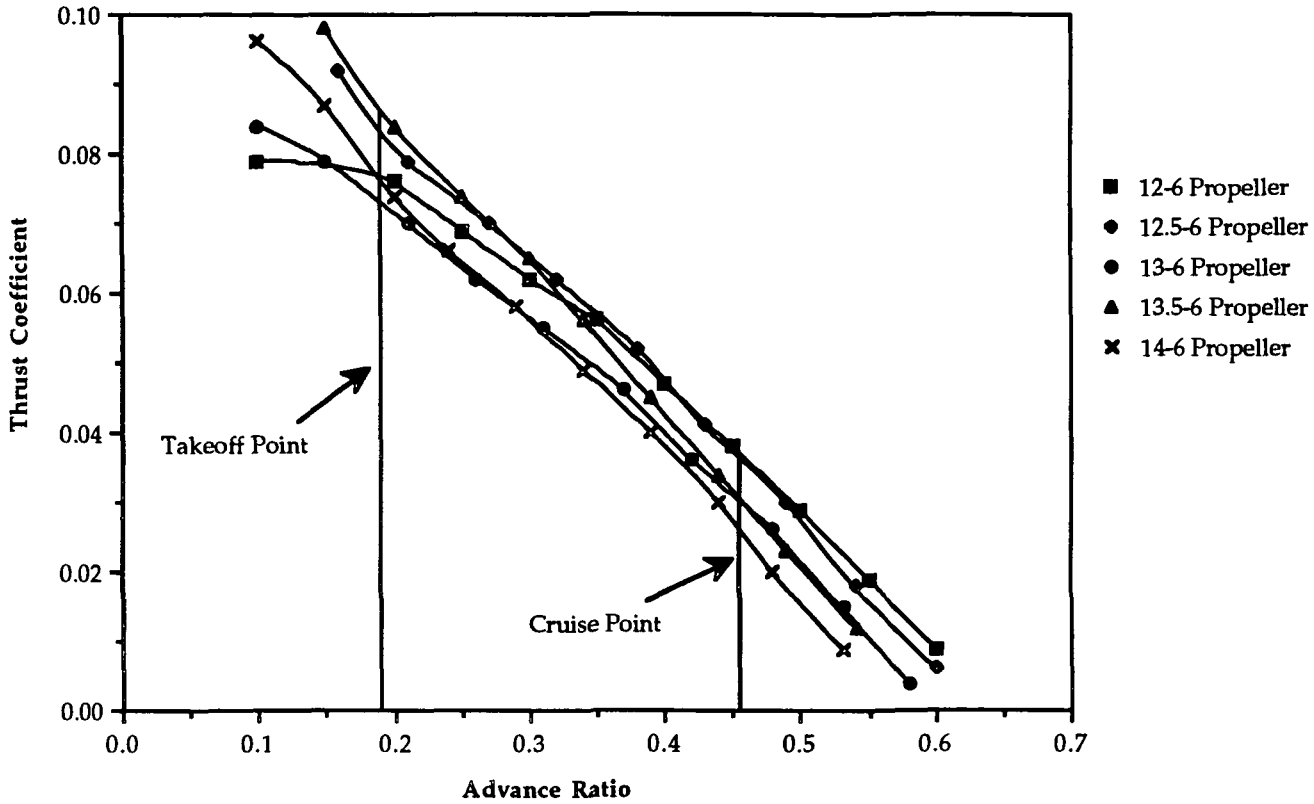

Finally, the power coefficients of the five propellers were examined. These curves are shown in Figure D-4. As with the thrust coefficient, the Zinger 12.5-6 propeller had the highest overall power coefficient values in the range between takeoff and cruise. These three analyses showed that the Zinger 12.5-6 propeller was indeed the best choice for the RTL-46.

Figure D-4 - Propeller Power Coefficient vs. Advance Ratio

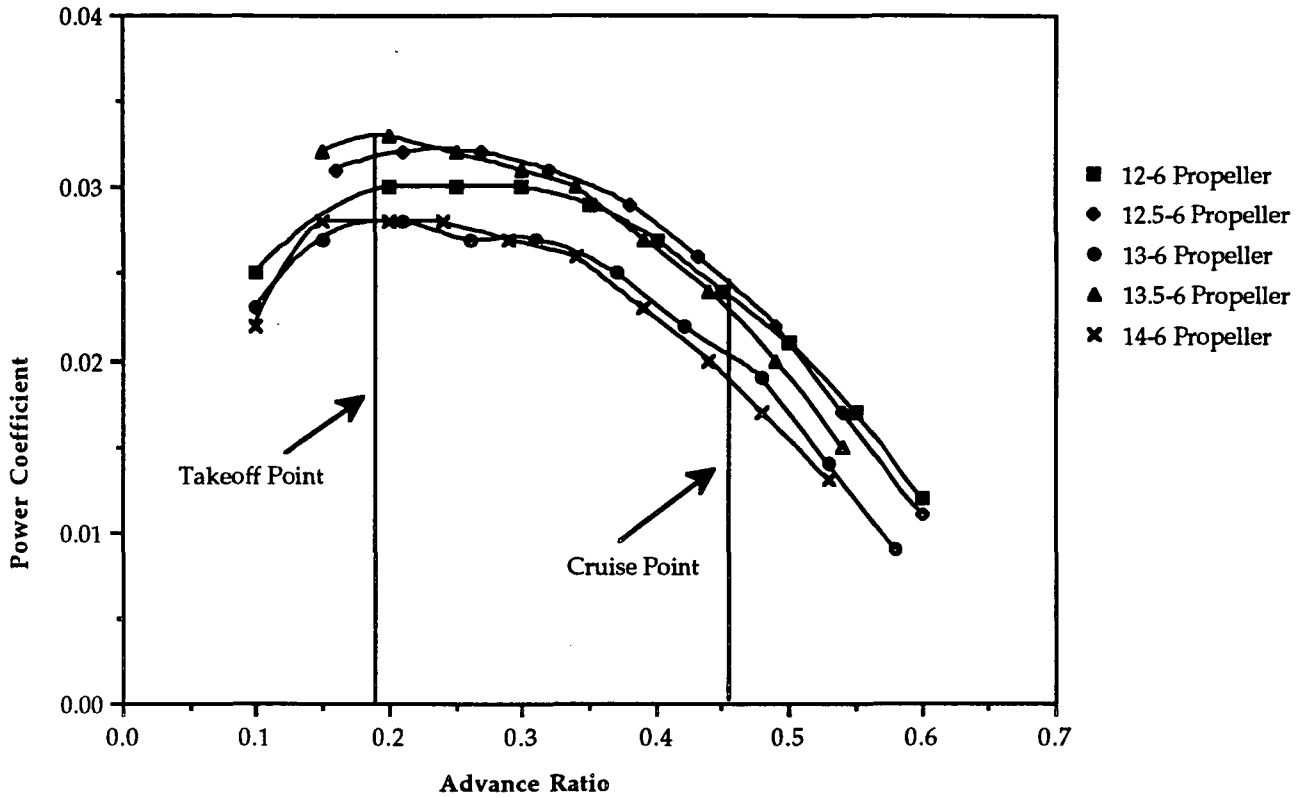

D.4 - ENGINE CONTROL AND FUEL

The throttle setting for the aircraft will need to be adjustable in order to achieve efficiency in all phases of flight. The takeoff and climb phases will require the maximum throttle setting of 14.4 volts, but the throttle setting must be reduced during the cruise phase so that the power required is equal to the power available for the aircraft. This adjustability of the throttle will be controlled by the pilot's control stick, which will control a Tekin speed controller. This speed controller will send the necessary voltage to the motor for the different throttle settings.

As stated above, the maximum throttle setting of 14.4 volts will be used for the takeoff and climb phases of flight. This maximum throttle will provide a rate of climb immediately after takeoff of 11.8 ft/s, rising to a maximum of 13.4

ft/s once the aircraft has reached a velocity of 30 ft/s This will allow the aircraft to climb to the cruise altitude of 25 ft in approximately 2 seconds.

For cruise, however, the full voltage will not be necessary, and the pilot will need to throttle back to maintain straight-and-level flight. In order to decrease the pilot's workload, a value of throttle voltage was required to give the pilot an idea of the cruise throttle stick setting. At cruise, the voltage was calculated as 9.26 volts. This corresponded to a throttle setting of approximately 65%. Therefore, the pilot will need to operate the aircraft at approximately two-thirds of the full throttle position when in cruise.

As mentioned in Section D.1, twelve 900 mah batteries were required in order to provide the necessary power to takeoff in under twenty feet and to minimize battery weight and cost. It was assumed that a total of about 3% of the total battery capacity would be used by the taxi, takeoff and landing procedures. This left 870 mah for the cruise and turning phases of the flight. By using this capacity with the cruise analysis for the Astro 15 motor, the total allowable range produced by these batteries was 19,450 feet - a 33% increase over the range defined by the Design Requirements and Objectives. By allowing for the 2 minute loiter at 25 ft/s, the maximum trip range was calculated to be 16,450 feet.

This increase in range indicated that a smaller battery capacity should be used for the RTL-46. The battery capacity necessary for the 13,000 foot range was calculated and found to be just under 700 mah. Therefore, 700 mah capacity batteries, if made available, would be adequate for the RTL-46 airplane. This would cause a decrease in the weight of each cell, and of the complete aircraft. Because 700 mah batteries were not available for use with the technology demonstrator, the 900 mah batteries will be used for flight testing purposes.

D.5 - MANUFACTURING AND INSTALLATION

One of the requirements for the propulsion system was that the motor and batteries be able to be removed from the aircraft in under 20 minutes. In order to achieve this, the batteries and motor had to be easily accessible. As discussed in Section A.4, the batteries will be contained in the undercarriage, which will contain 2 battery access doors. These batteries will be connected to one another with heat-shrink plastic to allow them to be handled as a package, rather than individually. This battery pack will be attached to the bottom surface of the lower passenger deck with Velcro, rather than screws, in order to allow quick removal.

The motor will slide into a mounting sleeve which will be attached to the firewall with four mounting screws. A nose section will surround the motor in order to reduce fuselage blockage effects. This nose section will be hinged in order to minimize removal time.

D.6 - PROPULSION SYSTEM SUMMARY

Motor	Astro 15
Motor, Gearbox and Mount Weight	10.24 ounces
Motor Cost	$ 124.95
Propeller	Zinger 12.5-6 (cut down from 13-6 model)
Propeller Weight	0.866 ounces
Propeller Cost (estimate)	Approximately $5.00
Battery Selection	12 Panasonic P-90 SCR cell (900 mah)
Total Battery Weight	14.76 ounces
Total Battery Cost	$ 36.00
Speed Controller	Tekin Model
Speed Controller Weight	1.77 ounces
Speed Controller Cost (estimate)	Approximately $ 70.00
Radio System Package	4NBL/Attack model
Radio System Package Cost	$ 299.95
- Receiver weight	0.95 ounces
- System Battery Weight	2.0 ounces
Total Weight	30.6 ounces
Total Cost (estimate)	$ 535.90

E PRELIMINARY WEIGHT ESTIMATE DETAIL

E.0 - GENERAL OVERVIEW

The weight analysis for the aircraft can be broken down into five main sections -1)the structure, 2)the landing gear 3)the control systems, 4)the propulsion systems and, 5)the payload. The maximum take off weight of the aircraft is 4.9 pounds with an uncertainty of 0.2 pounds. The main five sections were analyzed on the basis of their weight percentages which were 42% structure, 32% propulsion, 12% control systems, 10% payload and 4% landing gear(see Figure E-1.)

FIGURE E-1

Overall Weight Component Breakdown

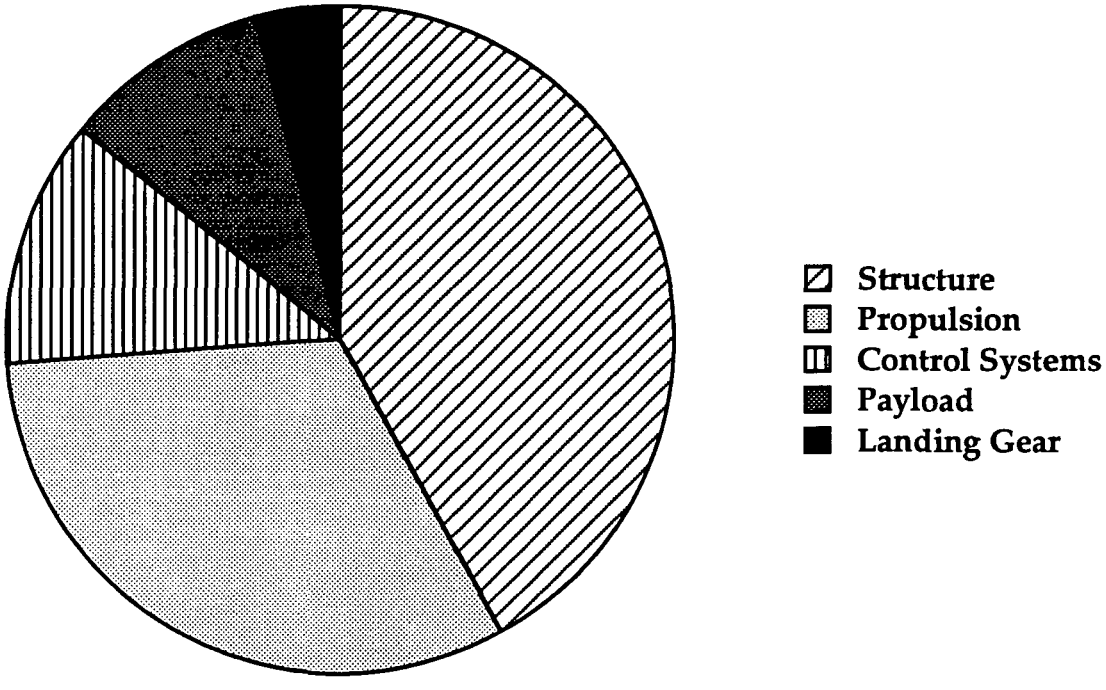

E.1 - COMPONENT WEIGHT ESTIMATE

The weight component breakdown is shown in Table E-1. The Table illustrates the components' weights, weight percentages and the X- position of the center of gravity. Some of the weight percentages and center of gravity points are left out of the table due to associating components in a system and referring to them collectively.

Level Zero weight estimates used the data base of past years' aircraft to estimate, based primarily on size, the weight of the RTL-46. This first estimate was a high 5.5 pounds compared to the final estimate of 4.9 pounds. The wing size was estimated to be the same as the other prototype aircraft while the fuselage size was estimated to be twice that of the HB-40 and other prototype transports of Aeroworld. Level One estimates used actual component estimates and reduced the weight estimate to 5.1 pounds. The weight component breakdown data was taken from a large data base and its specific application to the aircraft. The data base consisted mainly of experimental data. The weight per unit length of varied balsa cross sectional areas and the weight of the landing gear were experimentally taken and designed to minimize the overall weight of the aircraft. This selection process was very important because over 45 per cent of the total body weight is composed of the structure of the aircraft. Selection of Balsa wood for its high strength to weight ratio was unquestionably the most important weight decrease between the HB-40 and the RTL-46. The last level of weight of estimation was purely done by using the weights of every thinkable component from glue to monokote to hinges and hardware. This estimate was iterated to decrease the overall weight below 5.0 pounds. By decreasing the overall weight of the aircraft the design takeoff distance was easily achieved.

The control over the structural weight was a large issue and many design concepts were attempted as discussed in the Structural Design Detail Section (Chapter H.)

TABLE E-1

COMPONENT	WEIGHT oz.	WEIGHT %	CG POINT(X)in.
STRUCTURE			
Decking	4.86	5.7	27.5
Empennage	1.7	2	62
Wing	21	25	18
Fuselage	7.2	8.5	27.8
Monokote	3.54		22
subtotal	35.3	42%	
LANDING GEAR			
Nose	1.4		6
Main	2.2		20
subtotal	3.6	4.2%	
CONTROL SYSTEMS			
Servos	2.4		12
Receiver	.95		12
Syst. batteries	2		12
Speed controller	1.77		12
Push rods	1.82		12
Surface horns	.5		n/a
subtotal	9.44	11.6%	
PROPULSION			
Engine mount	1.2		2
Astro 15 w/ grbox	10.3	12.2	2
Batteries	14.75	17.5	16.6
Propeller	.866		-.2
subtotal	27.12	32%	
PAYLOAD	8.818	10.4%	33
MISC.			
velcro and glue	2		n/a
TOTAL	82.6+/- 3 oz. 5.1+/-.2 lbs	n/a	19.0 +/-.4 full 16.5 +/- .4 unload

E.2 - CENTER OF GRAVITY LOCATION AND TRAVEL

The center of gravity is governed by the placement of large mass-percentage components in variable positions. Figure E-2 is a schematic of critical center of gravity positions for the aircraft's components. The center of gravity for the RTL-46, with full passenger payload, is at the quarter chord of the wing with an uncertainty of less than +/- 0.03c. On the other hand, the center of gravity without a full passenger payload(empty) is at 0.12c. It is an undesirable characteristic to have the center of gravity highly dependent on passenger loading.

FIGURE E.2

CENTER OF GRAVITY DIAGRAM

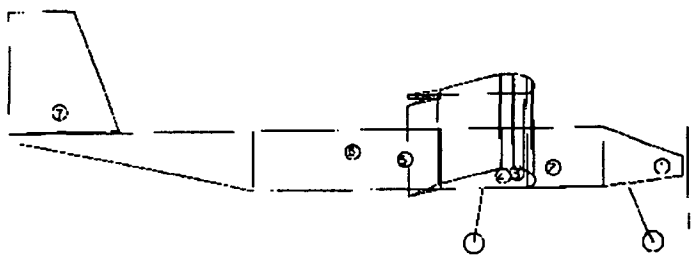

1. CG. OF PROPULSION SYSTEM
2. CG. OF CONTROL SYSTEMS
3. CG. OF FUEL BATTERIES
4. CG. OF THE WING
5. CG. OF THE FUSELAGE STRUCTURE
6. CG. OF FULL PASSENGER PAYLOAD
7. CG. OF THE TAIL SECTION

There are a few ways to compensate for this change. The first, which is the most desirable, is to have the larger mass-percentage components nearer to the center of gravity. This would be done by moving the control systems aft, closer to the center of gravity. A second possible solution would be to strategically load the aircraft with a varied passenger load to help facilitate aft movement of the center of gravity. The third solution which would help in the center of gravity movement is battery placement. The batteries are easily

movable and constantly changing their position to accommodate the design center of gravity at the quarter chord would be effective. One aspect to keep in mind is that due to the RTL's target market, it is designed to fly at a minimum of 70 per cent capacity. This shifts the center of gravity from the .25c to the .21c position. This center of gravity travel is more easily accommodated by second proposed method. The desired methods of determining center of gravity travel therefore is a combination of the first and second methods.

F. STABILITY AND CONTROL

F.1 - OBJECTIVES

The purpose of stability and control was:

- To determine the size of the horizontal tail to provide for longitudinal static stability.
- To determine the size of the vertical tail to provide for directional and lateral stability.
- To provide enough lifting surfaces to counteract disturbances in roll, pitch, and yaw attitude, and to aid in the maneuverability of the RTL-46 in the different phases of flight.

F.2 - STATIC LONGITUDINAL STABILITY

In order to possess longitudinal stability, the RTL-46 must first meet a few basic requirement. These are:

- The pitching moment curve slope must be less than zero. i.e.

$$\frac{dC_m}{d\alpha} < 0$$

This is due to the fact that as the angle of attack of the aircraft increases due to a positive (nose-up) moment, the aircraft will tend to create a negative (nose-down) moment in order to trim itself. Should the pitching moment curve slope, Cm_α, be greater than zero, then, as the aircraft experiences a nose-up disturbance, it will continue to pitch up until the aircraft stalls.

- The pitching moment coefficient at zero angle of attack, Cm_o, must be greater than zero. Failure to achieve this will leave the aircraft unable to trim at positive angles of attack.

The aircraft's wing, fuselage, and horizontal tail, or stabilizer, all contribute to the pitching moment. As presented in Chapter C, the SD7062 airfoil was used for the wing mounted at 1.5° with respect to the fuselage. The contributions of each component to the pitching moment can be seen in the definition of the Cm_o and Cm_α. They are defined as:

$$C_{mo} = C_{mac} + C_{Low}\left(\frac{X_{cg}}{c} - \frac{X_{ac}}{c}\right) + C_{mo_f} + \eta V_H(\varepsilon_o + i_w - i_t)$$

and

$$C_{m\alpha} = C_{L\alpha w}\left(\frac{X_{cg}}{c} - \frac{X_{ac}}{c}\right) + C_{m\alpha_f} + \eta V_H C_{L\alpha t}\left(1 - \frac{d\varepsilon}{d\alpha}\right).$$

Methods of finding Cm_{of} and $Cm_{\alpha f}$ are found in Appendix [4].

Thus, the contributions of the wing and the fuselage to the pitching moment are negative for the RTL-46. Therefore, one of the primary concerns of the horizontal tail design is that it must provide enough pitching moment to counteract the unstable contributions of the wing and the fuselage. This can be done through variations in the tail airfoil section, tail incidence angle, tail positioning, length from the center of gravity to the tail aerodynamic center, the tail area, and the tail aspect ratio.

However, longitudinal stability is not the only concern of the horizontal tail. It also contributes to the static margin of the aircraft, which is a measure of the responsiveness of the aircraft.

The static margin is defined as the distance between the neutral point position aft of the wing leading, X_{NP}, and the center of gravity position aft of the wing leading edge, X_{cg}. i.e.

$$\text{Static Margin} = \frac{X_{NP}}{c} - \frac{X_{cg}}{c}$$

where the neutral point is defined as:

$$\frac{X_{NP}}{c} = \frac{X_{ac}}{c} - \frac{C_{m\alpha_f}}{C_{L\alpha w}} + \eta V_H \frac{C_{L\alpha_t}}{C_{L\alpha w}}\left(1 - \frac{d\varepsilon}{d\alpha}\right)$$

The neutral point can be found by solving the pitching moment slope equation for the center of gravity position for a pitching moment slope of zero. i.e. $C_{m\alpha} = 0$. If the center of gravity is located at the neutral point, the aircraft is neutrally stable. This corresponds to a pitching-moment curve

slope equal to zero. Movement of the center of gravity aft of the neutral point will render the aircraft statically unstable.

For conventional aircraft, acceptable values of the static margin range from 5 to 10 percent. But, for a Remote-Piloted Vehicle (RPV) such as the RTL-46, this value is deemed to be too small. Acceptable values for the static margin are at least 20 percent.

Thus, the stabilizer, must contribute to both the static longitudinal stability and the static margin of the RTL-46. Therefore, the characteristics of the stabilizer must be determined with these conditions in mind.

Recall that the tail contributions are:

$$C_m = \eta V_H(\varepsilon_o + i_w - i_t) + \left[\eta V_H C_{L\alpha t}\left(1 - \frac{d\varepsilon}{d\alpha}\right)\right]\alpha$$

(Note: Terms not explicitly defined in the equation, are explained in Appendix 4.) From the equation, it can be seen that as the tail incidence of the stabilizer is increased, the horizontal tail volume ratio, V_H, must be increased. This is due to the fact that a higher tail incidence leads to a greater tail lift and therefore a greater pitch-down moment on the aircraft. Therefore, it was decided that the tail be mounted at a negative incidence angle in order to aid in the stability of stability of the aircraft. However, the possibility of negative stall over the various aspects of the flight regime of the RTL-46, required that the stabilizer be mounted at a small negative incidence. Therefore, it was decided that the stabilizer be mounted at -2° with respect to the fuselage.

Thus, the number of parameters to be considered were narrowed to the tail moment arm, the stabilizer area, the tail airfoil section, and the tail aspect ratio. From Reference [8], it was found that for RPVs, it was preferable that V_H range from approximately 0.4 to 0.6, and the tail moment arm range from 2.5 to 3 times the wing chord length aft of the center of gravity.

Initially, the center of gravity was placed 20 inches aft of the nose of the aircraft. It was also decided that a flat plate would be used as the airfoil, primarily due to the fact that no modifications would be made. In order to decrease the size of the stabilizer area, the moment arm was determined to be 39 inches. A FORTRAN program (see Appendix 4) was written in order to determine the variations of the pitching moment and the static margin as the other parameters varied. The tail area was sized at 214.4 in^2. After viewing several different articles concerning RPVs, it was found that most RPVs place the center of gravity at the wing quarter chord, 18.25 inches from the nose in this case, thereby increasing the moment arm to 40.75 inches. However, it was not inherently possible to find and adequate Cm_o. A more accurate assessment of the weight placements placed the furthest aft position of the center of gravity at 19 inches behind the nose of the RTL-46. This satisfied the adequate Cm_o and Cm_α criteria, and provided a static margin of approximately 12 percent. However, as previously discussed, this value would lead to an aircraft difficult to control from the ground. Thus, it was necessary to increase the stabilizer area. In order to avoid having too large an area, it was decided to vary the aspect ratio in order to provide for moment contributions. Therefore, the stabilizer chord was kept constant, and the span was increased from its initial value of 23 inches, thereby increasing the aspect ratio. After several variations, the stabilizer span was set at 30 inches, yielding an aspect ratio of 3.22. This provided a static margin of approximately 28 percent.

The following values for longitudinal stability and horizontal tail geometries were used.

Table F-1 - Values for longitudinal stability parameters for RTL-46

horizontal tail area, St	279.9 in^2
V_H	0.61
mean chord, c	9.33 in
span, b	30 inches
moment arm, lt	40.75 in
Tail incidence, it	-2.0°
$X_{c.g.}/c$	0.31
Static margin	29 percent

Figure F-1 - Pitching moment coefficient vs. α for RTL-46 and components (without flaps)

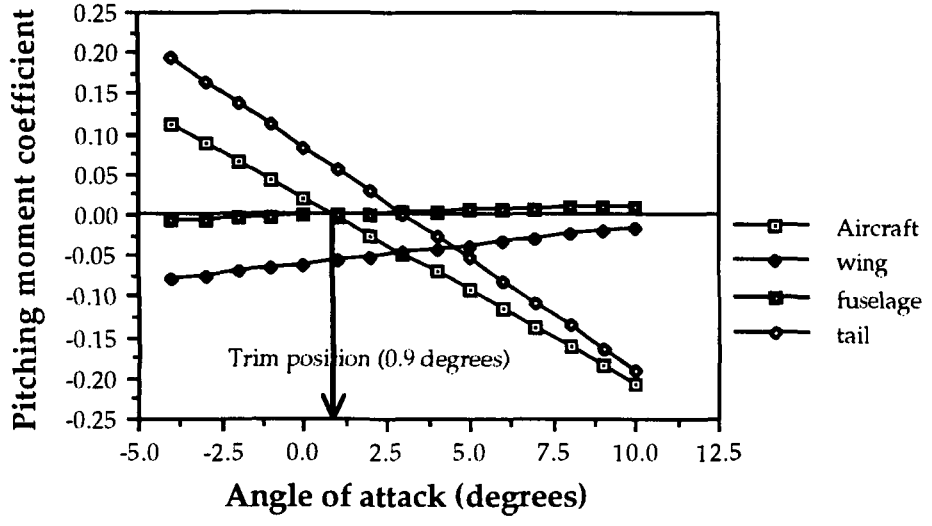

The contributions of the horizontal tail to the pitching moment are displayed above in Figure F-1. As can be seen, the wing and fuselage pitching moment curves have slopes greater than zero, and therefore are unstable. In addition, both have Cm_o values less than zero. The tail has a large negative slope and a large positive Cm_o. These combine to yield the aircraft pitching moment curve slope with adequate values of Cm_o and Cm_α. The equation of the pitching moment curve slope for the flaps configuration of the RTL-46 is thus $Cm = 0.0206 - 0.02280\alpha$, where α, the angle of attack, is measured in degrees. By setting the value of the pitching moment coefficient to zero, the

trim angle of attack can be found. (This is the angle of attack at which the aircraft flies without any pitching moment.)

It was also necessary to find the furthest forward position of the center of gravity. i.e. the empty aircraft configuration as opposed to the full capacity configuration. The furthest forward position of the center of gravity was found to be 16.5 inches from the nose of the aircraft, or 11.5 percent of the wing chord. Figure F-2 shows the pitching moment curves for the forward and aft positions of the center of gravity. As the center of gravity moves forward Cm_α becomes more negative, however, Cm_o also becomes negative. Although the RTL-46 will not always fly with a full capacity, Cm_o can be made positive by seating passengers to vary the center of gravity accordingly.

Figure F-2 - Pitching moment coefficient vs. α for RTL-46 at forward and aft positions of center of gravity (without flaps)

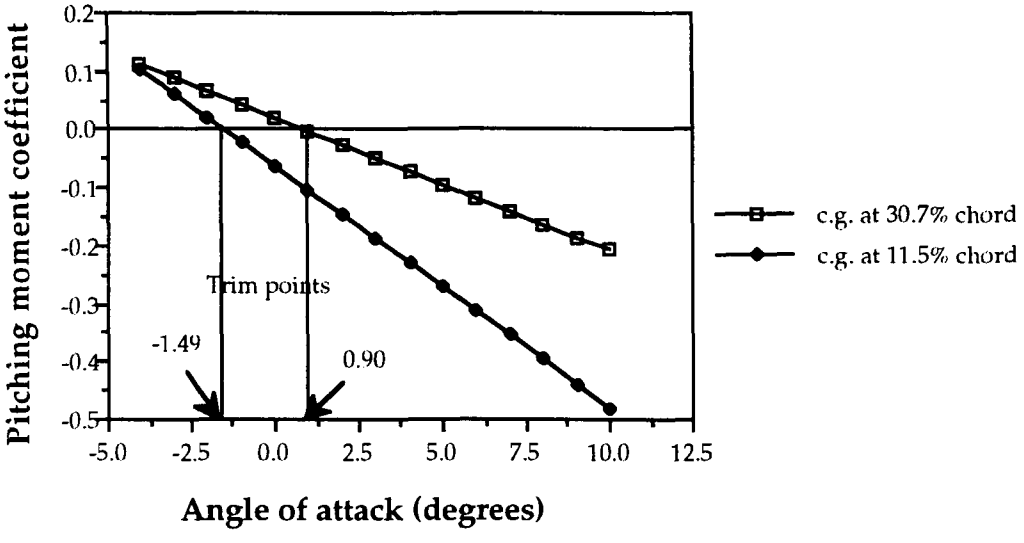

F.3 - LONGITUDINAL CONTROL

Longitudinal control is necessary to control the pitching moment of the aircraft during the different stages of flight. This control is attained by the inclusion of an elevator on the horizontal tail. In order to find the size of the elevator, it was first necessary to find the maximum angle of attack maintainable before the aircraft stalls. The elevator must be able to trim the aircraft at

this stall angle, with a maximum elevator deflection of +/- 15°. The pitching moment equation, taking the elevator contribution into account, then becomes

$$C_m = C_{mo} + C_{m\alpha}\alpha + C_{m\delta e}\delta$$

Thus, setting $C_m = 0$ and a maximum angle of attack of 10°, which was determined to be the stall angle of attack for the aircraft in Chapter C, the elevator control power, $C_{m\delta e}$ can be found. The elevators must be able to trim aircraft before the stall occurs. Once $C_{m\delta e}$ was found the flap effectiveness parameter, τ, could be found. (See Appendix 4). The flap effectiveness parameter is defined as a function of the ratio of the control surface area ratio to the lifting surface area which can be determined from Figure 2.20 in Reference [9]. In Figure F-3, for the given elevator control power, the effect of elevator deflection can be seen on the pitching moment curve. As the elevator is deflected up (a negative elevator deflection), the pitching moment curve shifts down, because this creates a pitch-down moment on the aircraft.

Figure F-3 - Effect of elevator deflection on pitching moment for horizontal tail for RTL-46

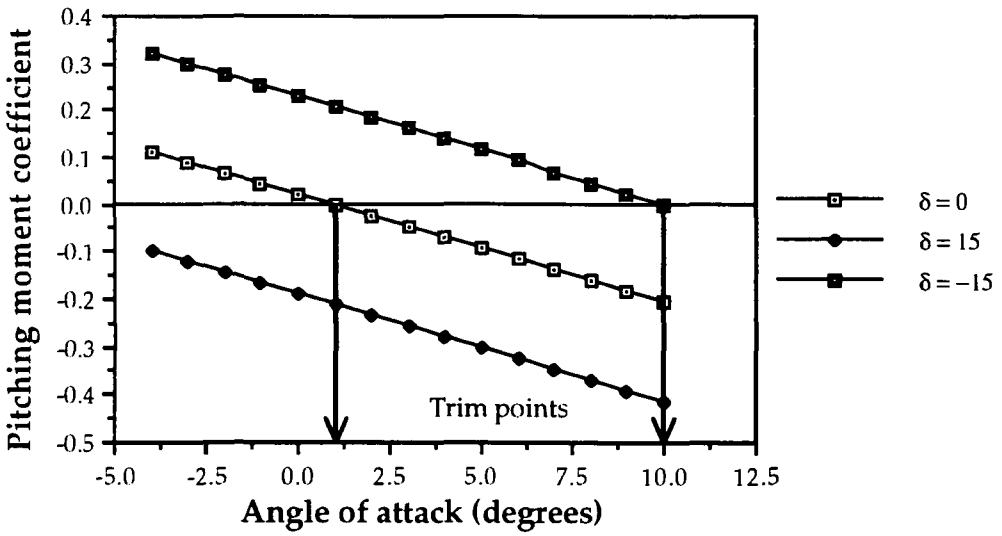

Thus the elevator characteristics are:

Table F-2 - Characteristics of elevator for RTL-46

$\delta_{e\,max}$ (no flaps)	+/- 15°
S_e/S_t	0.119
$C_{m\delta e}$	-0.743 rad^{-1}
c_e	1.11 in
$\delta_{e\,cruise}$	1.59°

Once the sizing of the elevator was completed, two important issues remained to be addressed. These are the effect of center of gravity movement and flaps on the pitching moment.

First, it is necessary to examine the effect that the center of gravity position will have on the pitching moment. As shown in Figure F-2, at the forward position of the center of gravity, the aircraft will not be able to trim at positive angles of attack. In the same way that the cruise elevator deflection was found, the cruise elevator deflection for the forward c.g. position can be found. This value is 5.27°.

The second important issue, the case where the flaps are deflected 20°, was of critical importance, as the flaps are needed to takeoff within the desired 20 foot objective. Figure F-4 shows the pitching moment coefficient in flaps up and flaps down configurations.

As can be seen in Figure F-4, the pitching moment curve is shifted down radically. Although $Cm_\alpha < 0$, the aircraft cannot trim at positive angles of attack without the aid of elevator deflection. The previous maximum elevator deflection limits would not be able to provide enough moment to trim the aircraft in a flaps down configuration. The pitching moment curve, in a flaps-deflected configuration, was found for different elevator deflections, and these curves are pictured in Figure F-5, below. Thus, it must be determined at what angle of attack the aircraft will fly in its flaps-deflected

configuration in order to determine what elevator deflection is necessary to trim the aircraft.

Figure F-4 - Pitching moment coefficient vs. α, with and without flaps

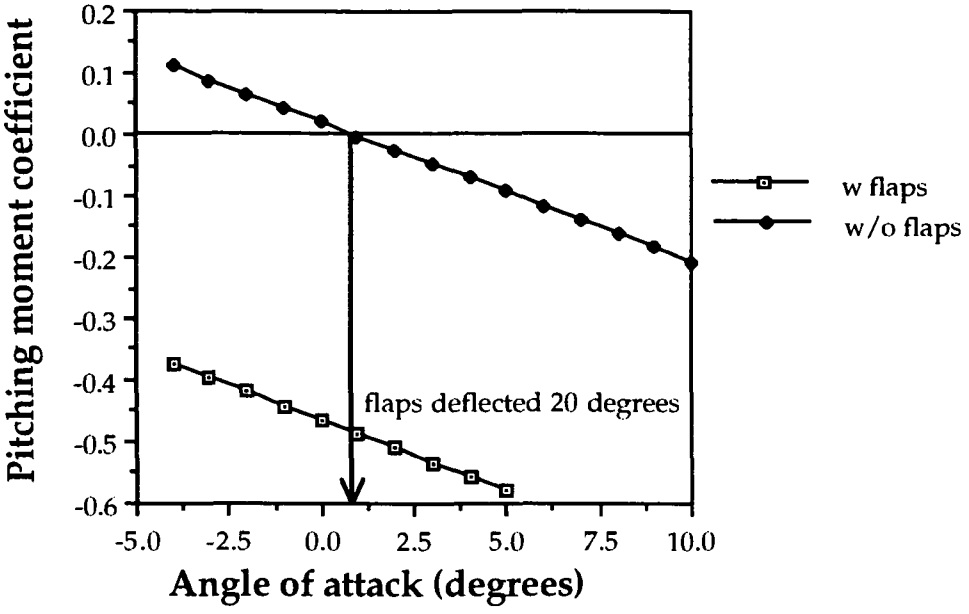

Figure F-5 - Effect of elevator deflection on pitching moment RTL-46 in flaps-deflected configuration

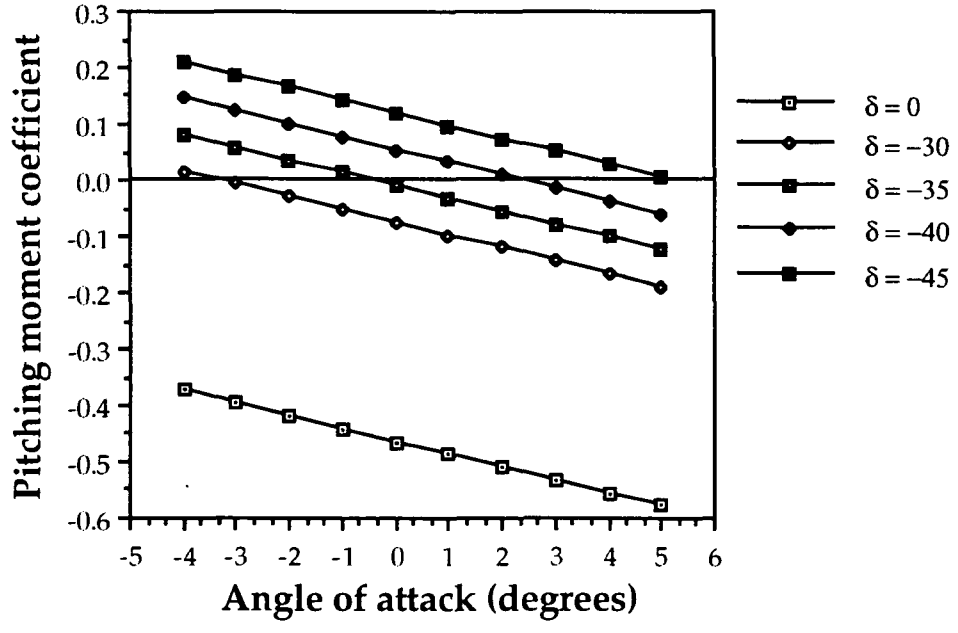

F.4 - LATERAL AND DIRECTIONAL STABILITY

Directional stability is necessary to keep the aircraft on a straight course or to maneuver. If the aircraft encounters a sideslip, it must be able to resume a trim condition. The yawing moment coefficient is defined as:

$$C_{n_\beta} = C_{n_{\beta_{wf}}} + C_{n_{\beta_v}}$$

where $C_{n\beta wf}$ is estimated using Equation 2.74 with Figures 2.28 and 2.29 in Reference [9]. The criterion for directional stability is $C_{n\beta} > 0$. It is readily seen that the wing-fuselage combination contributes to directional instability. $C_{n\beta v}$ must counteract this. It is found by combining Equations 2.80 and 2.81 for some given values to yield:

$$C_{n_{\beta_v}} = V_v C_{L\alpha_v}\left(0.93 + 1.03\frac{S_v}{S}\right)$$

The parameter k, similar to the vertical tail volume ratio, V_V, is now introduced and is defined by:

$$k = \frac{S_v l_v}{Sc}$$

According to Reference [11], for RC airplanes, a typical value for k is 0.22. Setting the moment arm l_v equal to l_t, a vertical tail volume ratio is found to be 0.027 and thus, an vertical tail area of 105 in^2 is found. Therefore, it is seen that $C_{n\beta v}$ is dependent on the 3-D lift curve slope of the vertical tail. It must be noted that the lift curve slope of the vertical tail area must be corrected for the presence of the fuselage and horizontal tail. According to Reference [7], the geometric aspect ratio must be multiplied by a factor of 1.6 to find the effective aspect ratio for the corrected lift curve slope. This is significant due to the fact that it will not be necessary to use a large geometric aspect ratio to obtain a favorable lift curve slope.

Roll stability is the ability of the aircraft to develop a restoring moment in response to a disturbance from a wings-level attitude. The requirement for

roll stability due to sideslip is $C_{l\beta} < 0$. The roll stability due to the wing is a function of the wing geometry and the dihedral angle of the wing. It is defined as:

$$C_{l_\beta} = -\frac{C_{L\alpha_v}}{6}\left(\frac{1+2\lambda}{1+\lambda}\right)\Gamma$$

where λ is the wing taper. Because there is no taper, this reduces to :

$$C_{l_\beta} = -\frac{C_{L\alpha_v}}{4}\Gamma$$

Thus, the characteristics contributing to the lateral and directional stability are:

Table F-3 - Values for vertical tail parameters for RTL-46

vertical tail volume ratio, V_v	0.27
vertical tail area, S_v	105 in^2
moment arm, l_v	40.75 in
wing dihedral, Γ	10 °
$C_{n\beta}$	0.092 rad^{-1}
$C_{l\beta}$	-0.196 rad^{-1}

F.5 - LATERAL AND DIRECTIONAL CONTROL

In order to achieve the necessary combined directional and lateral stability to perform a turning maneuver, the rudder, in conjunction with wing dihedral is necessary. The yawing moment coefficient is can be written as:

$$C_n = C_{n_\beta}\beta + C_{n_{\delta r}}\delta_r$$

while the rolling moment coefficient can be written as:

$$C_l = C_{l_\beta}\beta + C_{l_{\delta r}}\delta_r$$

It can also be written as $dC_l/d\delta r$. This is equivalent to

$$C_{l_{\delta r}} = \frac{\left(\frac{dC_l}{d\beta}\right)\left(\frac{dC_n}{\delta_r}\right)}{\left(\frac{dC_n}{d\beta}\right)}$$

which is simply

$$C_{l_{\delta r}} = \frac{C_{l_\beta} C_{n_{\delta r}}}{C_{n_\beta}}$$

This can be further simplified to

$$C_{l_{\delta r}} = \frac{\left(-\frac{C_{L\alpha_v}}{4}\Gamma\right)(-\eta_v \tau)}{\eta_v\left(1+\frac{d\sigma}{d\beta}\right)}$$

The denominator can be found through Equation 2.81 of Reference [9]. A rolling moment coefficient of at least 0.1 rad^{-1} was sought to account for the lack of ailerons in this configuration. This was found by assuming an HB-40 configuration with ailerons to aid in roll control.

Thus, necessary rudder control power can be found as function of the wing dihedral and the rudder effectiveness parameter. Once a desired value for the rudder control power is found, the corresponding rudder effectiveness parameter can be found resulting in the sizing of the rudder. For the RTL-46, Figure F-6 shows the dependency of the roll moment on the rudder effectiveness for varying dihedral angles. It must be noted that the lift curve slope, the vertical tail size, and the wing area were kept constant.
For the RTL-46, the following values were determined:

Table F-4 - Characteristics for rudder for RTL-46

$\delta_{r\,max}$	+/- 30°
S_r/S_v	0.539
$C_{l\delta r}$	0.131 rad^{-1}
$C_{n\delta r}$	-0.617 rad^{-1}

Figure F-6 - $C_{l\delta r}$ vs. τ for varying wing dihedral for RTL-46

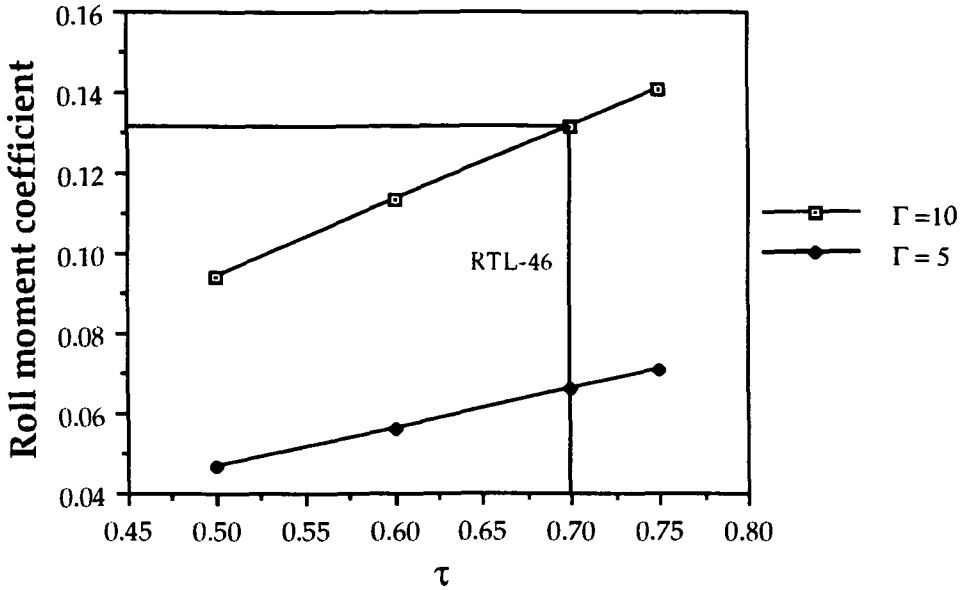

The need for ailerons is negated, as the rudder will be able to negotiate the same maneuvers without the need for servos and the disadvantage of added weight.

With the addition of dihedral, there is the possibility of tip stall due to a lateral gust which would causes sideslip. As sideslip is induced, the tips of the wings will effectively face a higher angle of attack than the root of the wing. Therefore, it is necessary to find the change in angle of attack between the root and the tip. Using small angle theory, the change in angle of attack, $\Delta\alpha$, is defined by:

$$\Delta\alpha = \beta\Gamma$$

The variation in angle of attack with respect to sideslip angle can be seen in Figure F-7. For a sideslip of 10°, there is only a change in angle if attack of 1.7°. This provides a guide as to what maximum angle of attack to achieve before stalling the tips of the wing.

Figure F-7 - Change in angle of attack vs. sideslip due to dihedral

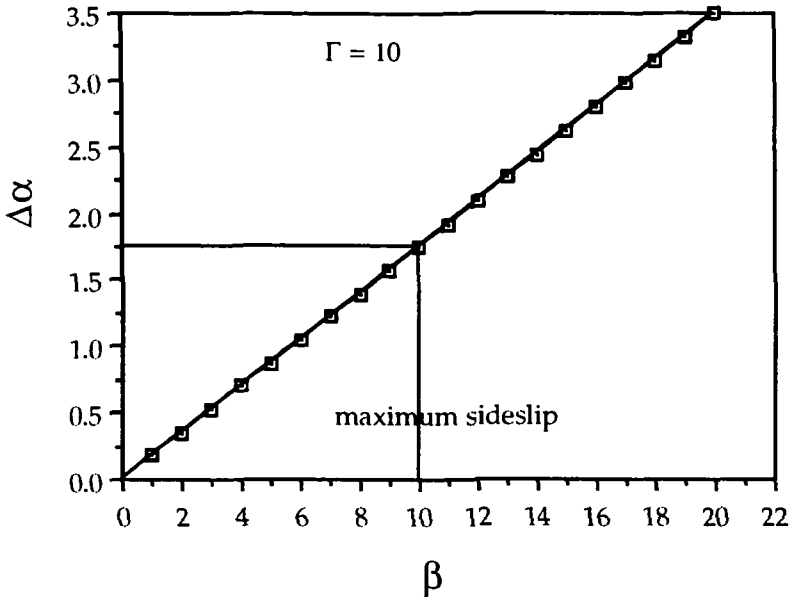

G. PERFORMANCE

G.1 - TAKEOFF

The takeoff performance for the RTL-46 was calculated using two different methods. The first method arising from Reference [6] and Reference [10], was used to provide the general guidelines for the takeoff configuration. The formula derived for the ground roll of the aircraft was:

$$X_{gr} = V_{to}^2/[2*g*(T/W - \mu)]$$

This relationship was used with a takeoff velocity of 120% of the stall velocity. This provided a factor of safety so that the aircraft would not stall during the takeoff maneuver. The values of the other components of the equation were also set assuming, that for the aircraft to fly, the lift must at least equal the weight, or:

$$\text{Lift} = \text{Weight} = 0.5*CLmax*r*S*Vstall^2$$

By estimating a value for the maximum lift coefficient of the aircraft, the stall velocity can be calculated. This allows for the calculation of the takeoff velocity. When combining these two equations, different values for the thrust required at takeoff, takeoff distance and takeoff velocity were calculated using iterations of a FORTRAN routine found in Appendix [5] which used data base information extrapolated to the first level approximations for certain design variables for the RTL-46. Once the design variables were set, the equation analysis provided a basis as to what conditions are needed for the RTL-46 to realistically takeoff within the parameters set forth in Chapter A.

The values listed in Table G-1 represent the final values calculated based upon the final design. In order to decide what types of values were necessary to achieve the objective values, iterations were performed and their results are presented in Figures G-1 and G-2.

Table G-1 - Design Variables for Takeoff of Aircraft

Aircraft Weight	4.9 lb
Wing Area	9.93 ft^2
Static Thrust	~2.6 lb
Runway coefficient factor	0.2
C_{Lmax} for aircraft (Flaps deflected)	1.8
Takeoff Velocity	19.7 ft/s
Wing Loading (W/S)	.493 lb/ft2
Thrust to Weight ratio (To/W)	.531

Figure G-1 Velocity and Static Thrust Required vs. CLmax for Aircraft

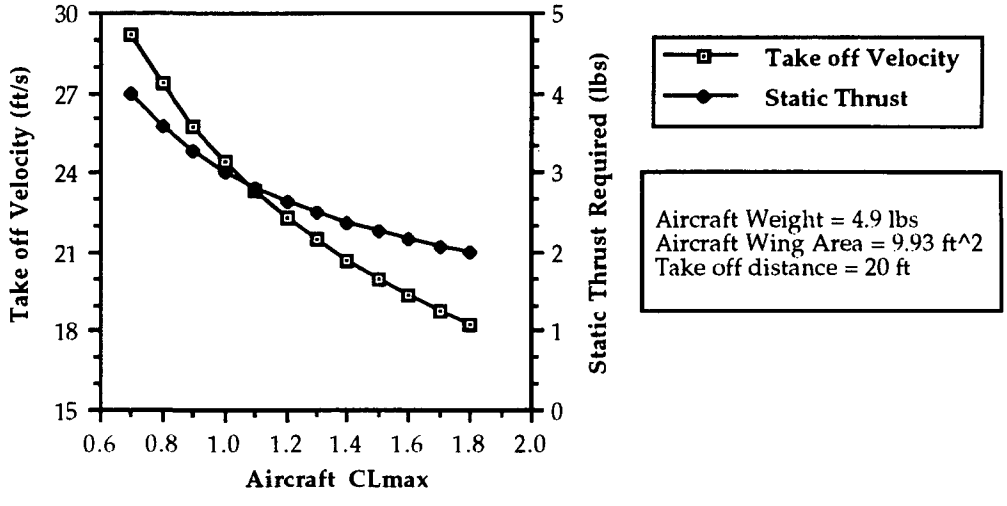

Figure G-1 displays the effect of the changes in takeoff velocity (left vertical axis) and thrust (right) with respect to changes in the maximum lift coefficient. If the aircraft had no flaps, its maximum lift coefficient would have been only 1.1 and thus the velocity necessary for takeoff would be over 24 ft/s or almost the minimum turn velocity and thus the 1.2 factor would have pushed the stall velocity very close to the 25 ft/s necessary to turn. For the case of a 20 ft

takeoff distance, the static thrust would have to have been about 3.7 lb - a high value for the 12.5-6 propeller.

The static thrust became the control variable from which the takeoff distance was calculated based upon the wing design and the aircraft weight settled upon in Chapter F. The takeoff weight of 4.9 lb was used in all calculations. At various maximum lift coefficients for the aircraft, the relation between the static thrust available to the aircraft at takeoff and the takeoff distance are shown in Figure G-2. As shown, the aircraft would have to have a static thrust of at least 2.2 lb for an aircraft with a maximum lift coefficient of 1.6 to achieve a 20 foot takeoff. Although, with the flaps, the maximum lift coefficient of the RTL -46 does slightly eclipse that value. Therefore with the propeller and motor design based upon these requirements as discussed in Chapter D, the maximum thrust at takeoff was calculated at ~2.6 lb. With this amount of thrust available, the aircraft could still takeoff if the flaps yield a maximum lift coefficient of about 1.2. Therefore the lift coefficient at takeoff became .83 when allowing for the takeoff velocity to be 120% stall velocity.

Figure G-2 Take off Distance vs. Static Thrust at constant Weight

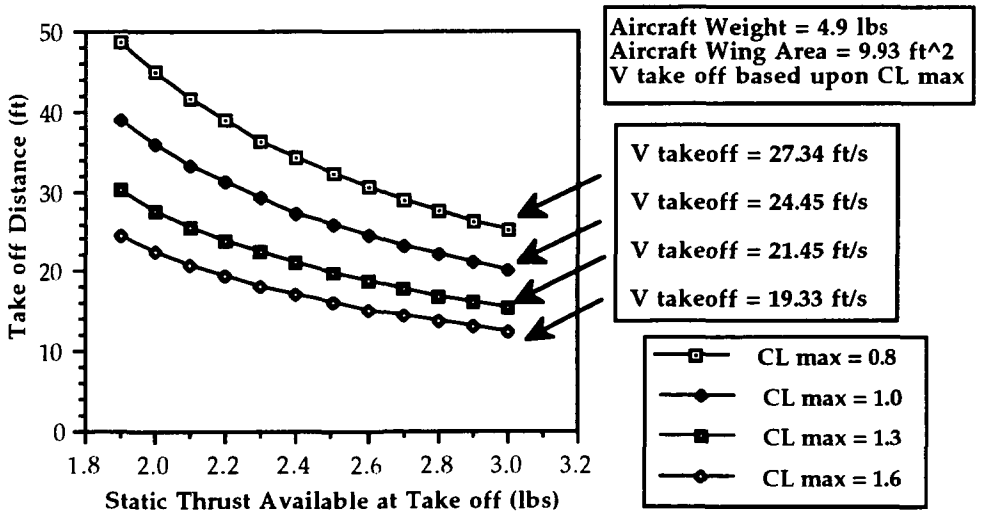

With the actual design configurations set at those values listed in table G-1, the design variables were entered into a takeoff performance program written by Reference [1]. Table G-2 lists these parameters. This program took into account the dimensions of the propeller and the motor and battery characteristics. These actual values combined with the aircraft configuration yield the data on the actual takeoff performance of the RTL -46. These values are shown in Table G-3. With the preliminary analysis of Figures G-1 and G-2 used to find baseline comparisons from which to base the design configuration for takeoff, the analysis of the Propeller program allowed for the actual values for the takeoff distance and velocity to be calculated. As can be shown, the numerical analysis based upon the ground roll formulation agrees with the results formulated through the propulsion system calculations.

Table G-2 - Takeoff Program Design Variables

Design Variable	Value
Weight	4.9 pounds
Wing Reference Area	9.93 square feet
Runway Friction Factor	$\mu = 0.02$
Battery Pack Voltage	14.4 Volts
Propeller	Zinger 12.5-6
Gear Ratio	2.38
Takeoff C_L	1.014
Takeoff C_D	0.078

Table G-3 - Takeoff Design Final Performance Values (Computer Based)

Takeoff Distance	15.4 feet
Takeoff Velocity	20.8 ft/s
Static Thrust	2.56 pounds
Battery Drain during Takeoff	3.7 mah

G.2 - CRUISE

Once in the air, the RTL-46 will cruise at 35 ft/sec. The cruise velocity is chosen to lower the cost of travel through Aeroworld as shown in Chapter I, and thus by traveling faster than the competitors increase the demand for the aircraft. Since the RTL-46 travels the Aeroworld routes at a velocity higher than the current HB-40, it can also expect to fly more flights in its lifetime than the other aircrafts vying for the market. With the cruise velocity set by economics of the market, the C_L necessary for this flight conditions naturally arises from the equation:

$$L = W = 0.5*r*Vcr^2*S*C_L$$

Thus the C_L necessary for the level cruise of the RTL-46 is .34.

The C_L at cruise of such a value proves to be beneficial because it can be achieved at a very low positive angel of attack of the wing (see Figure G-3). When the wing is mounted at the 1.5° incidence angle on the fuselage, the plane cruises at almost no angle of attack with respect to the velocity vector. The straight and level cruise provides extra comfort for the customers and ease for the pilot in flying the aircraft. The low power required to achieve this condition leaves plenty of excess power potential to maneuver at the cruise velocity. In fact as Figure G-6 will show in section G.5, only approximately 65% of the throttle is necessary to achieve the cruise velocity.

Figure G-3 - Lift Curve for RTL-46 With and Without Flaps Deflected

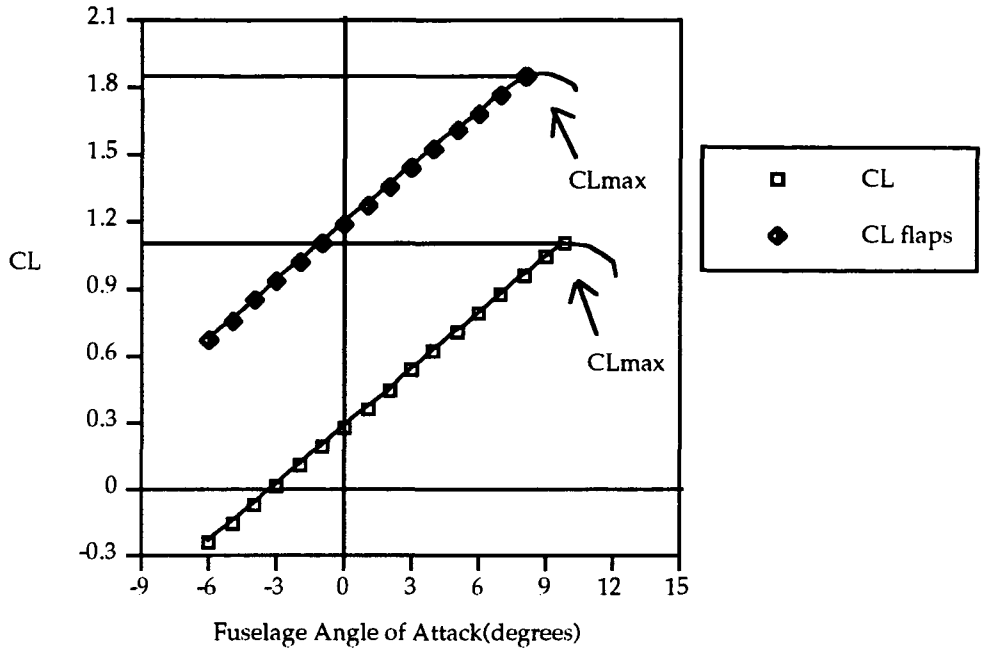

Figure G-4 - L/D vs. Angle of Attack For RTL-46

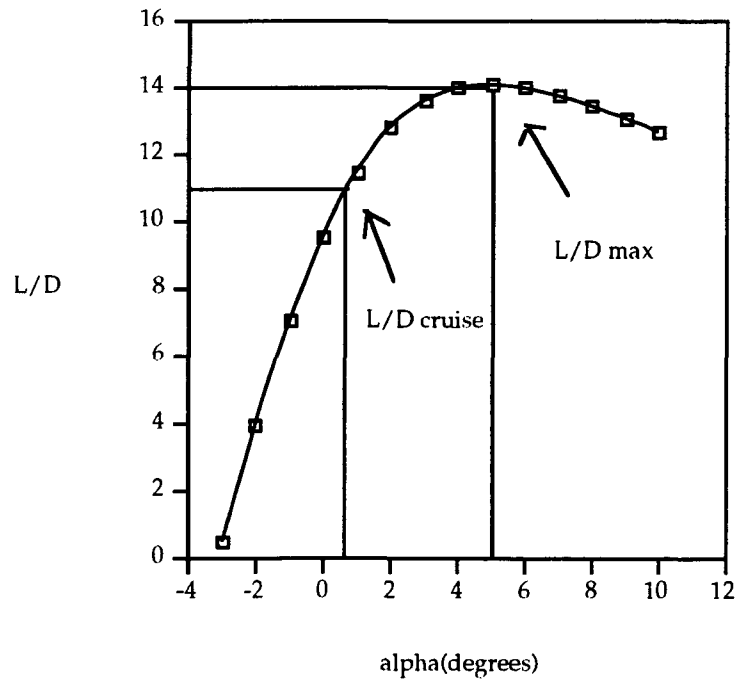

Another benefit to cruising at a low C_L is the lower induced drag effect the aircraft sees due to the lower lift being achieved. This low drag leads to a L/D at cruise of 11, which is near the maximum value of 14 (see Figure G-4). This L/D provides the optimal cruise conditions for the current configuration because if the aircraft were to fly at the maximum L/D, the lift coefficient present would lead to a velocity of only 26 ft/sec, which is a large economic disadvantage in Aeroworld.

G.3 - TURN

The aircraft will use the 10 degree dihedral of the wing in combination with the rudder control achieved by the maximum rudder deflection of 30°, in order to bank into the desired turn. The Request for Proposals stipulated that the aircraft be able to turn with a 60 ft radius at a velocity of 25 ft/s. Thus, the bank angle necessary for the turn is approximately 18 degrees based upon the equation:

$$\tan \phi = V_{turn}^2/(g*R)$$

where ø is the bank angle of the airplane and R is the radius of the turn (refer to References [7] and [10]). With the roll control power of 0.131 ($C_{l\delta r}$) for the aircraft (as discussed in chapter F), and the formula derived from chapter 5 of Reference [9], the roll rate of the aircraft was estimated by:

$$P_{SS} \text{ (steady state roll rate)} = \frac{-2*C_{l\delta r}*\Delta\delta r}{C_{lp}*b}$$

where C_{lp} (roll rate coefficient due to roll) = $-C_{l\alpha}/6$. For the aircraft, the value of C_{lp} was calculated to be -0.75/radian based upon the lift curve slope for the aircraft calculated in Chapter C. Thus, the maximum roll rate of the aircraft was found to be 28.3°/sec, or, in the case of maximum rudder deflection, the aircraft will roll to the desired bank angle in under one second.

G.4 - LANDING

The landing performance for the RTL-46 follows a parallel methodology as the takeoff performance because of the runway length restrictions (see Section A-2). If the aircraft only had 20 ft in which to takeoff, it would only have this distance (from point of touchdown) in which to come to a complete stop. The landing performance calculation arises from the relation derived in Reference [7] and is as follows:

$$X_{gr} = X_{breaking} = \frac{W}{g} * \frac{1}{2B} * \ln(1 + B/A * V_{touchdown}^2)$$

$$A = \mu_{breaking} * W + R \qquad (R = \text{Reverse Thrust} = 0)$$

$$B = C_D * .5 * \rho * S \qquad (C_D \text{ calculated from drag polar})$$

The values used in the distance calculation are listed in Table G-4.

Table G-4 - Landing Performance Calculation Values

Parameter	Value (or Range of Values)
Weight	4.9 lb
Runway Friction Coefficient (μ)	.2 (same as takeoff - no brakes)
$V_{touchdown}$	16-28 ft/sec
C_L at touchdown	0.6 - 1.5
C_D at touchdown	0.0432 - 0.140
Wing Area	9.93 ft^2

With the range of parameters used, it became necessary to deflect the flaps at landing, thus causing a slower touchdown velocity and a higher drag due to the dirty aircraft configuration. Since the pilot will cut the motor completely for landing, the velocity at landing, as shown in Figure G-5, lies near the 20 ft/s

range. There was a problem here, because the aircraft would not be able to land in fewer than 24 feet, regardless of the lift coefficient at landing. This problem

Figure G-5 - Landing Distance vs. CL for Various Approach Velocities

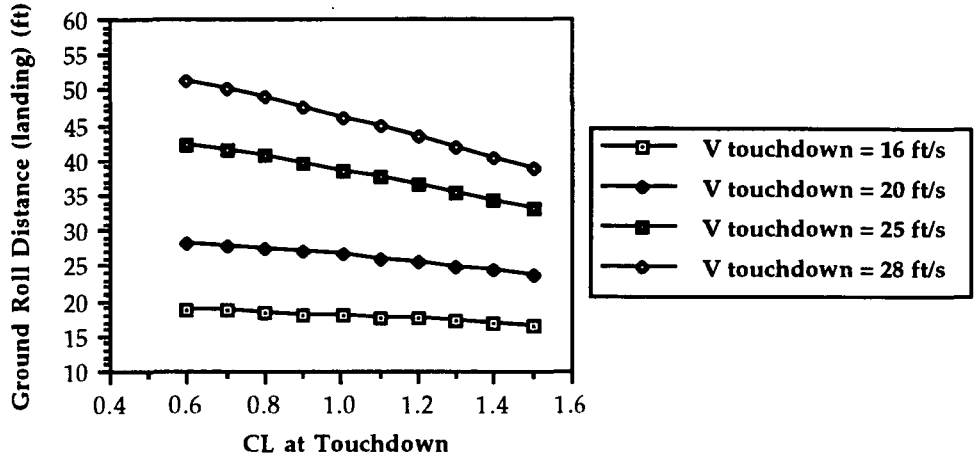

can be explained by the fact that the aircraft was not designed to use brakes on the landing gear. In a final design, breaks will be included thus providing landing ground roll distances of well under the 20 ft airport requirement. The RTL-46 prototype, however will not incorporate breaks into the design.

G.5 - POWER REQUIRED AND AVAILABLE

The power required and available ranges for the RTL -46 were required in order to gather information on the performance of the propulsion system. These values were calculated using Reference [3] for a variety of throttle voltage settings and velocities. The results of this analysis are shown in Figure G-6. This figure shows the maximum and minimum flight velocities (54 ft/s and 6 ft/s, respectively). Also, the cruise point at 35 ft/s is shown as the point where the power available and required graphs meet.

Figure G-6 - Power Available and Power Required vs. Velocity

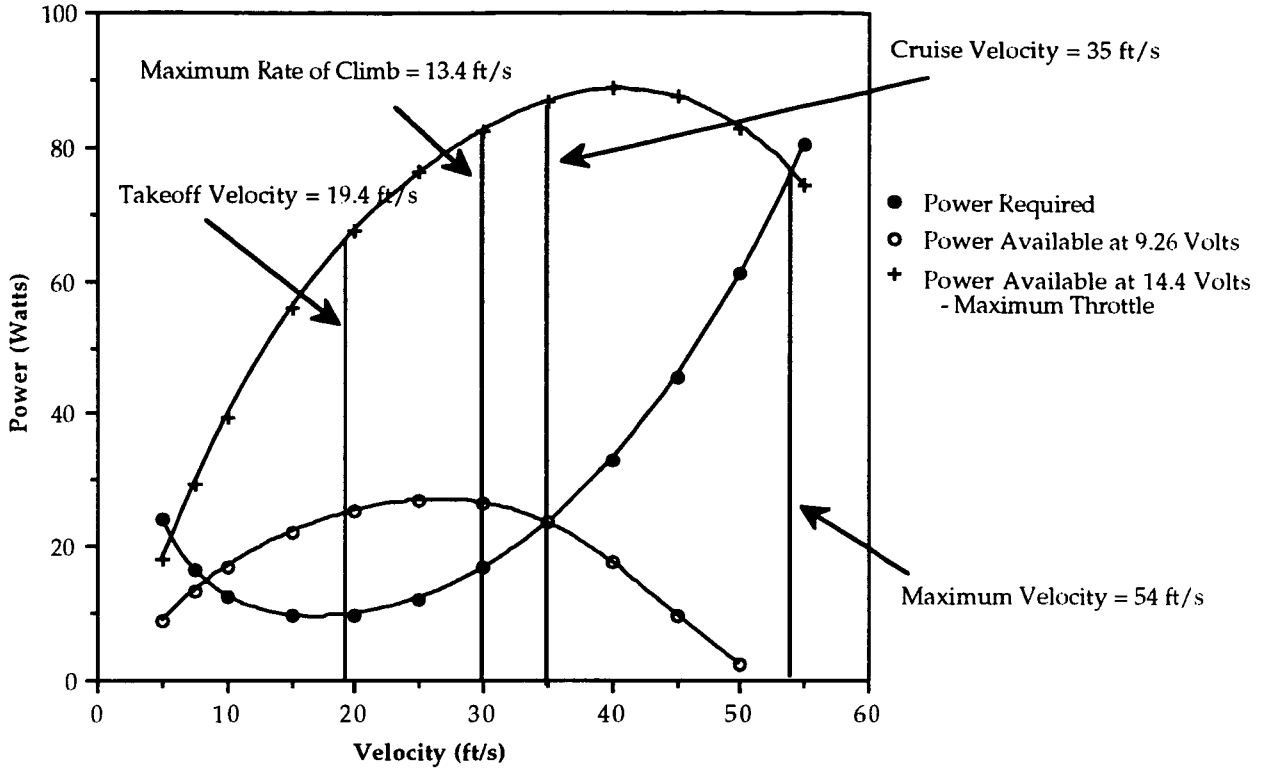

G.6 - CLIMBING AND GLIDING

The initial climb phase after takeoff will be performed at the maximum throttle voltage of 14.4 volts in order to achieve the design altitude of 25 ft as quickly as possible. At the takeoff velocity of 20.3 ft/s, this power setting will result in a 12 ft/s rate of climb. Immediately after liftoff, the rate of climb will increase as the velocity increases. Once a velocity of 30 ft/s has been reached, the rate of climb will be at its maximum of 13.4 ft/s. These rates of climb will produce a total time to design altitude of approximately 2 seconds.

Because of the possibility of complete motor failure, the glide performance was evaluated for the RTL-46 aircraft. These calculations were made using the information provided in Reference [10]. The minimum glide angle was calculated with the following relationship:

$$\tan \gamma_{min} = 1/(C_L/C_D)_{max}$$

where γ is the glide angle. With the maximum lift-to-drag ratio of 14.0, the minimum glide angle was calculated as 4.1 degrees. This corresponded to a maximum horizontal distance of 359 feet for a glide starting at a motor failure altitude of 25 feet.

G.7 - RANGE AND ENDURANCE

For the cruise condition at 35 ft/s, the battery capacity and current draw determined the maximum flight time (endurance) and range at cruise according to the following relationship:

$$\text{Endurance} = (\text{Battery Capacity})/(i_a)$$

where i_a is the cruise current draw. At cruise, it was found that the endurance would equal 9.3 minutes, and its corresponding range would be 19,451 ft.

In order to find the aircraft's maximum range and endurance, the motor/propeller analysis spreadsheet Reference [3] was used to calculate the range and endurance at different cruise conditions. The results of this analysis have been presented in Figure G-4:

This figure shows that the maximum endurance occurred at a velocity of 20 ft/s and was equal to 13.5 minutes. The corresponding range for this condition was 16,224 feet. The maximum range for the aircraft occurred at 30 ft/s and was equal to 19,788 feet, with a corresponding endurance of 11 minutes.

Figure G-7 - Range and Endurance vs. Velocity

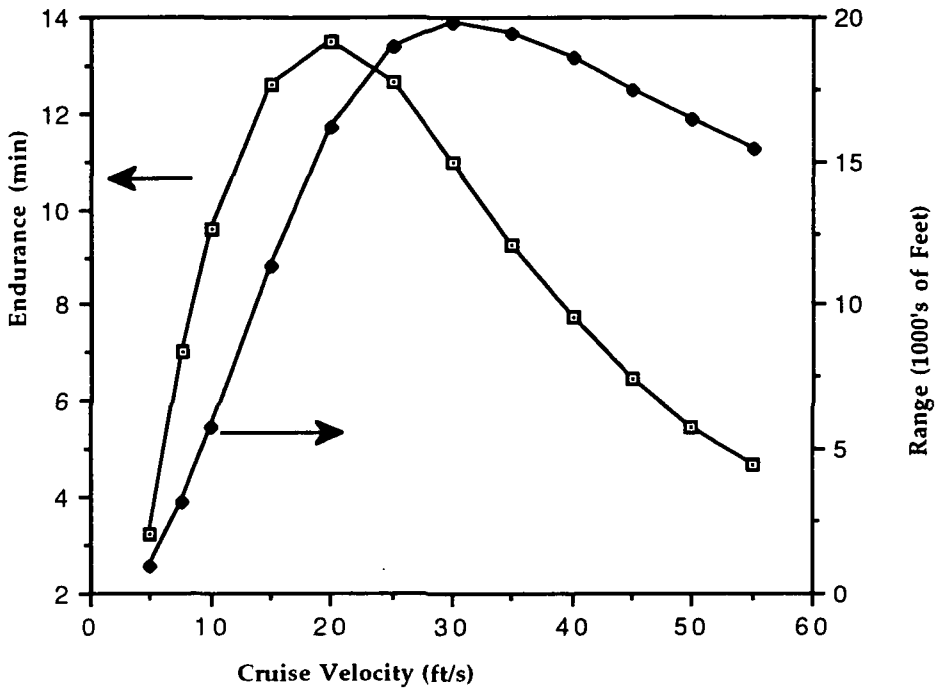

H. STRUCTURAL DESIGN DETAIL

H.1 - DESIGN OBJECTIVES

The goal of the design team was to design the structure of the aircraft in such a fashion as to provide the necessary support to maintain the structural integrity of the aircraft subjected to various expected maximum loading conditions. To accomplish this, the following objectives were formulated in accordance with all design group's input as to the design of the aircraft; in particular the aerodynamics and weight groups because their input has a direct bearing on the structural design.

Objectives:

- Design the structure to maintain the structural integrity of the aircraft under all expected loads, including
  - Normal maximum and minimum flight load factors of 2.0 and -1.5 respectively
  - Maximum ground loading of 3.0 G's due to accelerations caused by impact or hard landings
  - A 1.25 factor of safety above the expected normal loads
- Provide necessary space for 100 people, including passengers and flight crew
- Integrate the various components of the aircraft in a simple and straightforward manner to allow easy access to the various aircraft systems
- Design the structure for a maximum take-off weight of no more than 4.9 pounds to achieve the desired takeoff performance
- Design the structure so that it lends itself to minimizing the cost of manufacturing the aircraft

H.2 - LOAD ESTIMATIONS

Before structural design could begin it was necessary to obtain estimations of the loads acting upon the aircraft. It is important to note that there are many loading conditions beyond flight loads. The most noteworthy of these are the loads experienced on the ground, while at rest or even under severe conditions such as hard landings or crashes. As it turns out, the wing is governed by flight loads, while the design of the fuselage is dictated by the ground loads it experiences. This is primarily because the

wing experiences loads due to the lift distribution which the fuselage does not. It should be noted the fuselage experiences aerodynamic loads which the wing does not--for example the load caused by the lift force on the horizontal stabilizer--but they are minor compared to the effects of the lift distribution on the main wing.

The estimation of the loads on the wing at various flight conditions was obtained from the program *LinAir* by Desktop Aeronautics (see Reference 6). The loading distribution was then input into a program (see Appendix 6) developed to determine the shear and bending moments. Figure H.1 shows the bending moments experienced by the wing during operation at normal cruise conditions at a cruise velocity of 35 ft/sec. The rate at which the moment increases rises as the wing root is approached. Thus the root bending moment of the wing is a primary factor governing the design of main wing of the aircraft.

Figure H.1 - Wing Root Bending Moment at Cruise (load factor=1.0, weight=4.9 lbf)

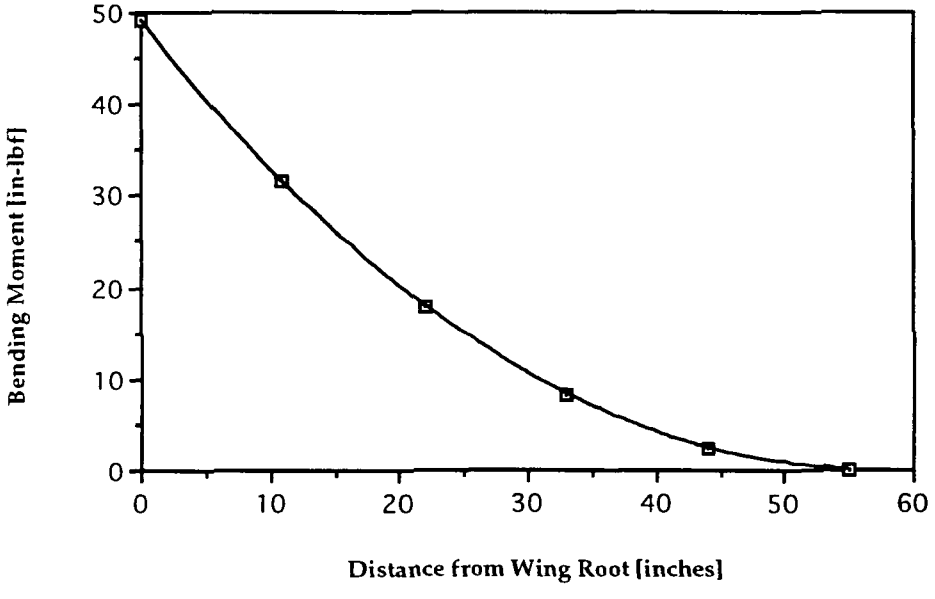

Ground loads are as important to the structural design of the fuselage as flight loads are to the design of the wing. Extreme load factors can be produced by hard

landings. It was desired to design the fuselage to withstand a landing load of three G's. This load factor was determine from a simple dynamic model of a predicted normal landing. The landing model began with the aircraft, at zero vertical velocity, dropping from three inches above the ground. It was assumed the landing gear would deflect one inch to absorb the impact. The acceleration caused by this landing was three G's. Drops from higher heights were considered, but the load factors generated soon became extremely high. A fuselage built to withstand these load factors would be overdesigned in the sense that only a crash or very hard landing would produce the load. It was therefore decided to build the fuselage to withstand a landing as originally modeled.

Figure H.2 - Fuselage Bending Moment Diagram (load factor=3.0, weight=4.9 lbf)

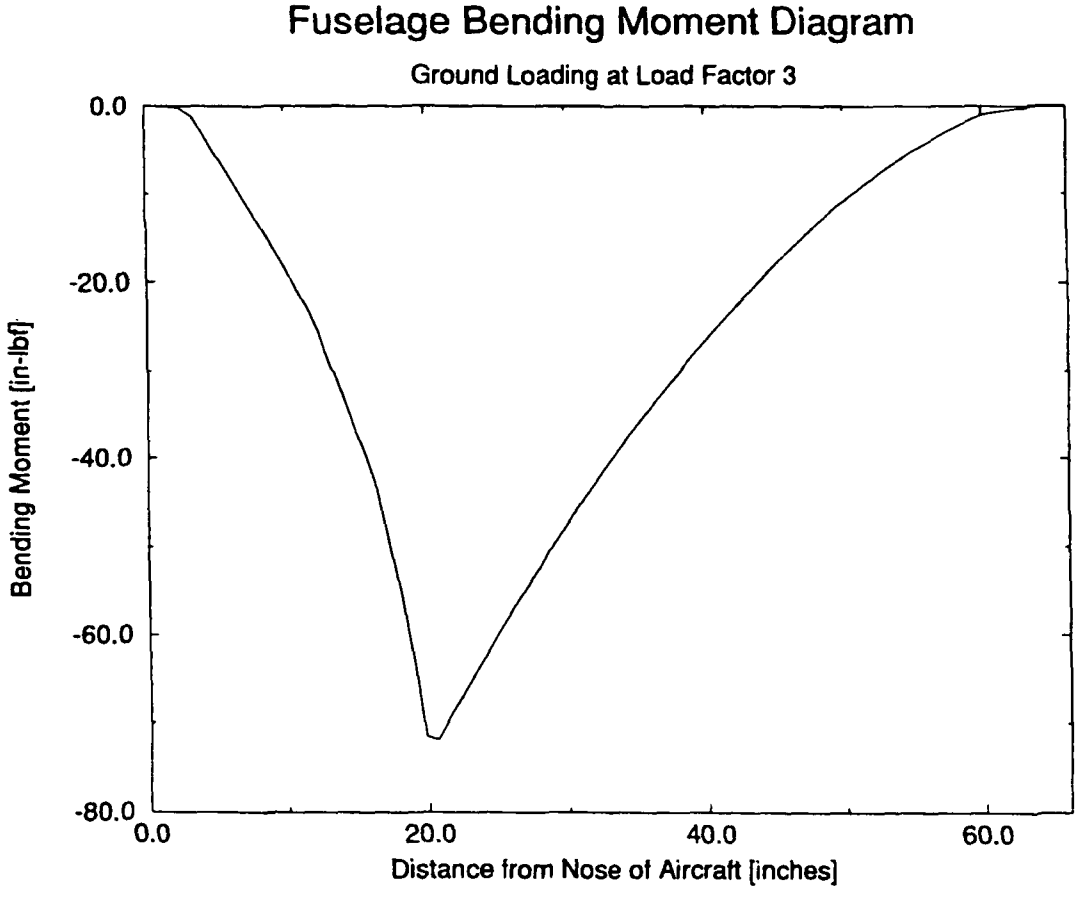

The bending moment experienced by the fuselage, at a landing load of three G's, as a function of distance from the nose of the aircraft is shown in Figure H.2. This

bending moment diagram corresponds to the moments experienced upon landing impact as mentioned previously. Specifically, at this condition the aircraft is not experiencing aerodynamic loads, but only loads produced by the impact. As is clearly indicated, the magnitude of the bending moment is very high at a distance of about twenty inches from the nose. This is because of the high concentration of mass at this point, including the wing and batteries. Thus the structural design of the fuselage must take into account the high stresses caused by the moments in this portion of the fuselage.

A helpful way of determining the flight loads, and thus the critical conditions leading to maximum aerodynamic loads acting upon the aircraft, is the development of a V-n diagram. The V-n diagram for the RTL-46 aircraft at the maximum takeoff weight of 4.9 pounds is shown in Figure H.3. The operating envelope for the fully loaded plane is shown for two flight configurations. The first condition is clean with no flaps deployed. The second condition depicts the aircraft with flaps lowered twenty degrees for a maximum performance take-off. These two conditions lead to two very different operating envelops, marked by differences in stall speed and the achievable load factor.

Once the operating envelop was determined it was possible to find those flight conditions which yielded maximum structural loads. In the case of the RTL-46, the predicted maximum normal structural loading in flight occurred at a flight velocity of 25 ft/sec at a load factor of 2.0 with the flaps lowered. At this flight condition the root bending moment, primarily due to the high lift coefficient developed, was predicted to be 113 inch-pounds.

Also shown on the V-n diagram is a normal load factor and an ultimate load factor. The normal load factor of 2.0 corresponds to the maximum positive load factor expected during normal flight operations. The ultimate load of 2.5 depicts the load factor at which failure of the structure is predicted to occur. Designing the wing for a flight load factor of 2.5 allows for a 1.25 factor of safety.

A final note concerns the load factor at minimum lift coefficients. In the clean configuration the maximum achievable negative load factor is approximately 1.1. With flaps lowered, the wing is not capable of producing negative lift. This means the maximum negative load factor that must be designed for is only 1.1 because the wing will stall before any lower load factors are encountered.

Figure H.3 - V-n Diagram at Maximum Takeoff Weight = 4.9 lbf

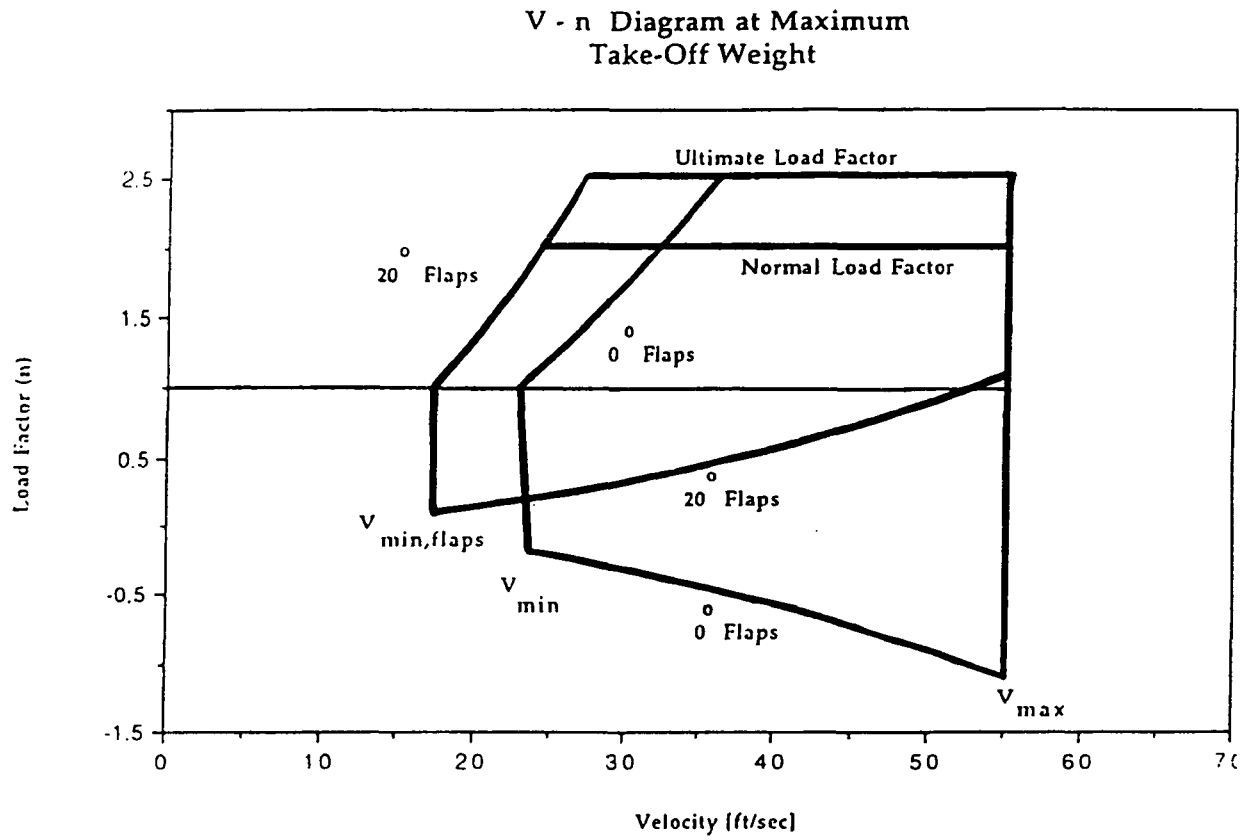

H.3 - PRIMARY COMPONENTS, SUBSTRUCTURES, AND ASSEMBLY

Primary components of the RTL-46 aircraft are the wing, fuselage, empennage, and landing gear. Primary substructures are the wing carry-through structure, the firewall, and the main gear support. Each is discussed in detail below, including characteristics of the component and its integration into the whole aircraft.

Wing: The wing of the RTL-46 is rectangular with no sweep, geometric twist, or aerodynamic twist. The span is 110 inches and the chord is thirteen inches. Wing construction is complicated by the inclusion of full span flaps with a length of 0.25 chord. See Figure H.4 for a schematic of the wing construction.

Figure H.4 - Main Wing and Airfoil Section

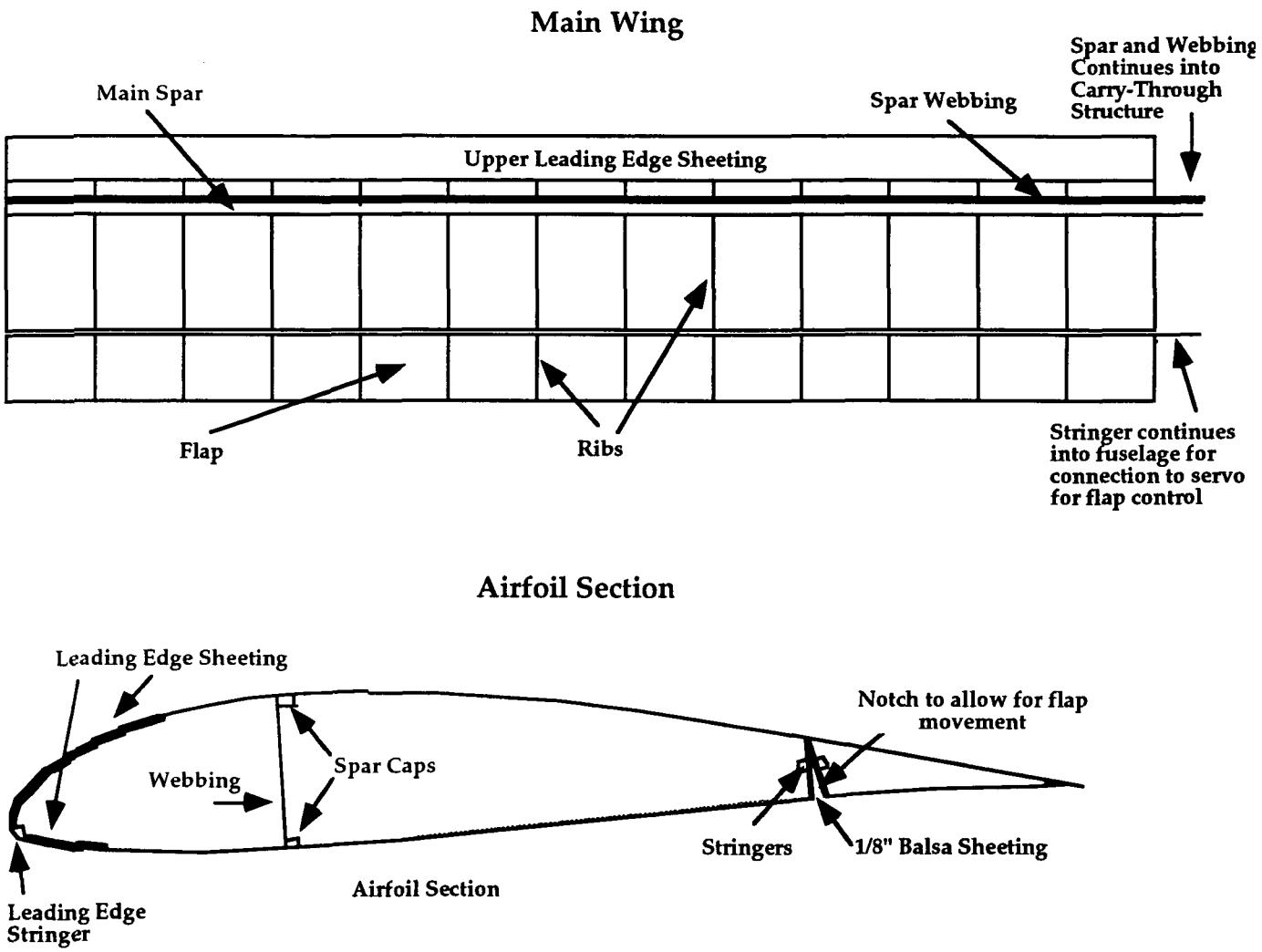

The main spar of the wing is located at 0.25 chord or 3.25 inches from the leading edge. The upper spar cap is 5/16"x1/4" balsa. The lower cap is 3/16"x3/16" balsa. The spar caps are connected by webs made of 1/16 balsa sheeting. Leading-edge sheeting is used on the upper and lower surfaces to maintain the integrity of the airfoil

shape at high curvature between the ribs, which are 4.2 inches apart. The width of the upper and lower sheeting is 2.5 and 1.5 inches respectively. The main spar continues into the wing carry-through structure.

The leading edge of the wing is formed from 1/4"x1/4" balsa sanded to match the shape of the leading edge. The trailing edge of the main wing section is constructed in two parts. The first is a 3/16"x3/16" balsa stringer. The second is a 1/8" thick balsa sheet with a width equal to the airfoil thickness at this point. This cap is necessary to prevent the Monokote covering from sagging too much between ribs at the sharp corner of the trailing edge.

The flap is basically an extension of the main wing. It is formed from the same ribs that make up the main portion of the wing. The leading edge of the flap is identical in construction to the trailing edge of the wing, including the 3/16"x3/16" stringer and 1/8" sheeting. The leading edge of the flap also continues into the fuselage where it connects to the servo linkage. The total weight of the wing is 18.3 oz.

Fuselage: The fuselage serves as the place of attachment for all the other components as well as provides the space for the passengers and all aircraft systems. The basic fuselage construction is shown in Figure H.5. Four longerons run the length of the 6"x6" fuselage, one at each corner. The longerons are 3/16"x3/16" in cross section. Due to the high stresses due to bending in the constant area portion of the fuselage, the longerons here are made of spruce; elsewhere they are balsa. Separating the longerons are 3/16"x3/16" balsa members, running perpendicular to the longerons, on all four sides of the fuselage. Placement of these members was based on the critical buckling length of the longerons at the point of maximum stress (approximately twenty inches from the nose). These members were placed to reinforce the longerons at a spacing less than the critical buckling length to ensure buckling did not occur. Additionally, 3/16"x3/16" diagonal members on the sides of the fuselage support any torsional loads experienced by the fuselage.

Figure H.5 - Fuselage Structural Schematic

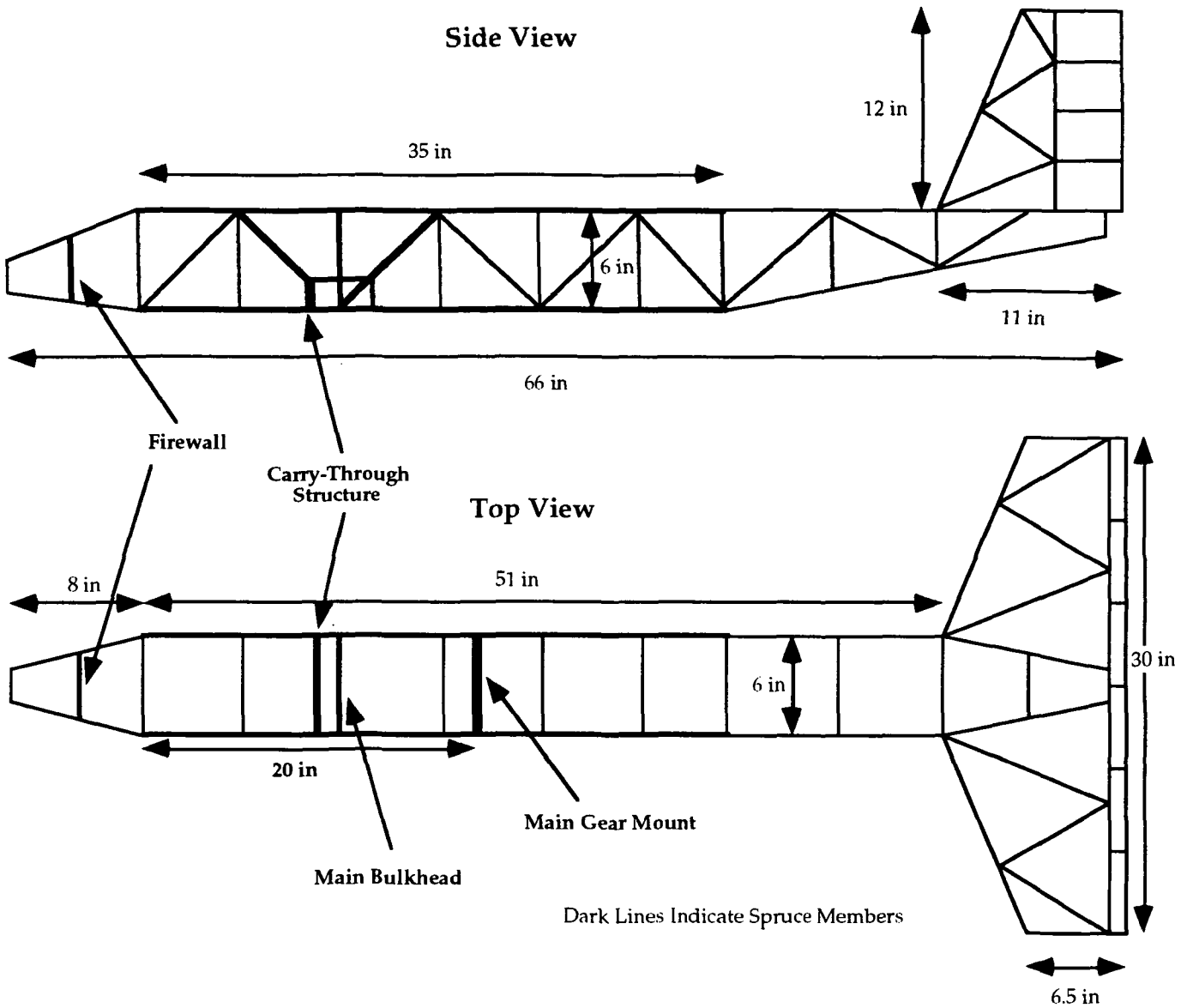

The area where the wing is attached to the fuselage is reinforced as shown in the figure. The wing carry-through structure is attached to these members. Access to this area is through hinged openings in the bottom of the fuselage. The fuselage also contains the firewall substructure to which the engine mount and front landing gear are attached, as will be discussed later. The structural weight of the fuselage is 4.8 oz.

Empennage: Also shown in Figure H.5 is the structure and location of the vertical and horizontal stabilizers. Simple truss-type design is utilized in the main

portions of the stabilizers. The perimeter of the stabilizers are made from 3/16"x3/16" balsa, while the inner truss members are of 3/16"x1/8" balsa. Control surfaces are formed by parallel 3/16"x1/8" pieces of balsa. The carry-through structure for the horizontal stabilizer is simply the continuation of the perimeter structure of the stabilizer through the fuselage. The weight of the empennage is 2.2 oz.

The horizontal stabilizer will be built around the fuselage. Thus the fuselage longerons will form part of the support structure of the horizontal stabilizer. Connection of the vertical stabilizer to the fuselage will be achieve by gluing a continuation of the perimeter structure of the stabilizer into a slot built into the fuselage directly underneath the vertical stabilizer.

Wing Carry-Through Structure: The most important substructure of the aircraft is the wing carry-through structure. This is the structure that connects the wing halves, holds the wing rigid, and supports the bending moments carried to it by the main wing spar.

Composition of the main wing spar is different in the carry-through. The webbing is now 5/16" spruce, which is connected to the main carry-through structure by 3/16" diameter threaded steel bolts. The bolts are held in place by blind nuts that bite into the spruce. The spruce carry-through structure is 1/8" thick, two inches high, and runs the width of the fuselage. Narrow holes are cut in the top and bottom of this structure to provide room for control linkages that run the length of the fuselage. The carry-through structure itself is mounted to the fuselage at the reinforced spruce structure shown on Figure H.5. The carry-through structures weighs 0.4 oz.

Firewall: The firewall is the structure to which the engine mount and nose gear are connected. This 1/8" thick piece of spruce is mounted vertically in the nose of the aircraft at four inches from the tip of the nose. The engine mount is connected to the firewall by four steel bolts. The bracket which holds the nose gear wire is connected to the rear of the firewall, again by steel bolts. The firewall is connected to the structure of

the nose by vertical balsa members which run between the longerons in the nose. Easy access to the firewall will be accomplished through the use of a removable nose section forward of the firewall. The firewall weight is 0.6 oz.

Main Gear Mount: The last substructure is extremely important in supporting the reaction force imparted on the fuselage by the main gear upon landing. The gear mount is a 3/16"x1.5" piece of spruce which runs the width of the fuselage and is glued to the spruce longerons. The gear strut, made of nylon or plastic, is mounted to this structure with screws at a position twenty inches from the nose of the aircraft. Thus the main gear are directly below the mount. The main gear mount weighs 0.3 oz.

Total Aircraft Weight: The weight of the structural components listed above plus the weight of all the other equipment and components is 4.8 pounds. This is 1.6 ounces below the design goal of 4.9 pounds, and leaves room for items not yet taken into account such as bolts, hinges and glue.

H.4 - PRIMARY MATERIAL SELECTION

Two materials, balsa wood and spruce, were chosen to be used in the construction of the structure. Their material properties are given in the following table. Note the direction associated with the axial tension and axial compression strength is along the grain of the wood. See Reference 16 for complete tables of the properties of various woods.

Table H.1 - Selected Properties of Building Materials

Material	Strength [psi] Axial Tension	Axial Compress	Shear	Mod. of Elas. [psi]	Density [lb/in cubed]
Balsa	10.6E3	1.30E3	160	.37E6	.0058
Spruce	12.2E3	4.35E3	770	1.32E6	.016

Balsa wood is by far the most widely used material in the construction of this class of aircraft. Balsa has the highest strength to weight ratio of any wood and is

therefor an excellent choice for a wide range of building applications. Spruce is a good alternative where a high compressive strength is needed to prevent axial compressive failure or buckling. Such is the case in portions of the fuselage longerons. Spruce is also better in places where screws or bolts are to be used. Spruce is much harder than balsa and can more readily support the blind nuts and washers used in such connections. The firewall, wing carry-through structure, and main gear support are examples where spruce is used for this reason, in addition to higher strength.

Other woods that have commonly been used in the past, such as bass, were not considered simply because there was no demand for their higher strength. Sole use of balsa and spruce results in a substantial weight savings since these materials are less dense than other hardwoods.

Another important material not listed in the above table is the Monokote covering material. This material was not modeled in any of the analyses, but it is quite strong in tension and shear and will definitely add to the structural strength of the aircraft, as well as maintaining the desired shape of the aircraft between wooden supports.

H.5 - STRESS ANALYSIS

A stress analysis was performed on all of the load carrying components. The primary load paths occur along the wing spar, fuselage longerons, wing carry-through structure, and main gear support structure. In the case of the wing and fuselage, the structure was modeled as a statically determinate beam. Bending moments (See Figure H.1 and H.2) along the length of the beam were determined analytically from a computer routine developed specifically for this purpose. Another computer code determined the direct stress due to bending at specified cross-sections along the length of the beam. Idealized lumped areas were used to model the longerons in the fuselage and the spar caps and leading and trailing edges in the main wing. Using these

analytical techniques, the minimum size of load bearing components needed to withstand the predicted loads could be calculated. See Appendix 6 for listings of all computer codes used in the structural analysis.

In the case of the substructures such as the wing carry-through and main gear support, other techniques were used to determine the stresses which could lead to failure. The wing carry-through was modeled as a beam subjected to the root bending moment of the wing. For the carry-through structure then,

$$\sigma_{max} = \frac{Mc}{I}$$

where the bending moment (M), the distance to the neutral axis (c), and the moment of inertia (I) are known. For the main gear support the shear stress in the longerons to which it is connected was analyzed. Presented in the following table is a summary of the stresses under normal loads, the maximum stresses that can be carried, and the factor of safety, for the various load bearing members. Note that the maximum stress for the wing spar and wing carry-through occur with flaps fully deflected at a flight velocity of 25 ft/sec at load factor of 2.0, while the maximum stresses in the fuselage longerons and the main gear brace occur during the landing load factor of three G's.

Table H.2 - Stress Analysis Summary

Component	Normal Stress [psi]	Max. Stress [psi]	Factor of Safety
Wing Spar	965	1300	1.35
Longeron (spruce)	2096	4350	2.08
Longeron (balsa)	603	1300	2.16
Carry-Through	648	4350	5.71
Main Gear Brace	39.2	770	18.6

The factors of safety for the carry-through structure and the main gear support are very high. The necessity of using spruce in these structures to support the bolts and

blind nuts in these areas lead to the high factors of safety. It is apparent the aircraft will first fail structurally in the wing spar or in the fuselage longerons before any of load bearing subsystems. Overall, the factors of safety are very reasonable. The factor for the wing spar of 1.35 is close to the 1.25 limit imposed on manned aircraft, although the actual factor of safety is higher because there are structural materials such as Monokote and spar webbing unaccounted for in the model. The larger factor of safety of the fuselage is beneficial in that the landing loads are very unpredictable without knowing the exact material properties and behavior of the landing gear. Therefor a larger factor of safety may save the aircraft from a particularly hard landing or underestimation of landing loads.

It is important to note that although bending moments were the structural design drivers, the shear forces and buckling loads in the wing spar and fuselage longerons were also checked to ensure they did not exceed the maximum allowable limits. The fuselage was examined at the critical load condition of a three G landing. The wing was examined at the flight condition which produced the highest compressive stress in the leading and trailing edge. This occurred while flying at the highest achievable negative load factor of 1.1 at a the maximum flight velocity of 55 ft/sec in the clean configuration. The buckling analysis assumed fixed end conditions.

Table H.3 - Shear and Buckling Analysis

Component	Max. Predicted Shear [psi]	Max. Allowable Shear [psi]	Critical Buckling Length [inches]
Wing Leading Edge	20.8	160	7.3
Wing Trailing Edge	20.8	160	24.3
Longeron (spruce)	78.6	770	8.5
Longeron (balsa)	3.9	160	8.4

It as clear from these results the maximum allowable shear stress is not exceeded in any portion of the structure. Additionally, the critical buckling length of each of the structural components is not exceeded because they are reinforced at intervals less than the buckling length. In the wing the ribs are spaced at 4.2 inches, well under the leading edge buckling length of 7.3 inches. Similarly, the fuselage longerons are reinforced at intervals less than 8.4 inches. The spar was not checked for buckling as it is reinforced continuously by the spar webbing. The spar has a maximum shear stress of 20.8 psi, which, like the leading and trailing edge, is well below the maximum allowable shear stress of 160 psi.

H.6 - LANDING GEAR

The last major structural component to be considered was the landing gear. The gear configuration is shown in Figure H.6. The RTL-46 employs a tricycle gear configuration. As mentioned before, the stearable nose wheel is mounted to the back of the firewall, and the main gear are braced by a spruce structure located on the bottom of the fuselage, between the longerons.

Figure H.6 - Landing Gear Schematic

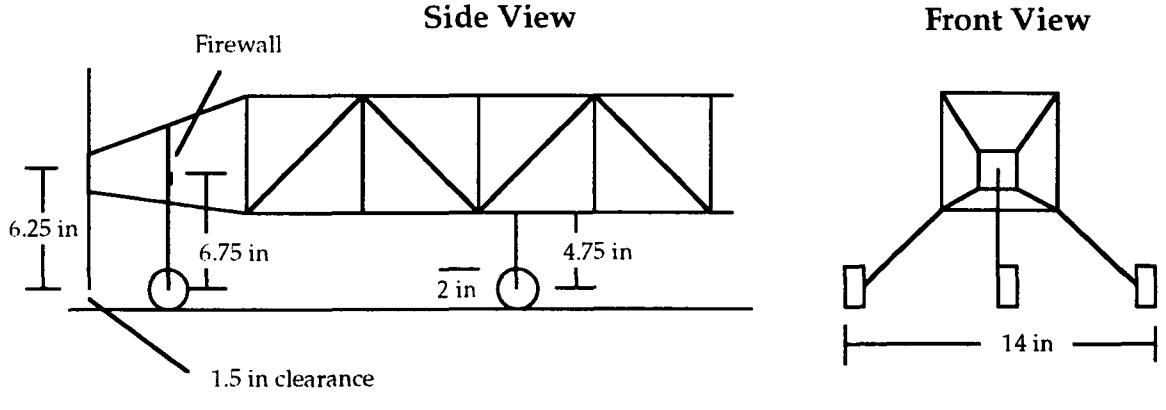

The governing constraint in the design of the gear was propeller clearance. It was decided to allow 1.5 inches between the propeller tip and the ground. The fuselage is to be kept level while on the ground. With two-inch diameter foam wheels, this

requires a front nose wheel strut length of 6.75 inches as measured from the mounting bracket on the firewall, and main gear struts that are 8.46 inches long to provide a clearance of 4.75 inches from the fuselage and a distance between the wheels of fourteen inches. The diameter of two inches was chosen because it was decided that gear of this size were the minimum required to smoothly roll over the runway surface.

Based on previous model experience with aircraft of this class, an assumption was made to arrive at this design. The gear deflection was estimated to be one inch upon a hard landing. This still leaves 0.5 inches of propeller clearance. In reality, the main gear will compress more than the nose gear, in effect helping to keep the propeller out from hitting the ground.

H.7 - SUMMARY

Design of the aircraft structure began with an examination of the loads acting on the plane in various configurations in the air and on the ground. Once these loads were known, a stress analysis of the load carrying components was carried out. It was then a relatively straightforward matter to select the materials and to size the components. The result is a structure capable of withstanding all expected normal loads, and flight loads up to 1.25 those predicted, and ground loads up to 2.0 times the predicted loads. Manufacturing costs were kept in mind during the design process. Wherever possible, the same size and type of materials were used to help reduce waste. Straightforward methods of assembly were developed and access to various systems was simplified through the use of removable access panels. Integration of flaps as high lift devices for increased takeoff performance was obtained. Finally, the maximum takeoff weight of 4.9 pounds was achieved. Thus accomplishment of the design goals yields a structure that is lightweight, simple and cost-effective to manufacture, and easily accessible. Overall, the design helps achieve characteristics which will allow the RTL-46 to outperform the current market leader.

I. ECONOMIC ANALYSIS

I. 0 - GENERAL OVERVIEW

The economics of the RTL-46 were one of the more important driving factors in design decisions. Such major decisions such as passenger load, range, cruise velocity, manufacturing plans and motor selection hinged on economic repercussions. The design point for the aircraft (100 passengers, cruise velocity of 35 ft/s, range of 13000 feet) produced a CPSPK(cost per seat per thousand feet of travel) of 0.42cents, a value 57% less than the HB-40. Achievement of this reduction in cost was done by increasing the cruise velocity and passenger load, while decreasing production costs.

I.1- CPSPK EVALUATION

The CPSPK was the calculated figure of merit for economic evaluation. The CPSPK was derived by using the DOC(direct operating cost) and dividing by the number of passengers and the range (in thousands of feet.) The DOC was the sum of the Depreciation Costs, the Operational Costs and the Fuel Costs. The lower bound of the CPSPK is obviously the preferred value. The Depreciation Costs accounted for 76% of the overall DOC. The other 24% were incurred by the Operational and Fuel Costs. The way these values are optimized is greatly effected by the range of the flight the passenger loading and cruise velocity. Figure I-1 illustrates the relationship of the three parameters and shows the overall trend of decreasing CPSPK by increasing passenger load, increasing cruise velocity and increasing range.

FIGURE I-1

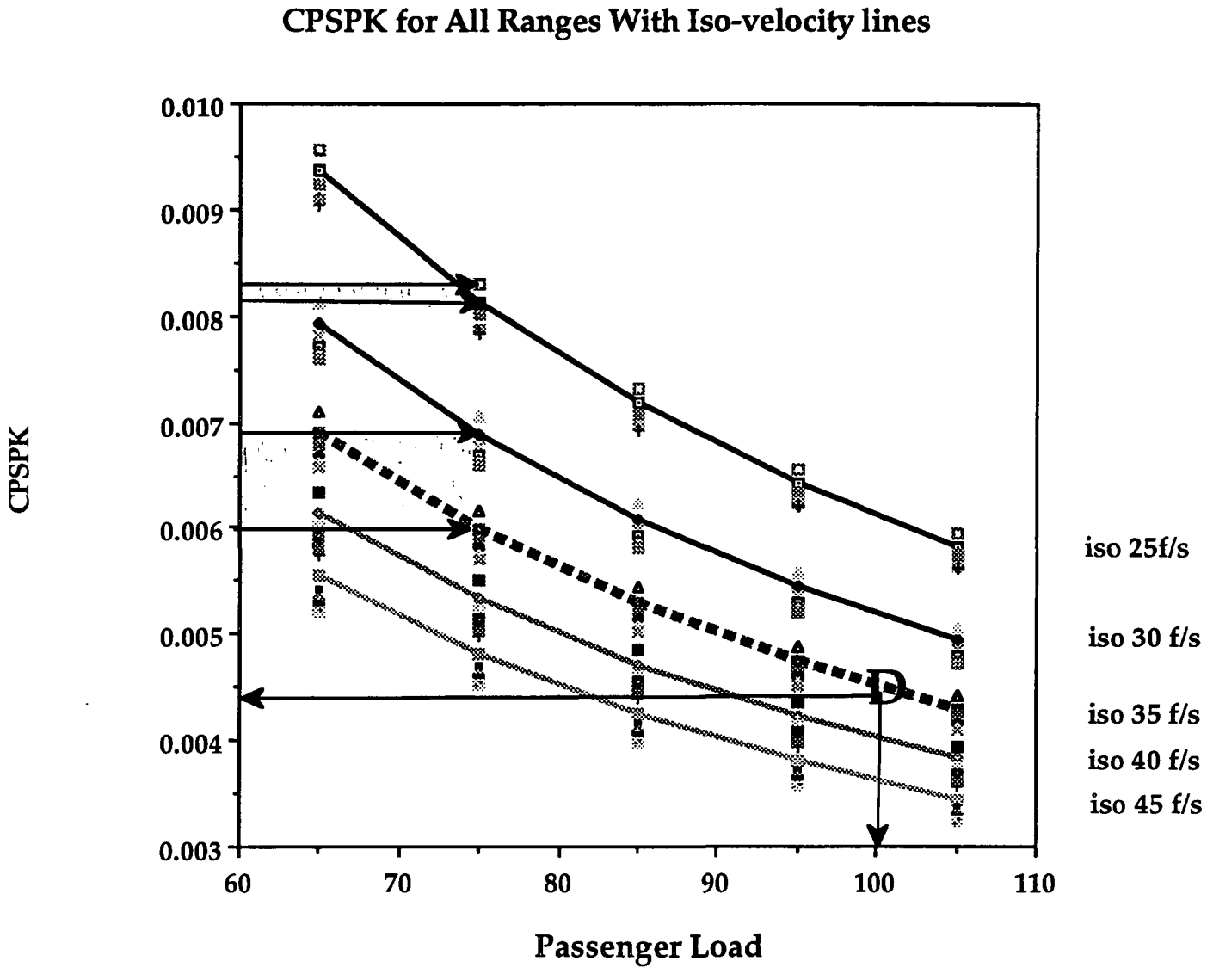

Analysis of the shaded regions on Figure I-1 showed that a 5% increase in passenger load decreased the CPSPK by 11% while a 5% increase in range only decreased the CPSPK by 6%. This shifted emphasis of design to the maximum payload within reasonable bounds. Those reasonable bounds were based primarily on volume maximums for the fuselage. The same shaded regions showed that the same range increase was not as beneficial as a 5% increase in

cruise velocity. Therefore, a rank of design parameters driven by their influence on the CPSPK was derived and assessed. The most important was the cruise velocity. Although there were penalties in L/D and Fuel Costs due to the selection of cruise velocity based on economics the overall decrease in the figure of merit exceeded 23%.

A second figure of merit was introduced by our economics department which relates the actual CPPPK(Cost Per Passenger Per Thousand Feet.) This new figure of merit is used to illustrate the incurred cost of flying at less than 100% capacity. Market analysis showed that RTL-46 would be flying at no less than 70% capacity, with an overall average capacity in excess of 76% for a single day's flights to all 15 airports on the specified flight per day schedule. This translated the CPSPK to a CPPPK of 0.51cents, most notably, still 45% less than the HB-40.

I.2 DIRECT OPERATING COSTS

The DOC for the aircraft was the sum of three influential costs. The Depreciation Costs, which were based on the production of the aircraft, the Operational Costs, which were driven mainly by the Crew Costs, and the fuel Costs, which were dependent on many factors, are the three influential costs driving the overall DOC.

I.2-a DEPRECIATION COSTS

The Depreciation Cost dominated the DOC of the aircraft. The single most important factor was the Cost per Aircraft. This was an accumulated cost of production, materials and wastes. Table I.1 shows the breakdown of the Cost per Aircraft factors. This lead to an estimation of the Cost per Aircraft for the Depreciation Cost.

TABLE I.1

Fixed Subsystems	$430
Raw Materials Cost	$120
Manufacturing Cost (person hrs)	$1000
(tooling)	$105
Disposal of Hazardous Mat.	$325
Change Orders	$205
TOTAL	$2185 +/- $150

The **fixed subsystem** cost accounts for the control subsystems and their support. The number of servos, the motor selection and the number of fuel batteries are the only variable quantities involved in this quantity. The raw materials cost was taken from the data base with preliminary estimates of additional costs due to steerable landing gear and the materials for the flap configuration.

Manufacturing costs were emphasized throughout the design process. **Tooling** costs were assumed to be slightly higher due to the advanced technology involved in the aircraft's design and mass production of parts to decrease person hours. The **person hour** estimate is based primarily on an efficient production plan, an emphasis on ease of manufacturing during the design process and experience of team members in the field of RPV production.

The **disposal and hazardous material** costs were assumed to be similar if not lower than that of the data base. A round number that the team felt was a conservative estimate was 15% of the overall cost of the aircraft. With the detailed design production layout the disposal and hazardous material costs will most likely be less than the estimated 15%. **Change order** costs were also

estimated using a baseline percentage of the overall aircraft cost. The estimate for these costs was 10%.

The cost of production of the aircraft is expected to vary from estimates based on the difficulty of analysis before the production stage of the design. Therefore there is a conservative $150 uncertainty added to the Cost per Aircraft estimation. An overall decrease in Cost per Aircraft of 14% was gained over the HB-40 through careful planing and experience.

FIGURE I-2

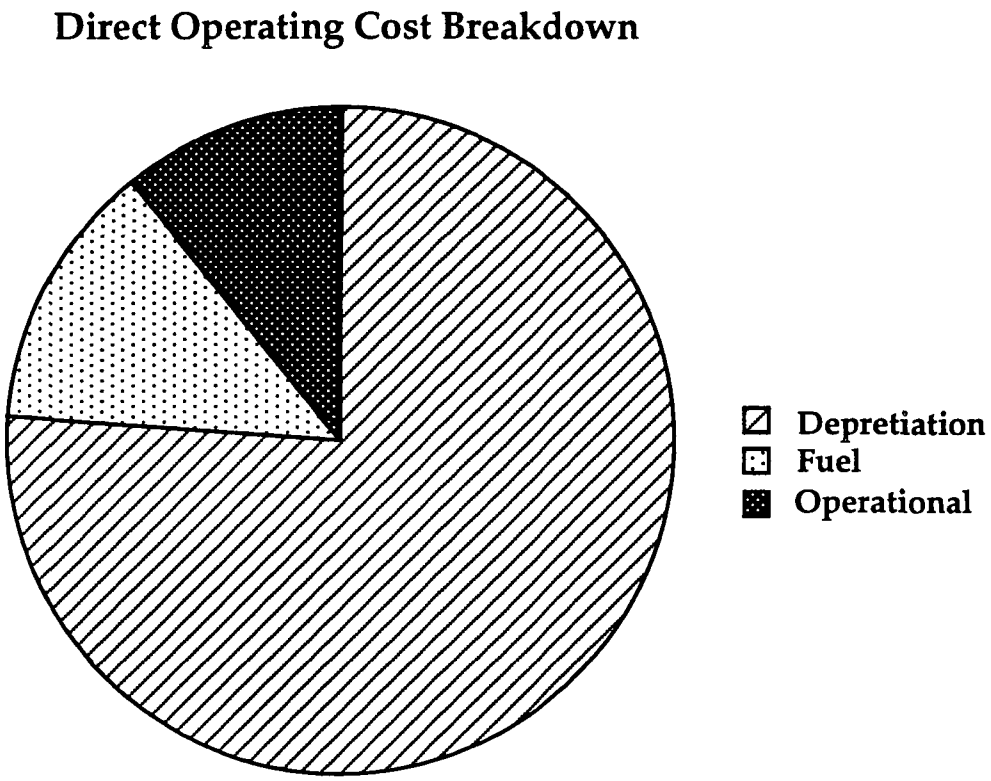

I.2-b. OPERATIONAL COSTS

Over 10% of the DOC was due to the Operational Costs. The Operational Costs were influenced most by the 'Flight Crew' costs. This was a static cost

based on the number of servos used for control systems. The aircraft, originally designed to have five servos, has four control servos which decreased the overall DOC by 5%. The Maintenance costs for the aircraft were dependent on the class of seating and the time of flight. The two quantities were summed to get an Operational Cost at the design point of $0.454, 89% of which was attributed to the Flight Crew Cost.

I.2-c FUEL COSTS

The Fuel Costs were responsible for 13% of the DOC. The Fuel Costs consisted of the Current Draw multiplied by the flight time and the constant FAC3. The Fuel Costs for the aircraft at the design point were $0.75. The Current Draw was dependent on many factors. The maximum takeoff weight was multiplied by the flight velocity and a units conversion factor of 1.36. This quantity was divided by the Lift over Drag ratio, the propulsion efficiency and the throttle voltage. The propulsion efficiency for the aircraft's system was the product of the propeller efficiency, the motor efficiency and the gear efficiency, 0.45. Using the throttle voltage for cruise, 9.3V, the Current Draw was 4.85 A/hr. The Fuel Costs were relatively static based on such numbers as design L/D, the Max T.O. Weight, and efficiencies.

APPENDIX 1 - FIGURES

- RANGE-PAYLOAD DIAGRAM
- AIRFOIL LIFT CURVE WITH C_{Lmax} INDICATED
- AIRCRAFT LIFT CURVE WITH C_{Lmax} INDICATED (WITH HIGH LIFT DEVICES)
- AIRCRAFT DRAG POLAR - FOR BASIC CONFIGURATION WITH TABULAR COMPONENT DRAG BREAKDOWN
- L/D CURVE FOR COMPLETE AIRCRAFT
- PITCHING MOMENT COEFFICIENT VS. ALPHA FOR THE MOST FORWARD AND AFT CG POSITIONS
- POWER REQUIRED AND POWER AVAILABLE VS. FLIGHT SPEED FOR ENTIRE FLIGHT REGIME
- PROPELLER EFFICIENCY VS. ADVANCE RATIO
- WEIGHT/BALANCE DIAGRAM
- WEIGHT ESTIMATE FOR EACH COMPONENT
- V-N DIAGRAM
- DETAILED THREE VIEW EXTERNAL SCHEMATIC
- DETAILED TWO VIEW INTERNAL DRAWING

Range - Total Weight Diagram

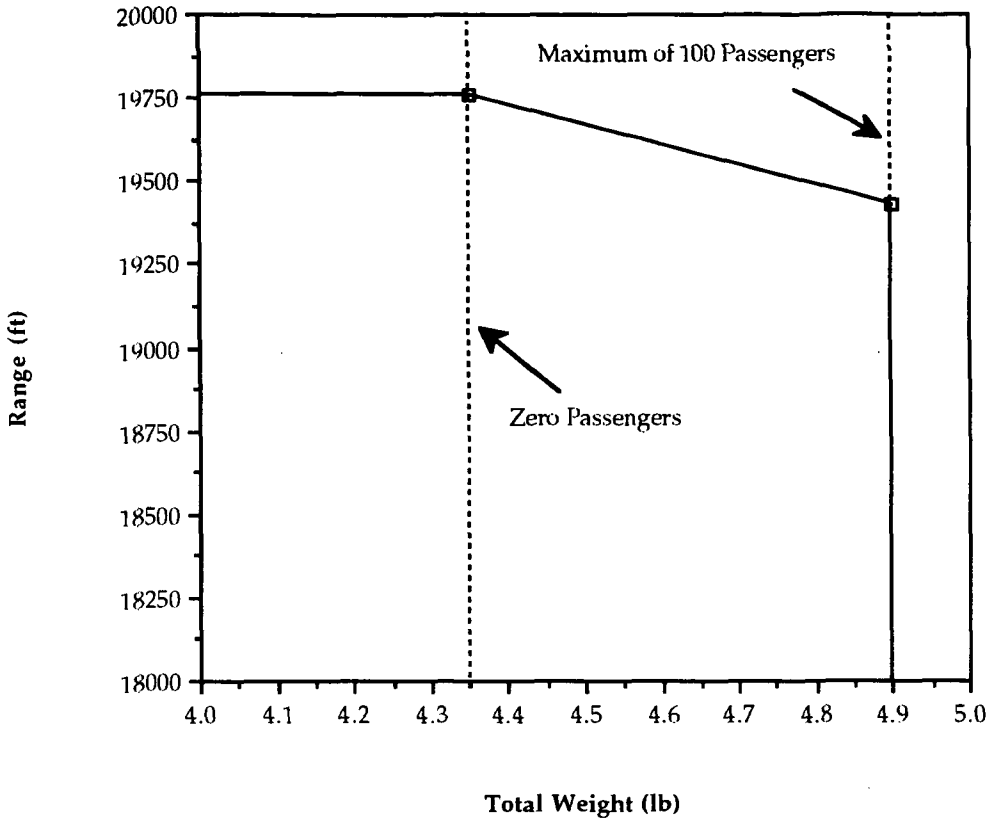

Lift Curve for the SD7062 Airfoil (AR = 8.46)
With and Without Flaps Deflected 20 degrees

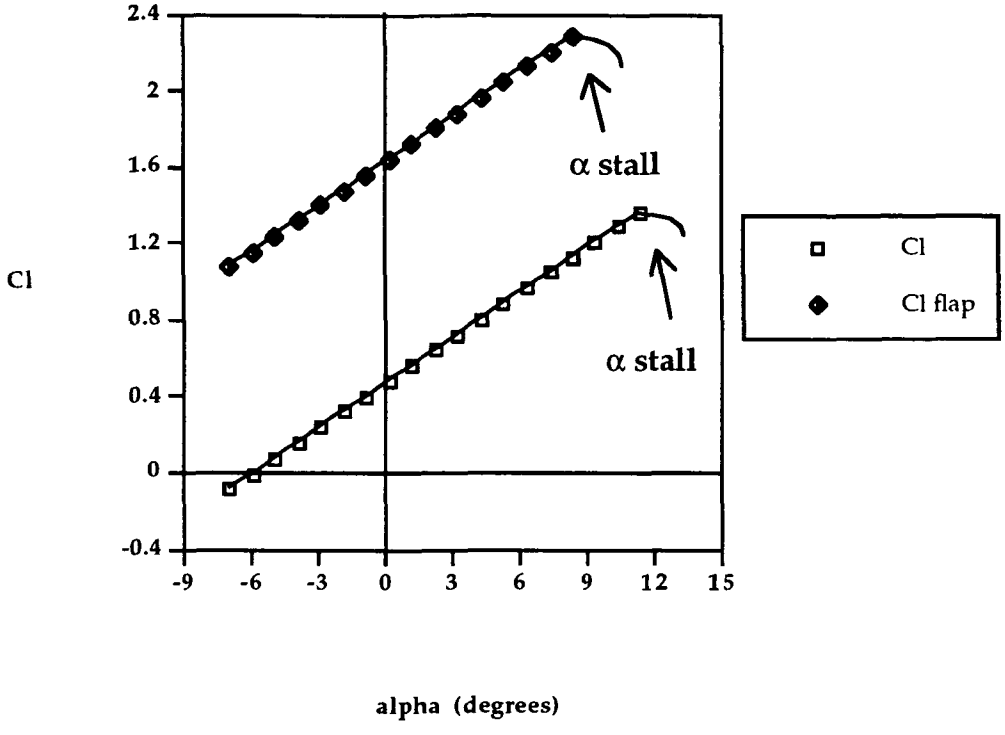

RTL-46 Aircraft Lift Curve
With and Without Flaps Deflected 20 degrees

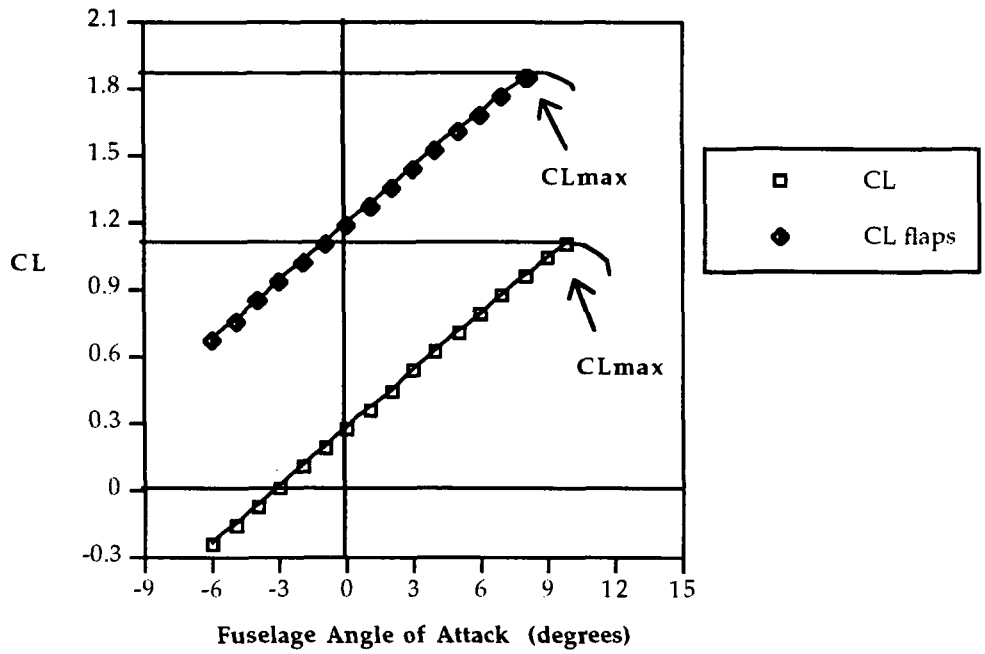

RTL-46 Aircraft Drag Polar
With and Without Flaps Deflected 20 degrees

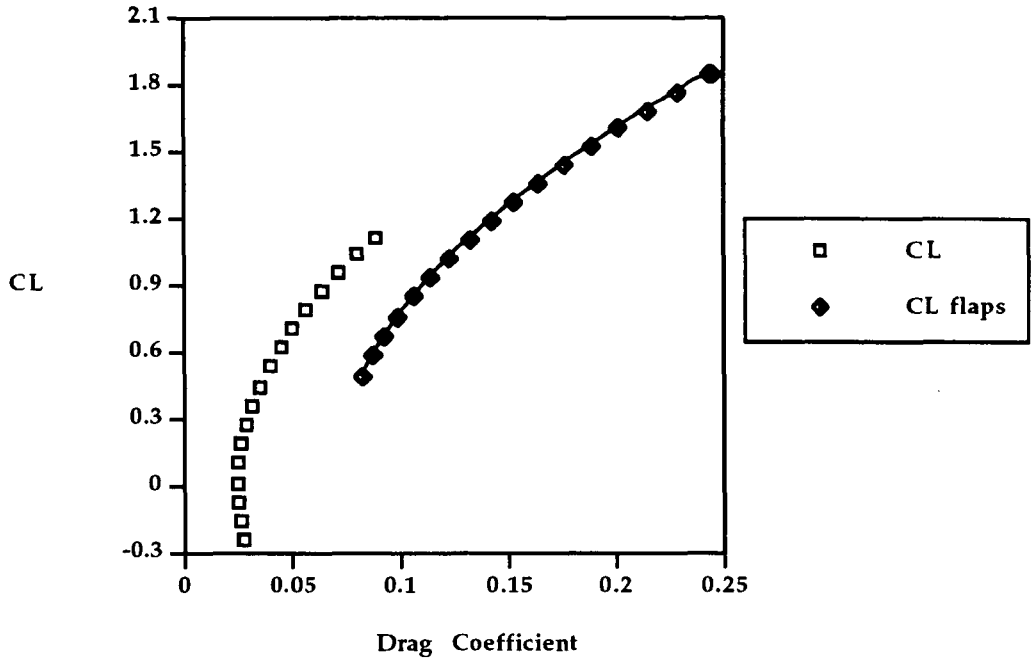

RTL-46 Aircraft Drag Breakdown

Component	$C_{D\pi}$	A_{π}	% of total drag
Fuselage- frontal area component	0.11	0.25	
Fuselage- surface area component	0.0033	9.223	
Fuselage- total %			29
Front landing gear	0.25	0.0348	4
Back landing gear	0.5	0.0919	24
Wing	0.007	9.93	35
Horizontal tail	0.008	1.458	5
Vertical tail	0.008	0.729	3
Interference	20%		

RTL-46 Aircraft Lift to Drag Ratio

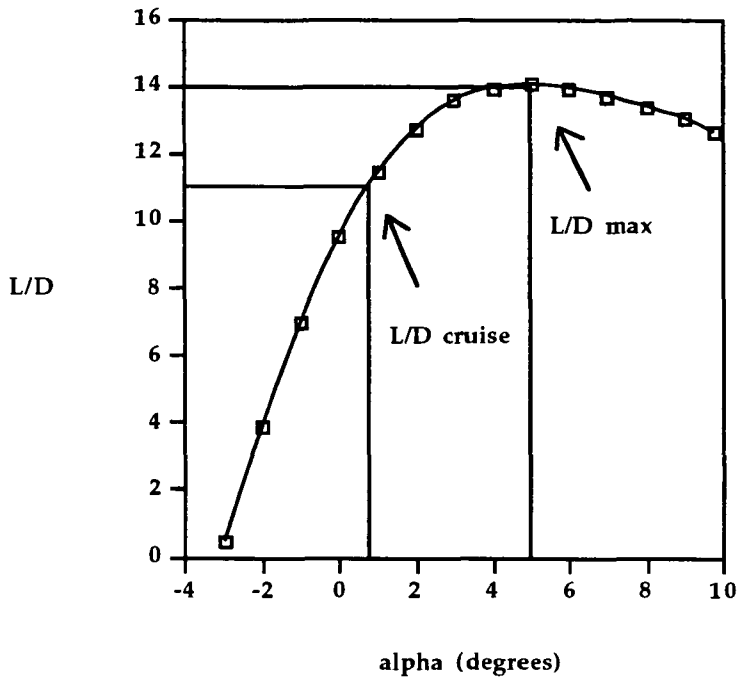

Pitching moment coefficient vs. α (forward and aft c.g. positions)

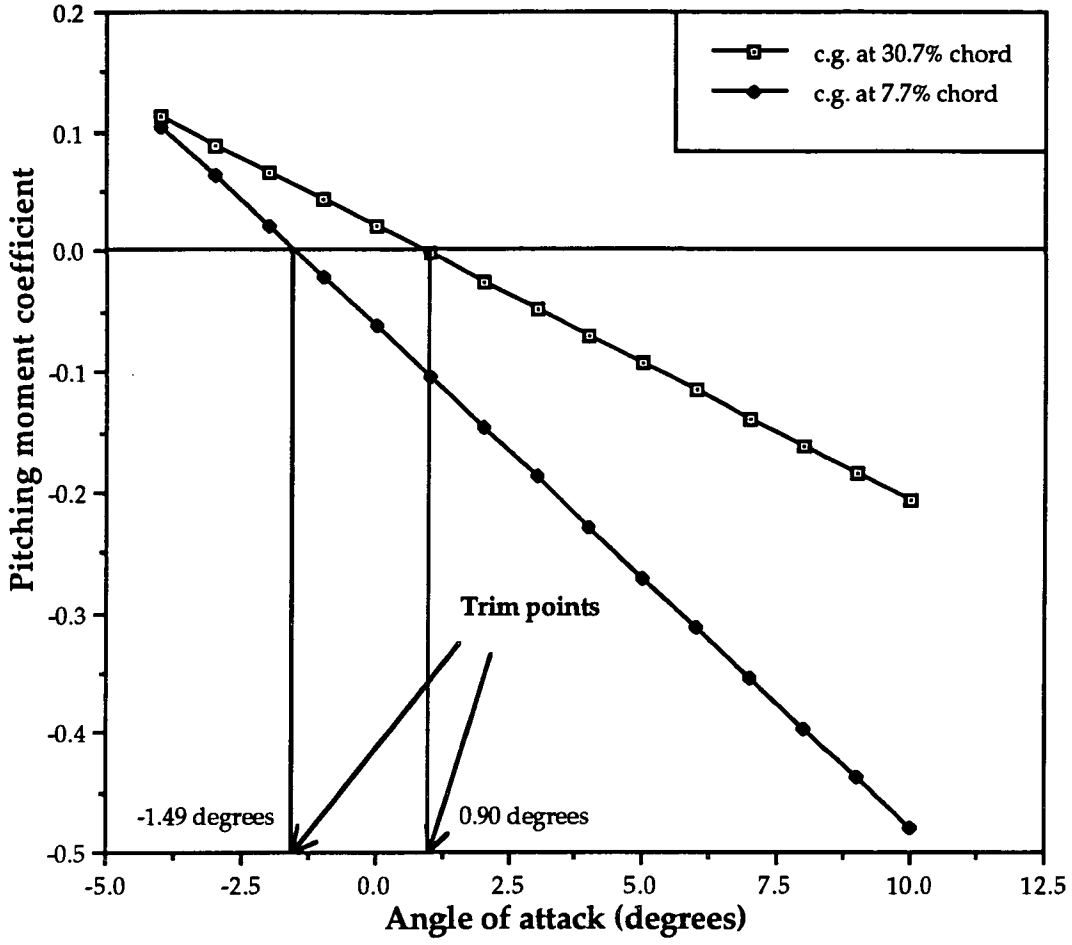

Power Available and Power Required vs Velocity

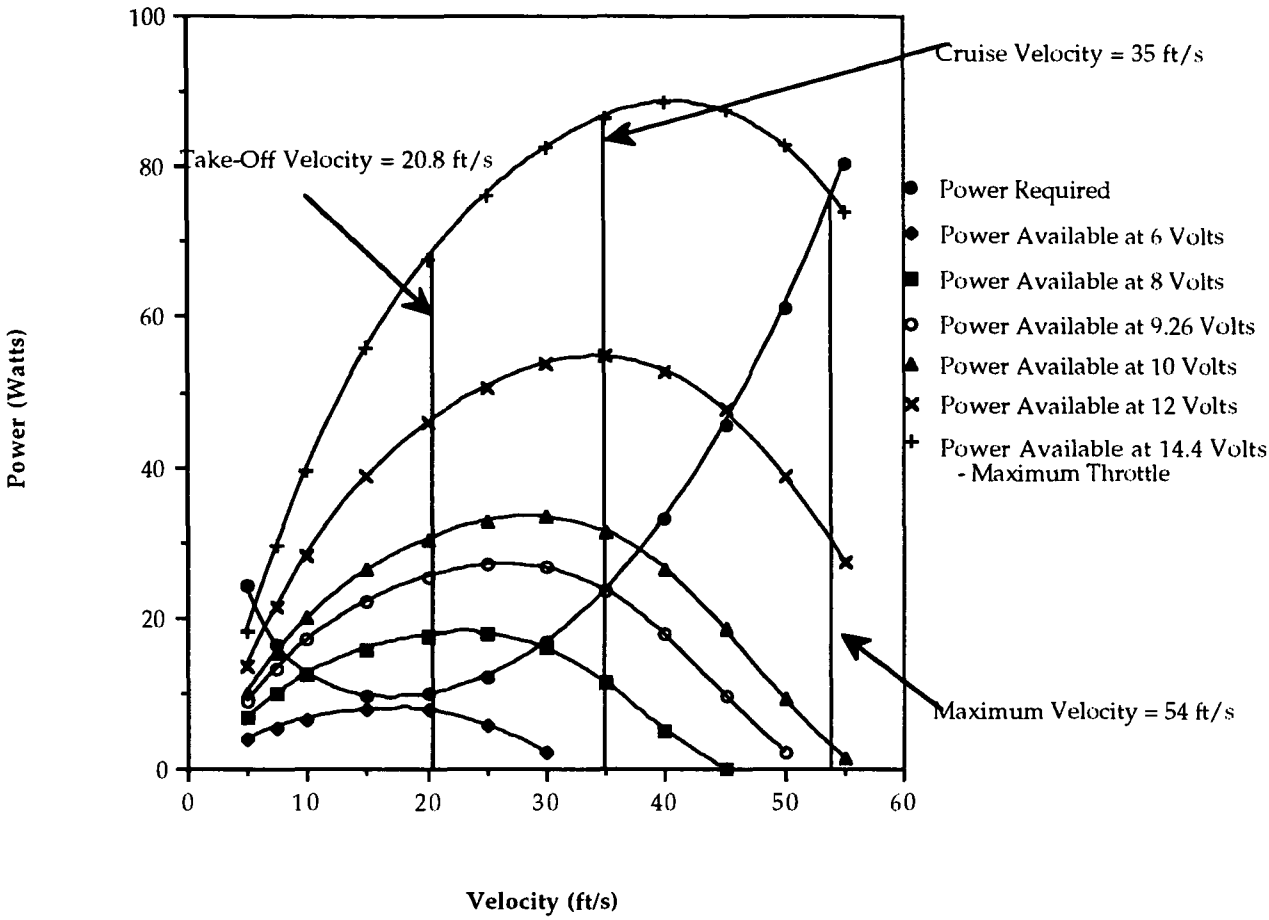

12.5-6 Propeller Efficiency vs. Advance Ratio

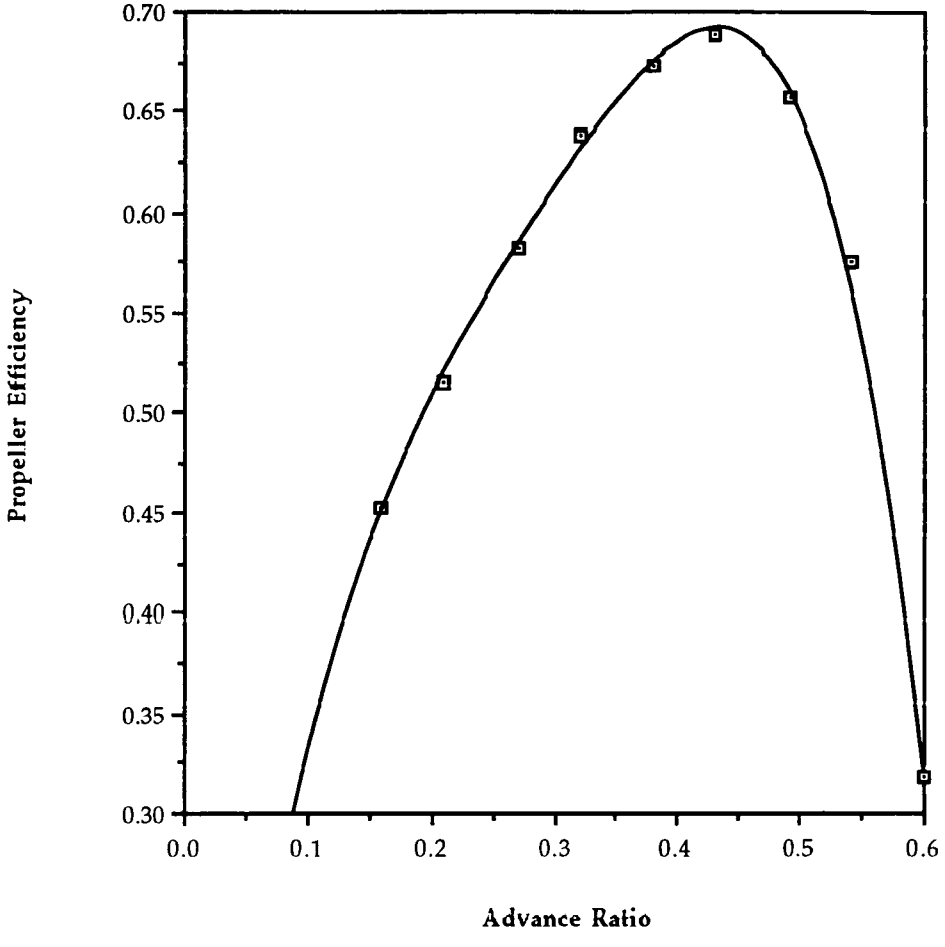

WEIGHT BALANCE DIAGRAM

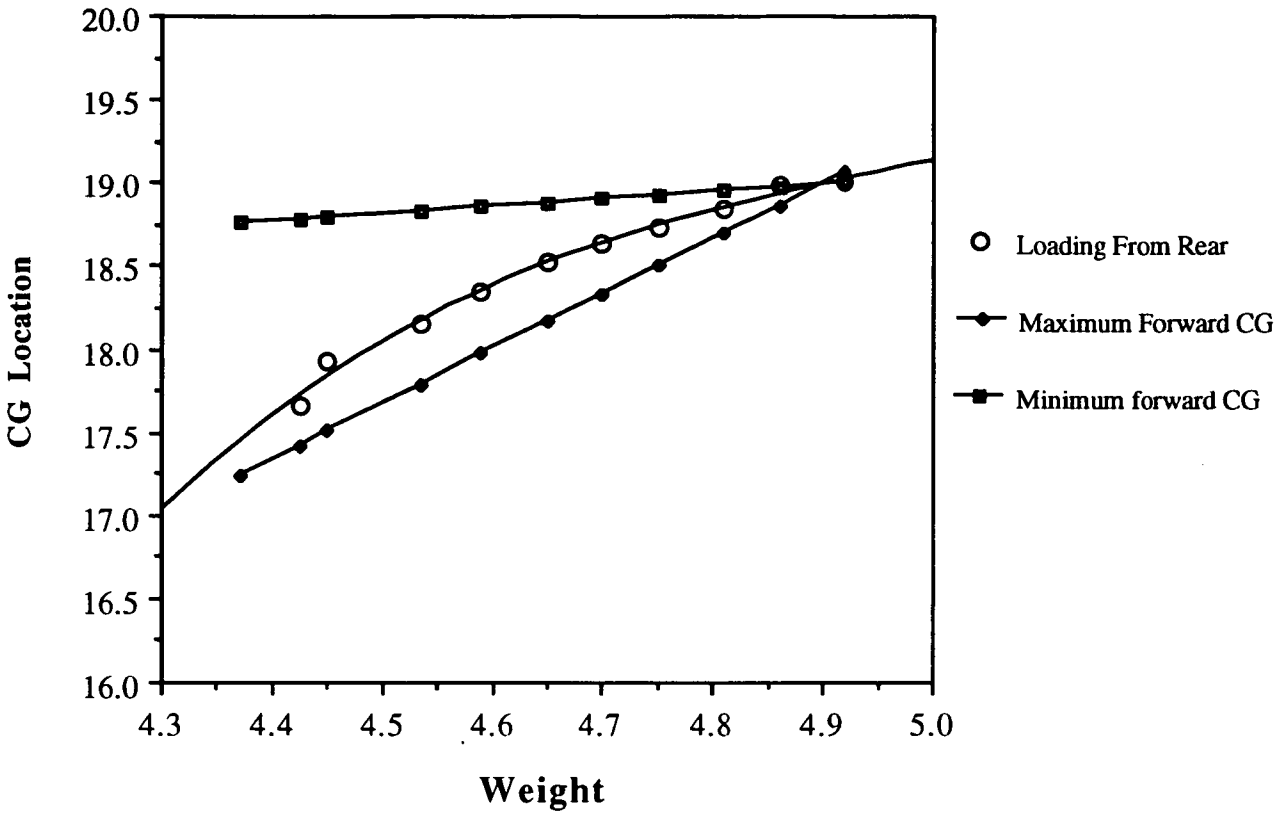

COMPONENT WEIGHT BREAKDOWN

COMPONENT	WEIGHT oz.	WEIGHT %	CG POINT(X)in.
STRUCTURE			
Decking	4.86	5.7	27.5
Empennage	1.7	2	62
Wing	21	25	18
Fuselage	7.2	8.5	27.8
Monokote	3.54		22
subtotal	35.3	42%	
LANDING GEAR			
Nose	1.4		6
Main	2.2		20
subtotal	3.6	4.2%	
CONTROL SYSTEMS			
Servos	2.4		12
Receiver	.95		12
Syst. batteries	2		12
Speed controller	1.77		12
Push rods	1.82		12
Surface horns	.5		n/a
subtotal	9.44	11.6%	
PROPULSION			
Engine mount	1.2		2
Astro 15 w/ grbox	10.3	12.2	2
Batteries	14.75	17.5	16.6
Propeller	.866		-.2
subtotal	27.12	32%	
PAYLOAD	8.818	10.4%	33
MISC.			
velcro and glue	2		n/a
TOTAL	82.6+/- 3 oz. 5.1+/-.2 lbs	n/a	19.0 +/-.4 full 16.5 +/- .4 unload

V - n Diagram at Maximum
Take-Off Weight

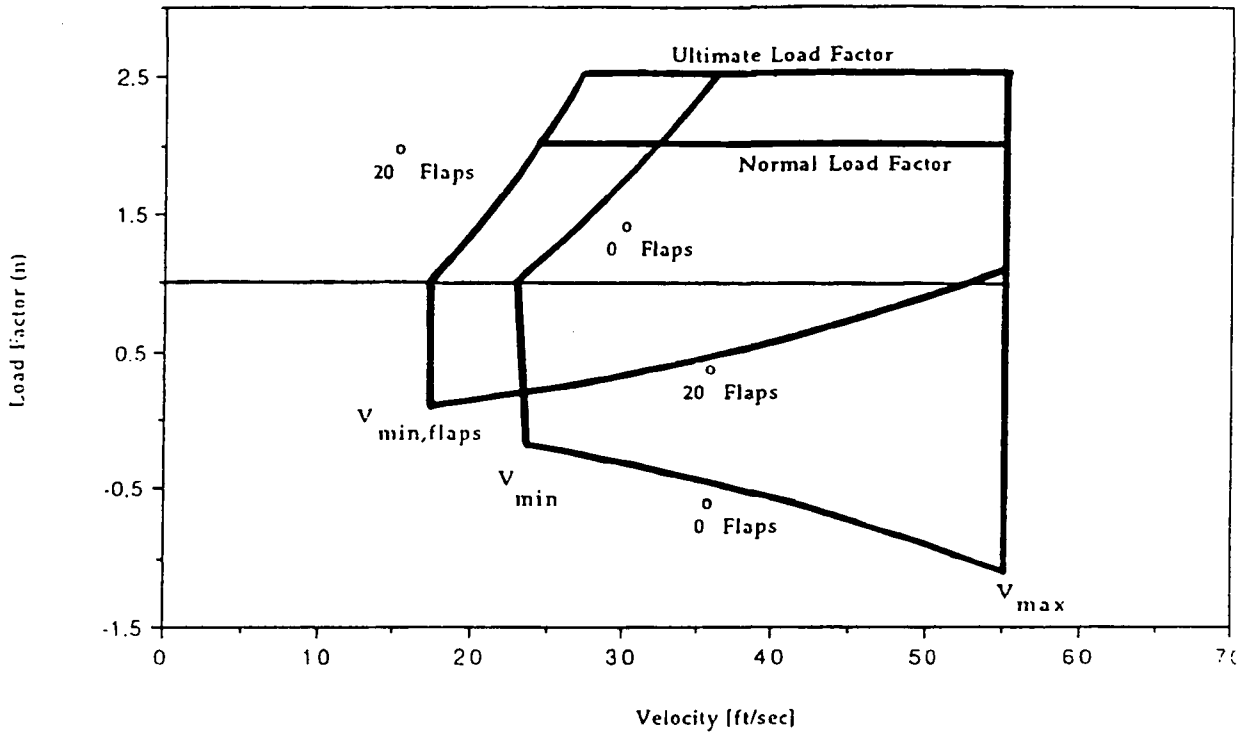

THREE VIEW EXTERNAL SCHEMATICS

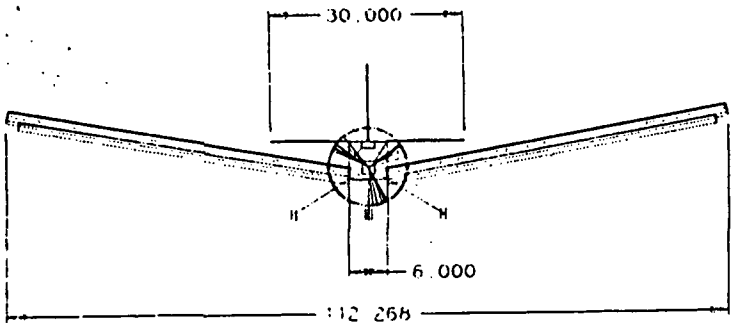

FRONT VIEW

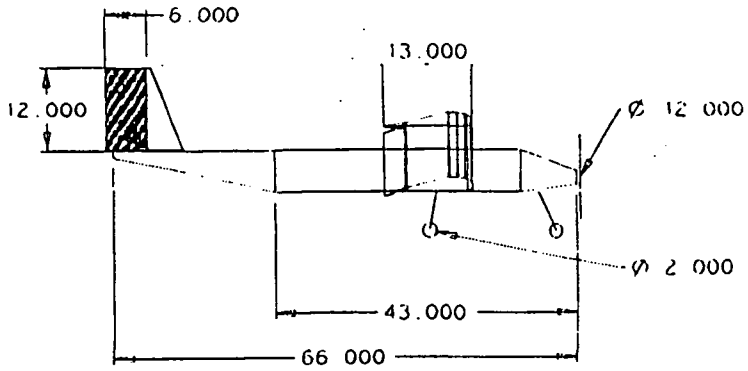

SIDE VIEW

TOP VIEW

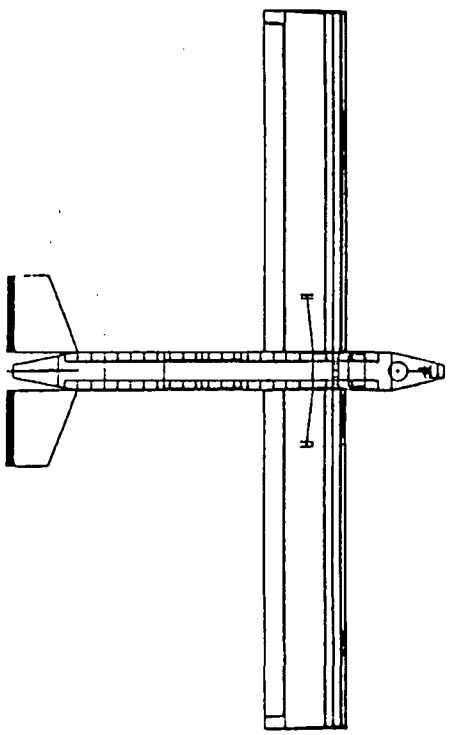

TWO VIEW INTERNAL CONCEPT SCHEMATIC

TOP VIEW

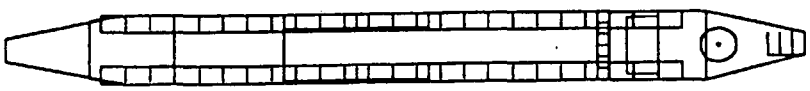

SIDE VIEW

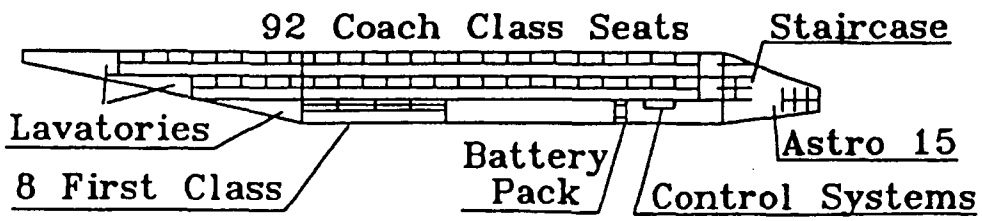

APPENDIX 2 - AERODYNAMICS

- **CALCULATIONS OF FLAP EFFECT ON AIRCRAFT LIFT**